AD-772 708

STUDY OF ADVANCED STRUCTURAL CONCEPTS FOR FUSELAGE

Sidney C. Swatton

Boeing Vertol Company

Prepared for:

Army Air Mobility Research and Development Laboratory

October 1973

AD

USAAMRDL TECHNICAL REPORT 73-69

STUDY OF ADVANCED STRUCTURAL CONCEPTS FOR FUSELAGE

By

S. Swatton

October 1973

EUSTIS DIRECTORATE
U. S. ARMY AIR MOBILITY RESEARCH AND DEVELOPMENT LABORATORY
FORT EUSTIS, VIRGINIA

CONTRACT DAAJ02-72-C-0056
THE BOEING VERTOL COMPANY
(A DIVISION OF THE BOEING COMPANY)
PHILADELPHIA, PENNSYLVANIA

DISCLAIMERS

The findings in this report are not to be construed as an official Department of the Army position unless so designated by other authorized documents.

When Government drawings, specifications, or other data are used for any purpose other than in connection with a definitely related Government procurement operation, the United States Government thereby incurs no responsibility nor any obligation whatsoever; and the fact that the Government may have formulated, furnished, or in any way supplied the said drawings, specifications, or other data is not to be regarded by implication or otherwise as in any manner licensing the holder or any other person or corporation, or conveying any rights or permission, to manufacture, use, or sell any patented invention that may in any way be related thereto.

Trade names cited in this report do not constitute an official endorsement or approval of the use of such commercial hardware or software.

DISPOSITION INSTRUCTIONS

Destroy this report when no longer needed. Do not return it to the originator.

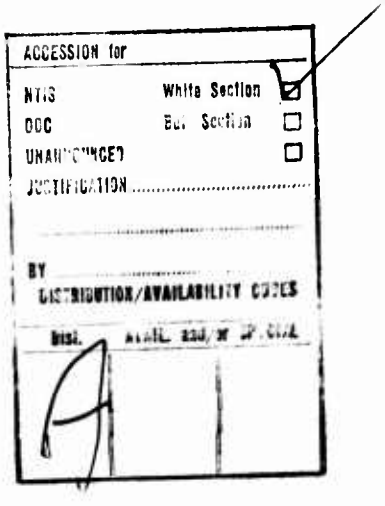

Unclassified

Security Classification

AD772708

DOCUMENT CONTROL DATA - R & D

(Security classification of title, body of abstract and indexing annotation must be entered when the overall report is classified)

1. ORIGINATING ACTIVITY *(Corporate author)*
The Boeing Vertol Company
Box 16858
Philadelphia, Pennsylvania

2a. REPORT SECURITY CLASSIFICATION
Unclassified

2b. GROUP

3. REPORT TITLE

STUDY OF ADVANCED STRUCTURAL CONCEPTS FOR FUSELAGE

4. DESCRIPTIVE NOTES *(Type of report and inclusive dates)*
Final Report

5. AUTHOR(S) *(First name, middle initial, last name)*

Sidney C. Swatton

6. REPORT DATE	7a. TOTAL NO. OF PAGES	7b. NO. OF REFS
October 1973	186	14

8a. CONTRACT OR GRANT NO.	9a. ORIGINATOR'S REPORT NUMBER(S)
DAAJ02-72-C-0056	
b. PROJECT NO. Task 1F162208A17001	USAAMRDL Technical Report 73-69
c.	9b. OTHER REPORT NO(S) *(Any other numbers that may be assigned this report)*
d.	D210-10683

10. DISTRIBUTION STATEMENT

Approved for public release; distribution unlimited.

11. SUPPLEMENTARY NOTES	12. SPONSORING MILITARY ACTIVITY
	Eustis Directorate U. S. Army Air Mobility R&D Laboratory Fort Eustis, Va.

13. ABSTRACT

This report presents the results of a study conducted to develop advanced structural concepts and the application of fiber-reinforced composite materials for the Cobra AH-1G helicopter tail section.

This study comprised the following tasks: (1) analysis of existing AH-1G metal tail section to determine areas having highest potential structural improvement, (2) development and preliminary design studies of various advanced structural concepts and selection of three concepts for prelmiinary design trade-off study, (3) determination of parameters affecting cost effectiveness and performance of composite fuselage structure, (4) sensitivity analysis for reducing tail-section life-cycle costs, and (5) development of a math model for life-cycle costs and performance of composite fuselage, and utilization of model to recommend the optimum design.

The following structural concepts were selected for preliminary design study: (1) monocoque sandwich clamshell, (2) thin sandwich shell with longerons and frames, and (3) integrally molded skin/stringer clamshell.

The study results recommend the monocoque sandwich clamshell as the optimum design concept.

DD FORM 1 NOV 68 1473 REPLACES DD FORM 1473, 1 JAN 64, WHICH IS OBSOLETE FOR ARMY USE.

Unclassified

Security Classification

14. KEY WORDS	LINK A		LINK B		LINK C	
	ROLE	WT	ROLE	WT	ROLE	WT
Clamshell, sandwich, monocoque						
Clamshell, stringer						
Composite structures						
Cost effectiveness, composite structures						
Fiberglass-reinforced						
Fuselage, AH-1G, Cobra						
Math model, life-cycle costs						
Shell, sandwich, thin						
Skin, integrally molded						
Tail boom, helicopter						
Tail section, AH-1G, Cobra						

DEPARTMENT OF THE ARMY
U. S. ARMY AIR MOBILITY RESEARCH & DEVELOPMENT LABORATORY
EUSTIS DIRECTORATE
FORT EUSTIS, VIRGINIA 23604

This report was prepared by the Boeing Company, Vertol Division, under the terms of Contract DAAJ02-72-C-0056.

The information contained in this report is a result of research conducted to extend the basic understanding of advanced design concepts and composite materials and their application to aircraft fuselage primary structures.

This effort is one of two parallel studies to investigate advanced structural concepts for helicopter fuselages. The associated study program, under the same title, was conducted by Kaman Aerospace Corporation under the terms of Contract DAAJ02-72-C-0057.

Numerous design approaches, material selections, and fabrication techniques were investigated for the Cobra AH-1G helicopter tail section. A quantitative method (math model) for ranking the proposed design concepts was developed. Although each concept possesses specific areas of advantages and disadvantages, it was determined that a monocoque/sandwich structure was the preferred design concept.

The report has been reviewed by the Eustis Directorate, U.S. Army Air Mobility Research and Development Laboratory and is considered to be technically sound. It is published for the exchange of information and the stimulation of future research.

This program was conducted under the technical management of Mr. L. Thomas Mazza, Technology Applications Division.

Task 1F162208A17001
Contract DAAJ02-72-C-0056
USAAMRDL Technical Report 73-69
October 1973

STUDY OF ADVANCED STRUCTURAL CONCEPTS FOR FUSELAGE

D210-10683
Final Report

By

S. Swatton

Prepared by

The Boeing Vertol Company
(A Division of The Boeing Company)
Philadelphia, Pennsylvania

for

EUSTIS DIRECTORATE
U.S. ARMY AIR MOBILITY RESEARCH AND DEVELOPMENT LABORATORY
FORT EUSTIS, VIRGINIA

SUMMARY

This report presents the results of a study conducted to develop advanced structural concepts and the application of fiber-reinforced composite materials for the Cobra AH-1G helicopter tail section.

This study comprised the following tasks:

1. The review and analysis of the AH-1G existing metal tail section to determine the areas having highest potential structural improvement.

2. Development and preliminary design studies of various advanced structural concepts composed of fiber-reinforced composite materials and selection of three concepts for preliminary design trade-off study.

3. Determination of significant design parameters affecting the cost effectiveness and performance of a fiber-reinforced composite fuselage structure.

4. Generation of a sensitivity analysis for reducing overall fuselage tail section life-cycle costs.

5. Development of a math model for the overall life-cycle cost effectiveness and performance of a fiber-reinforced composite fuselage and utilization of the math model to recommend the optimum of the three designs selected for the preliminary design trade-off study.

The following structural concepts were selected for preliminary design study:

1. Monocoque Sandwich Clamshell

2. Thin Sandwich Shell with Longerons and Frames

3. Integrally Molded Skin/Stringer Clamshell

The study results recommend the Monocoque Sandwich Clamshell as the optimum design concept.

FOREWORD

This final technical report concludes the study of "Advanced Structural Concepts for Fuselage" initiated on April 27, 1972, for the Eustis Directorate, U.S. Army Air Mobility Research and Development Laboratory, Fort Eustis, Virginia, by the Boeing Vertol Company under Contract DAAJ02-72-C-0056, DA Task 1F162208A17001.

The program was conducted at the Vertol Company under the technical direction of Mr. P. Woods, Program Manager. Mr. C. McCall, Chief Stress Engineer, was responsible for the technology input.

Principal investigators for the program were Mr. S. Swatton, Design Project Engineer; Mr. R. Pinckney, Manager, Composites Manufacturing; Mr. S. Moszer, Technology; and Mr. G. Willetts, Systems Evaluation.

TABLE OF CONTENTS

LIST OF ILLUSTRATIONS

LIST OF TABLES

LIST OF SYMBOLS

A	section or stringer area, $in.^2$
A_e	enclosed cell area, $in.^2$
a	panel length or span, in.
b	panel width, in.
c	column fixity coefficient
D	panel stiffness parameter, lb-in.
d	total honeycomb sandwich thickness, in.
E	modulus of elasticity, psi
F_c	allowable column buckling stress, psi
F_{cc}	allowable crippling stress, psi
F_{cr}	allowable panel compression buckling stress, psi
F_{cu}	material ultimate compression strength, psi
F_{isu}	laminate interlaminar shear strength, psi
F_{scr}	allowable panel shear buckling stress, psi
F_{su}	material ultimate shear strength, psi
F_{tu}	material ultimate tensile strength, psi
f_c	applied compression stress, psi
f_s	applied shear stress, psi
G	shear modulus, psi
G_c	honeycomb core shear modulus, psi
h	distance between honeycomb sandwich facing centroids, in.
I	moment of inertia, $in.^4$
J	torsional rigidity, $in.^4$
K	general buckling constant

K_{mc}	compression buckling constant
K_{ms}	shear buckling constant
L	longitudinal direction; length, in.
L'	effective column length, in.
M	bending moment, in.-lb
N_{cr}	allowable compression buckling load per unit length of edge, lb/in.
$N_{xy,cr}$	allowable shear buckling load per unit length of edge, lb/in.
R	stress ratio
S	shear load, lb
s	distance between element centroids, in.
t	facing thickness; skin thickness, in.
t_c	honeycomb core thickness, sandwich, in.
U	honeycomb panel design parameter, transverse stiffness, lb/in.
V	honeycomb panel design parameter
V_f	fiber volume fraction
W	transverse core axis

Subscripts

c	compression
s	shear
t	tension
x	axis direction
y	axis direction
z	axis direction

Greek Symbols

θ	skin panel buckling parameter
λ	$1-\mu^2$
μ	Poisson's ratio
ρ	radius of gyration, in.

INTRODUCTION

The development and application of fiber-reinforced composite materials to primary and secondary airframe structures and dynamic components have increased rapidly over the last 10 years.

The increasing requirement for more efficient and reliable aerospace structural materials and systems has triggered extensive research and development in the application of new, high-modulus, high-strength fiber materials.

The increase in the use of composite materials has occurred only because composite materials and designs have been shown to reduce equipment life-cycle costs and/or increase productivity.

The structural properties of composite materials have improved to the point where major secondary airframe components have essentially become an industry production state of the art.

The major factors for this continued application growth have been:

1. Lower tool and production man-hours for complex contours on limited production runs.

2. Improved vibration, impact and crack growth resistance.

3. Elimination of corrosion and related maintenance costs.

4. Improved ballistic tolerance.

5. Improved aerodynamic surfaces; smoother, fewer joints; less rivets, etc.

The continued development of composite materials, design techniques and manufacturing methods and their improving structural properties now make them good candidates for primary airframe structures.

This report presents the results of a study conducted by the Boeing Vertol Company to determine specific structural design concepts for the AH-1G tail system by applying composite materials and material combinations and using their properties to the fullest advantage.

REVIEW AND ANALYSIS OF THE AH-1G EXISTING METAL FUSELAGE TAIL SECTION

The existing AH-1G metal fuselage tail section was reviewed and analyzed to determine areas having the highest potential for structural improvement.

The study included an examination and evaluation of engineering drawings, structural reports, and actual tail section hardware items supplied by USAAMRDL. Maintenance data for the Navy AH-1G, received from the Navy's 3-M reporting system, was also used.

In the evaluation, an attempt was made to identify any parts or areas which would limit performance or be subject to operational damage and/or environmental change, or in any other way have high maintenance potential.

The review of the actual tail section hardware, drawings, and structural data did not reveal any areas of structural deficiencies or design features which might cause maintenance problems.

Investigation revealed that the Navy 3-M data was probably the most comprehensive maintenance performance data available for the AH-1G aircraft. Data collected by the Navy during the period September 1969 through December 1970, representing 20,262 flight hours, were analyzed. The data segments were the tail-boom airframe, including the elevator and tail skid, tail rotor system components and tail drive system components. Additionally, to provide greater visibility, identical segments of UH-1E data collected during the November 1969 through December 1970 period, representing 44,865 flight hours, were also analyzed. The results of the analyses are presented in Table I. Preliminary review of this data indicates that the tail-boom airframe of the AH-1G is a four-to-one improvement over the UH-1E. Undoubtedly the AH-1G is an improvement; however, a true magnitude could not be determined by this study due to the fact that, although the data was collected during the same time frame, the AH-1G was a relatively new aircraft, while the UH-1E aircraft had been in service for some time with the attendant accumulation of flight hours. Therefore, fatigue-induced failures were low in this data sample for the AH-1G compared to the UH-1E.

At this point it should also be noted that the 3-M reporting system is not specific as to the particular component or the mode or type of failure. For example, a "tail-boom fairing" may be listed as a failed item and the mode listed as "broken or cracked." It is not always possible to determine which fairing is involved, the location, and the type of break.

TABLE I. TAIL-BOOM AIRFRAME - FAILURE ANALYSIS FOR AH-1G AND UH-1E

Failure Data:	AH-1G	UH-1E
Mean time between failures	163 Hr	43 Hr
Failures/1000 flight hours	6.12	23.51
	FR/1000	% of System
AH-1G Major Failure Items:		
Tail-boom assembly	1.33	21.8%
Gearbox access fin cover	1.09	17.7%
Bearing hanger support fitting	.99	16.1%
Fairing assembly	.79	12.9%
Elevator assembly	.49	8.1%
Remaining airframe	-	23.4%
UH-1E Major Failure Items:		
Tail-boom assembly	10.52	44.7%
Tail-boom door assembly	3.97	16.9%
Fairing assembly	2.45	10.4%
Elevator assembly	2.21	9.4%
Gearbox access fin cover	1.07	4.5%
Remaining airframe	-	14.1%
AH-1G Major Modes of Failure:	% of A/C	
Worn, chafed or frayed	16.7%	-
Missing or loose hardware	16.7%	-
Loose	15.8%	-
Broken or cracked	13.3%	-
Torn	8.3%	-
Other	22.0%	-

The AH-1G tail-boom airframe is a good, sound and durable structural design with a good maintenance history. Most of the problems encountered are typical of airframe structures, i.e., loose rivets or hardware, and broken or cracked parts. These types of failures can be reduced in composite structural designs whereby mechanical fasteners are eliminated or reduced by bonded joints, and by the crack-resistant properties of composite materials.

ADVANCED CONCEPTS

The primary task of this study was the development of advanced structural concepts using fiber-reinforced composites for the AH-1G tail section. The primary emphasis was placed on design ingenuity to produce new and innovative concepts so that the maximum benefit may be obtained from the properties of composite materials.

GROUND RULES FOR DESIGN STUDY

The design ground rules for this study were:

1. AH-1G structural loads and dynamics criteria
2. AH-1G structural attachment geometry at fuselage, gearboxes
3. AH-1G subsystems structural provisions
4. AH-1G access doors, panels and fairings - same number, accessibility, location and geometry.

In adopting the above ground rules, it was conceded that they would undoubtedly dictate compromises, resulting in less than optimum design solutions which might otherwise be obtained without constraints. In addition, because of these constraints, the evaluation of new composite design concepts results in somewhat conservative payoff calculations.

This conservatism is such that small structural weight reductions are shown over that of a conventional aluminum sheet-stringer shell configuration.

Figure 1 shows the original Cobra AH-1G hardware and assemblies used on the composite tail section. These parts are represented by the shaded area on the diagram.

SIGNIFICANT DESIGN PARAMETERS

One of the first tasks included in this study was the determination of the significant design parameters affecting the cost effectiveness and performance of fiber-reinforced composites as compared to improved metal components. This effort resulted in two unprioritized listings. The first list, shown below, contains general parameters common to both types of construction.

- Weight (structural efficiency)
- Maintenance

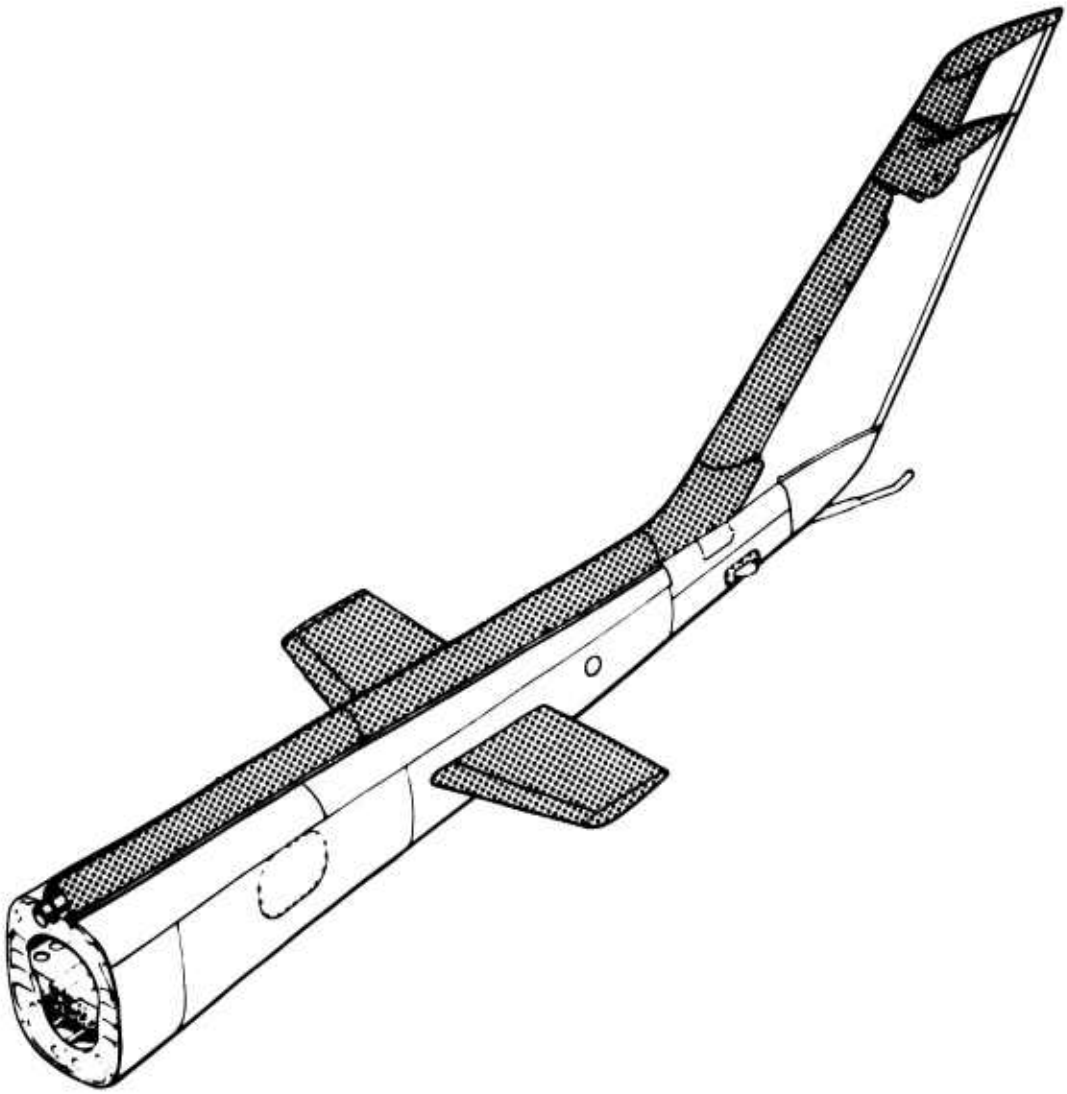

Figure 1. Original AH-1G Hardware.

- Repairability
- Material costs
- Fail-safe structure
- Survivable structure (gunfire and crash)
- Manufacturing cost
- Spares

A further examination was made of more specific (and generally unwritten) design criteria and considerations which the designer must consider. Those which influence the above-listed parameters are shown in Table II.

SENSITIVITY ANALYSIS

A sensitivity analysis was performed aimed at reducing overall fuselage tail section life-cycle costs. The following parameters were considered:

- Weight
- Maintenance
- Material cost
- Service-incurred damage and ballistic resistance
- Manufacturing costs
- Structural efficiency
- Dynamic response
- Performance

The analysis endeavored to determine the interrelationships of these parameters and their impact on the life-cycle cost. Table III shows these interrelationships. The impact of the parameters on the total life-cycle costs is summarized in Table IV. Total life-cycle costs are the summation of two basic cost areas: acquisition and user support costs. User support costs are those incurred in the use of the product. Basically the study reveals that weight, performance and structural efficiency are for practical purposes synonymous for weight alone and that a reduction in weight (improved structural efficiency and performance) generally results in higher acquisition cost but lower life-cycle costs. However, if maintenance accessibility is hindered or more inspection

TABLE II. DESIGN PARAMETERS

Metal Design	Composite Design
Minimize parts count	Minimize parts count
Automatic riveting	Automatic tape lay-up
Minimum of fasteners	Minimum secondary bonding
Single curvature	Avoidance of eccentricities
Minimum of machining	Gradual change in stress level
Avoidance of eccentricities	Fatigue quality (superior to metals)
Gradual change in stress level	Thermal compatibility
Fatigue quality of material	Anisotropic properties
Fretting and corrosion	Draft angle desired
Thermal compatibility	Fire resistance
Heat treating	Types of fasteners
Dissimilar metals in contact	Minimum gage
Types of fasteners	Vibration, flutter, dynamic response
Corrosion	Lightning protection
Minimum gage	
Vibration, flutter, dynamic response	

TABLE III. PARAMETER INTERRELATIONSHIP

	Weight	Maintenance	Material Cost	Service-Incurred Damage	Structural Efficiency	Dynamic Response	Manufacturing Costs	Performance (Range/Payload)
Reduced weight		Potentially higher cost	Generally higher	Potentially higher cost	Improved	Potentially reduced	Generally higher	Improved
Improved maintenance features	Increased weight	Reduced cost	No effect	No effect	Generally reduced	Generally reduced	Generally higher	Generally reduced
Low material cost	Generally increased weight	No effect		No effect	Generally reduced	No effect	Generally reduced	Generally reduced
Improved service incurred damage	Generally increased weight	Reduced cost	Potentially higher		Generally reduced	Generally improved	No effect	Generally reduced
Structural efficiency (improved)	Reduced weight	Potentially higher cost	Generally higher	Potentially higher cost		Potentially reduced	Generally higher	Improved
Dynamic response	Increased weight	Potentially higher cost	Generally higher	Generally reduced	Generally reduced		Generally higher	Generally reduced
Reduced manufacturing cost	Increased weight	Generally higher cost	Generally reduced	No effect	Generally reduced	No effect		Generally reduced
Improved performance	Reduced weight	Generally higher cost	Generally higher	Potentially higher cost	Improved	Generally reduced	Generally higher	

TABLE IV. EFFECT OF DESIGN PARAMETERS ON LIFE-CYCLE COSTS

	Acquisition Cost	User Cost	Life-Cycle Cost
Reduced weight	Increase	Potential reduction	Potential reduction*
Improved maintenance features	Potential increase	Potential reduction	Potential reduction**
Lower material cost	Reduction	Increase	Increase
Improved skin-damage resistance	Potential increase	Potential reduction	Potential reduction**
Improved structural efficiency	Increase	Potential reduction	Potential reduction*
Dynamic response	Potential increase	Increase	Increase
Reduced manufacturing cost	Reduction	Increase	Increase
Improved performance	Increase	Potential reduction	Potential reduction*

*Positive reduction if maintenance is not sacrificed.
**Positive reduction if weight is not sacrificed.

and/or maintenance is required, this favorable cost reduction may be lost. The same also applies for the reduced life-cycle costs shown by the improved maintenance features, the benefit of which may be lost if it incurs an increase in weight (reduced structural efficiency and performance).

Lower material and manufacturing costs, although reducing acquisition costs, generally result in a weight increase, thereby increasing the life-cycle cost.

CONCEPTUAL STUDIES

PRELIMINARY DESIGN SELECTION

In the proposal for this study, Boeing Vertol had shown nearly two dozen candidate design studies. These, in addition to others established during the current study, had to be reduced to three prime concepts for more detailed evaluation. The selection process involved first a preliminary screening followed by a final screening.

PRELIMINARY SCREENING SELECTION

This step was conducted using the considerations listed in Table V. As a result of this screening, eight concepts were selected for more detailed study and evaluation. (See Table VI.) Sketches of these concepts are shown in Figures 2 through 9. It should be emphasized that the design sketches are conceptual only and do not represent sized structures; they were mainly intended as exploratory schemes to establish viable construction concepts.

The delta configuration rigid frame and secondary panel concept did not meet interface requirements in the area of drive shaft support and fuselage/tail-boom attach points. Several construction ideas which appeared attractive when shown as independent sections were found to be unrealistic when applied to the overall composite concept, which has requirements for taper, curvature, access cutouts and interface fittings. The circular sleeve core concept and knitted sleeve concept are included in this category. The corrugated reinforced bonded shell is considered to be similar to the skin/stringer concept.

The sandwich shell with corrugated core idea was deemed to be sufficiently represented in the double-skinned monocoque/skin stringer/foam core concept. The Tetracore panel system was investigated and looked feasible but was not included as a conceptual design due to limited data available pertaining to the capability of specialized automatic machinery developed to weave lattice structures comprising compound curvature and tapering shell thickness.

In the I-beam primary structure concept, the secondary side panels were not specifically shown but were an attempt at fulfilling the concept of rigid frame/secondary panel with an innovative design.

TABLE V. DESIGN SELECTION CONSIDERATIONS - PRELIMINARY SCREENING

1. Customer requests
2. Technical confidence
   - State of the art
   - Qualified engineers
   - Qualified technicians
   - Successful past performance
3. Design engineer preferences
   - Optimum integration of all requirements
   - Performance vs risk and cost
   - Reliability
   - Simplicity
   - Interface problems
   - Thermal compatibility
   - Attachments, cutouts, subsystems, etc.
4. Stress engineer preferences
   - Quality
   - Strength critical
   - Stiffness critical
   - Fatigue resistance
   - Dynamic response
   - Minimum gage
   - Fail safety
5. Manufacturing engineer preferences
   - Producibility (automation and multifunctional cure, etc.)
   - Tooling cost/part (multipurpose tools)
   - Cost of materials (trend of costs)
   - Cost of labor/part
   - Cost of assembly (low parts count)
6. Cost effectiveness
   - Cost vs weight saving ($/lb)
   - Performance of system (life time)
   - Maintainability/repairability
   - Damage and ballistic tolerance
   - Corrosion resistance
   - Commonality of parts
7. Quality assurance
   - Simplicity of inspection
   - Reliability of inspection
   - Cost of inspection

TABLE VI. PRELIMINARY SCREENING SELECTION RESULTS
Concept
Monocoque sandwich - mandrel lay-up with female cure mold
Monocoque sandwich - clamshell
Monocoque sandwich - graphite filament wound
Thin sandwich shell with longerons and frames
Integrally molded skin stringer clamshell
Monocoque skin stringer with foam core
I-beam primary structure - secondary panels
Integrally molded waffle structure

The following is a brief description and review of each preliminary concept evaluated:

Monocoque Sandwich - Mandrel Lay-Up (Figure 2)

This sandwich-shell construction comprises graphite/epoxy inner and outer covers with Nomex honeycomb core, but no intermediate frames or stringers. Bulkheads are at forward and rear ends, and at vertical stabilizer front spar frame extension into tail boom (canted bulkhead). The internal secondary structure is fiberglass. Overlapping longitudinal joints, top and bottom, facilitate mandrel lay-up, enabling a complete shell to be laid up in one assembly prior to curing. The vertical fin is integral with tail boom and has sandwich type front and rear spar webs, same materials as shell.

Problems with this concept are: (1) high technical risk with numerous manufacturing difficulties, and (2) severe access limitations to locate and attach internal secondary structure. It requires extra female cure mold.

Monocoque Sandwich - Clamshell (Figure 3)

The structural arrangement is similar to mandrel lay-up (Figure 2), but the tail boom is made up in two separate halves, then affixed together via upper and lower splice joints. This arrangement allows all internal secondary structure to be easily attached to each open-half shell before the two halves are bonded together. The primary structure

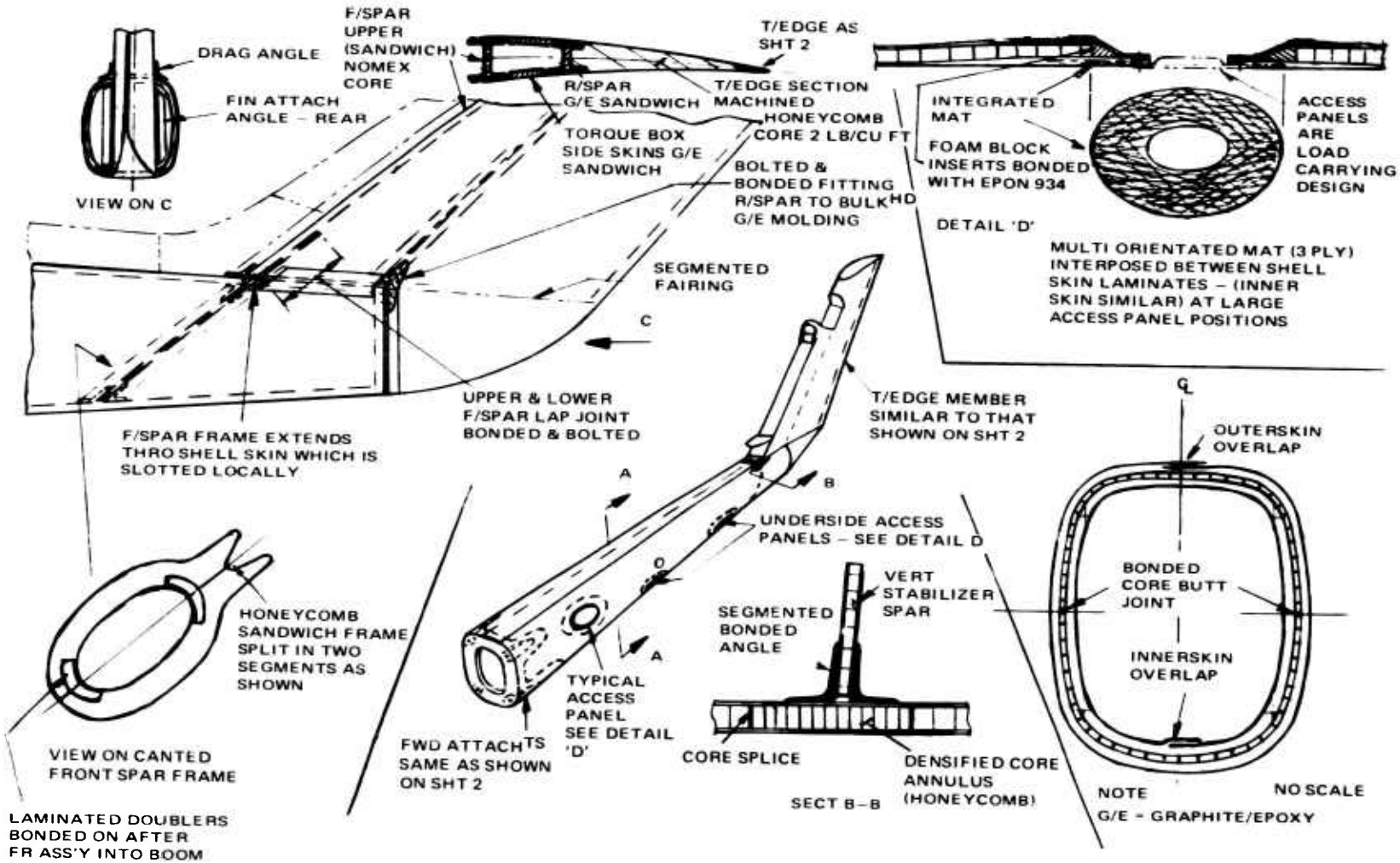

Figure 2. Monocoque Sandwich-Mandrel Lay-up.

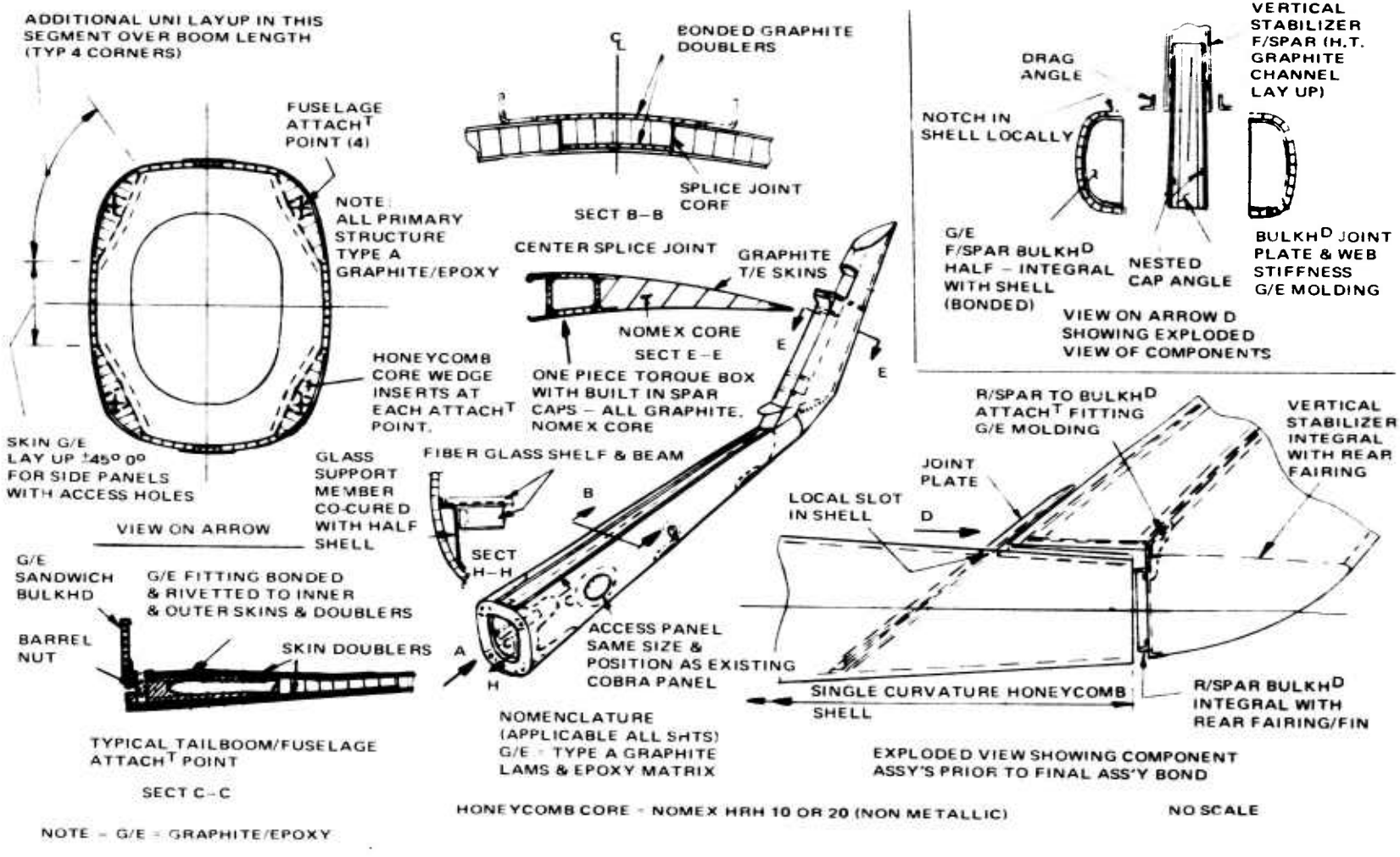

Figure 3. Monocoque Sandwich-Clamshell.

comprises graphite/epoxy covers with Nomex core. The compound curvature tail-cone section is molded graphite with internal stiffeners (load-carrying member). Heavy peripheral and longitudinal internal doublers at forward end of tail boom consolidate fuselage attachment fittings built in to locally thickened Nomex core shell. Internal secondary structure avionics tray supports, etc., are molded fiberglass construction. The HT graphite characteristics give best strength and stiffness for lowest weight, but type-A graphite is considered as giving acceptable performance for greatly reduced material cost.

Its problem is that graphite does not exhibit good low-velocity impact resistance without use of high elastic matrix material and/or dispersion of high impact resistant fibers (i.e., glass, PRD-49, etc.).

Monocoque Sandwich - Graphite Filament Wound (Figure 4)

This is basically a similar arrangement to that shown in Figure 3, in that it is a monocoque construction with the same bulkhead positions and vertical fin design and sandwich shell material. Moreover, manufacturing is done in a totally different way, which would facilitate production by affording maximum automated processes. The shell is produced by filament or tape winding the inner skin, hot mold forming the Nomex core, bonding into place, and then winding the outer skin similar to the inner cover. Frames, vertical stabilizer, and secondary structure are added after the shell has been cured in a female mold. The torque box of the stabilizer could also be of wound construction.

Problems - This would seem to be a satisfactory mass-production method for producing the tail-boom shell. However, it is doubtful that the tail boom, which, although it is a straight-line element but not symmetrical about the horizontal axis, could be fully automatically tape or filament wound with the specific ply orientations required. There are a number of considerations which could prove retrograde to the winding process, such as the doubler straps and surrounding reinforcings, which are added locally on inside skin surfaces or in some cases interposed between basic cover plies. It is doubtful whether the machine could be programmed to lay down special ply buildups with varying lengths, shapes and orientations, so the automated sequence would have to be stopped from time to time in order to hand lay-up doublers. There is also the question of accurate lay of tape or filament group; there should be no overlapping of tape edges of the same ply lay-up.

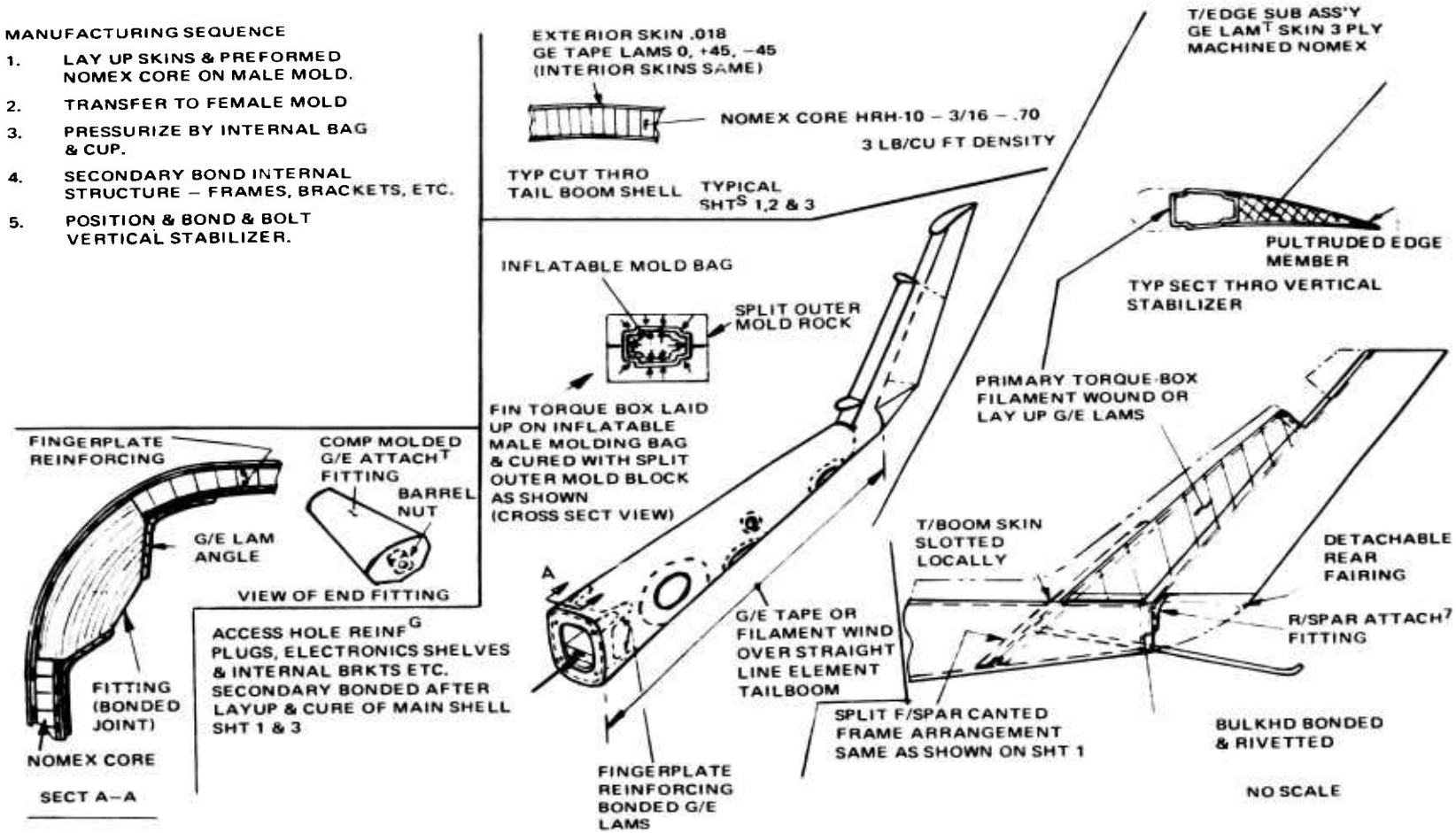

Figure 4. Monocoque Sandwich-Graphite Filament Wound.

Thin Sandwich Shell with Frames and Longerons (Figure 5)

This arrangement has considerable appeal from the design aspect, combining the advantages of two configurations. The skin/longeron system ensures a good fail-safe system with alternative load paths and skin panels divided into bays by stringers and frames to limit any possible skin crack propagation to one bay. The thin sandwich shell affords improved ballistic tolerance and reduces the number of stringers required to the extent that four heavy stringers or, more exactly, longerons are sufficient.

The combination of both systems confers even more redundancy, in that in the event of damage to one longeron, the sandwich skin locally is capable of acting as an alternate load path and taking the same bending load.

A mixed system of composite materials was selected for the tail-boom shell, comprising PRD 49-3/epoxy covers over Nomex core for the thin sandwich shell and graphite type-A bulkheads, frames, and longerons. Interior secondary structure is fiberglass "E" or "S." It was established that five intermediate ring frames would be required to support the shell in addition to the three bulkheads, which are positioned the same as those shown on the monocoque sandwich - mandrel lay-up with female cure mold, Figure 2.

The design incorporates a longitudinal upper and lower splice joint system to allow clamshell fabrication similar to that depicted in Figure 2.

Vertical fin structural arrangement, materials and installation are the same as those shown in Figure 2. (Graphite type-A skins are necessary for stress reasons.)

The longeron/frame system takes approximately 80 percent of the tail section bending load; sandwich skin, the other 20 percent.

Problems - Concept is a heavier structure, shows a larger parts count, and has all the manufacturing problems of both systems.

Integrally Molded Skin/Stringer Clamshell (Figure 6)

Construction is similar to conventional skin stringer aluminum alloy design but uses a mixed composite system. Primary structure comprises graphite type-A hat section stringers, floating ring type intermediate frames, and bulkheads. Cover material is S-glass (not sandwich). Secondary structure is fiberglass E or S.

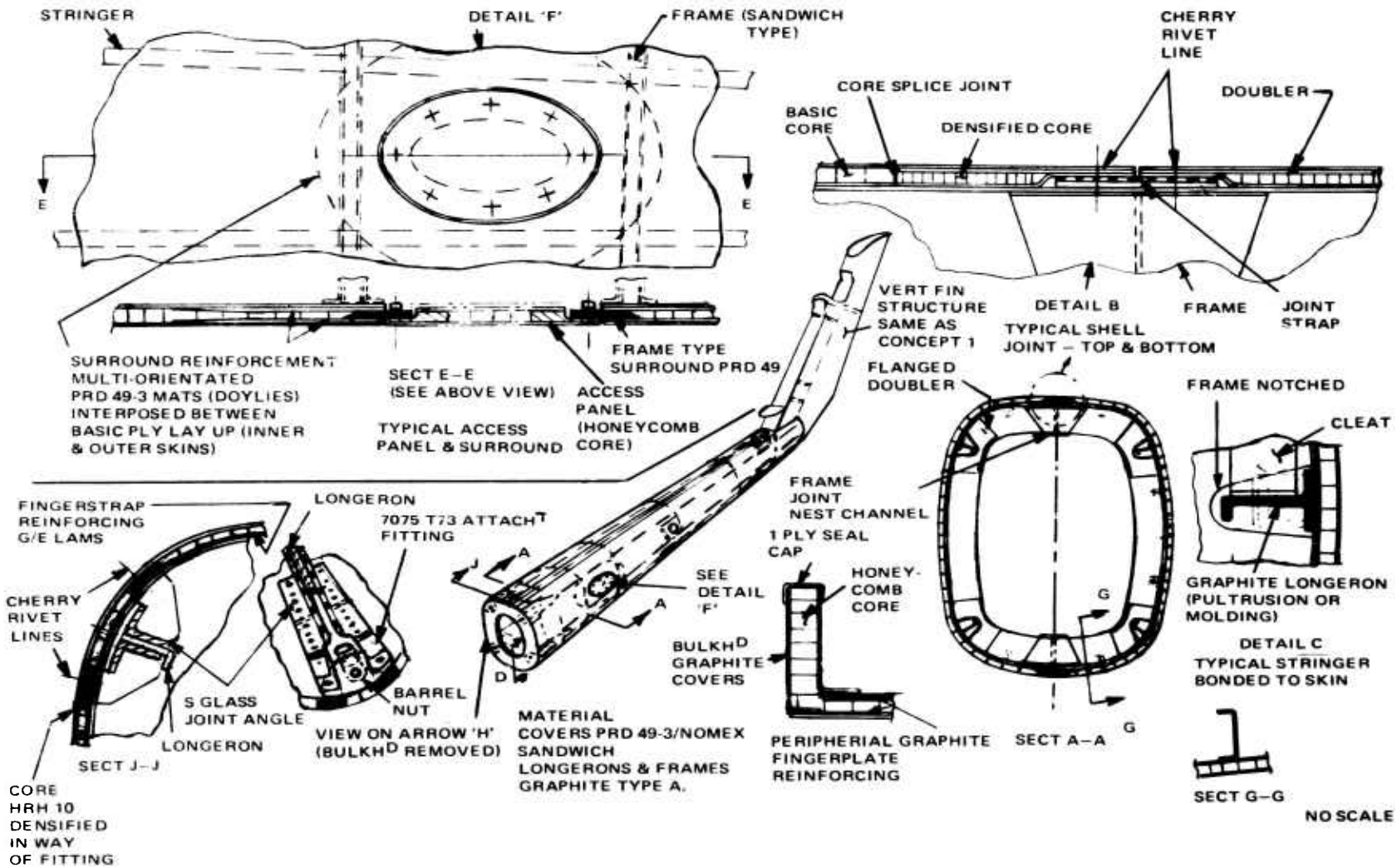

Figure 5. Thin Sandwich Shell with Frames and Longerons.

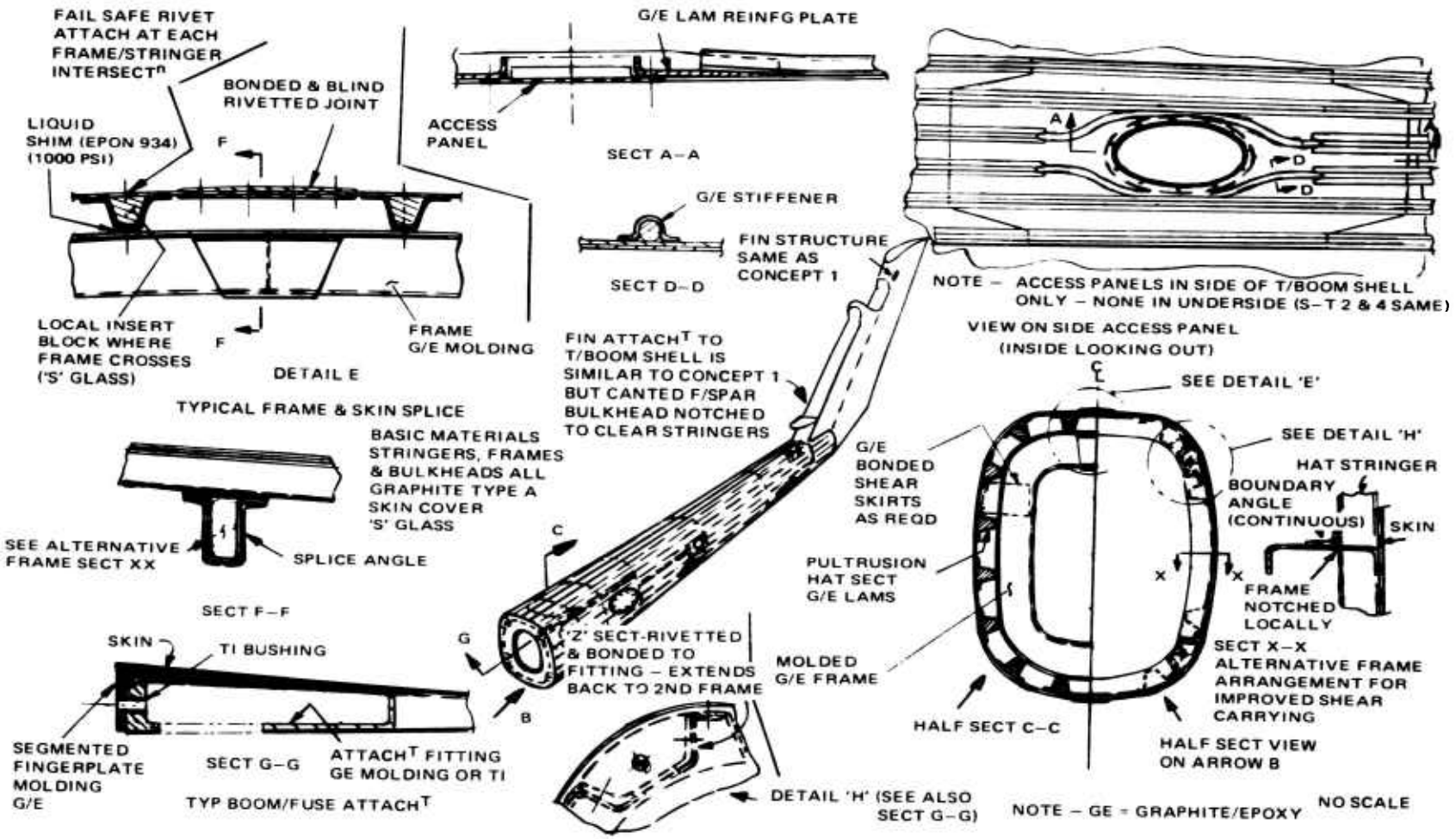

Figure 6. Integrally Molded Skin/Stringer Clamshell.

This arrangement obtained good ratings in the parametric studies due to the well tried and trusted design and for its good fail-safe qualities.

Again, the tail boom can be fabricated in two clamshell halves and bonded together, after the secondary structure is fit into each segment, by upper and lower splice joints running longitudinally down the length of the tail boom. Vertical fin structural arrangement, materials and installation are the same as shown in Figure 2. (Graphite type-A skins are necessary for stress reasons.)

Heavy graphite type-A finger-plate molding members serve as a collector to diffuse loads from the shell into the four integrated fuselage/tail-boom attachment fittings. These fittings are designed as "bathtubs" and are considered in titanium or as a graphite molding; they are positioned between stringers such that, as well as being primarily bonded to the surrounding structure, a system of blind attachments mechanically fastens fittings to stringers.

Problems - The fiberglass skin, although advantageous from the low-energy impact aspect, is thick and consequently contributes significantly to the excessive weight of this concept.

There are many fit-up problems due to the larger number of stringers and frames required.

High parts count also means increased time to manufacture.

Monocoque Skin/Stringer and Foam Core (Figure 7)

An unusual feature of this semimonocoque sandwich concept is that the core is envisaged as "foam-in-place" urethane rather than honeycomb. The tail section bending is carried by graphite type-A channel pultrusions which are integrated between inner and outer covers. There are three graphite bulkheads located in the same positions as shown in Figure 2, and the shell is fabricated in two halves with the usual joint at centerline, upper and lower.

Another interesting feature of this concept is the integral molding of the half segments of tail boom and vertical stabilizer covers forming a "hockey stick" configuration. When the two "hockey stick" segments are brought together for joining, the fin spar web, formed on one segment only, overlaps onto a bonded cap angle on the other segment, where it is attached by mechanical fasteners plus bonding. All secondary structure is fiberglass and is assembled to shell halves before being assembled together.

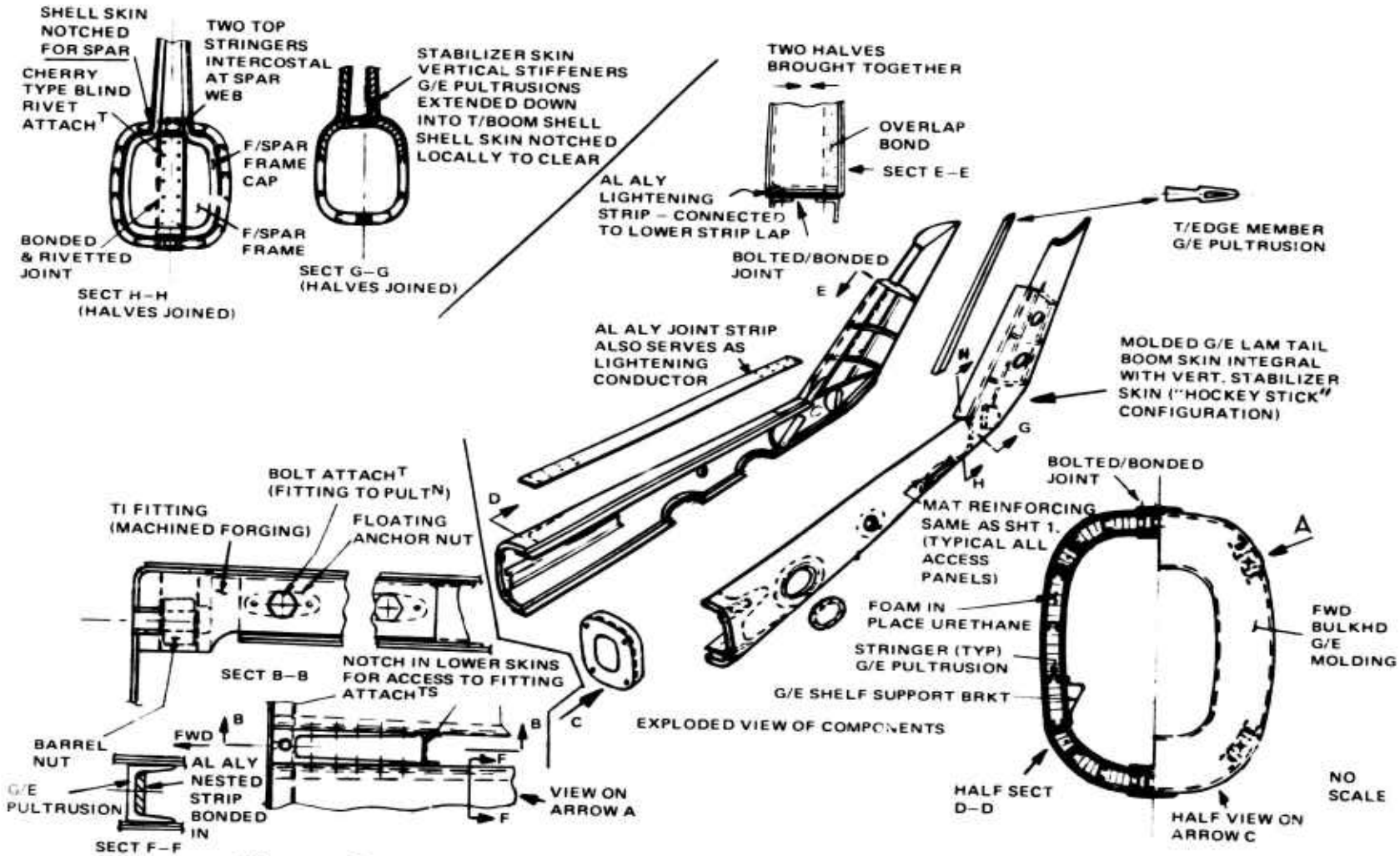

Figure 7. Monocoque Skin/Stringer and Foam Core.

The urethane foam filling is carried out after the curing sequence of each half clamshell, if using "foam-in-place" technique, or during lay-up operation, if bonding in pre-formed foam slabs. The main attachment fittings at the forward end of the shell are titanium and are detachable from the shell structure by unbolting and removing them through a notch in the inner skin.

Problems - The fabrication of this concept is considered to be a high risk. Foaming in-place is a difficult operation involving exact calculations of foam characteristics and expansion volume, etc. Due to the high pressures involved in this method, sophisticated and heavy molds would be required. Pre-foamed molded and machined urethane slabs bonded during lay-up would be a surer method, but it is expensive and time-consuming.

Fit-up problems in locating and bonding in the many pultrusion stringers, plus high parts count, are further detractions from this concept.

I-Beam Primary Structure - Secondary Side Panels (Figure 8)

The logic for this concept was that the tail boom configured as an I-beam, or more exactly a rotated H-beam, would be the optimum arrangement for a structure carrying high vertical and lateral bending loads. The secondary structure panels capable of carrying shears between intercostal frame segments would form an aerodynamic cover and carry the required access panels.

Upper and lower segments of urethane foam are bonded onto the basic section caps and have built-in tapering graphite channel members to afford added beam stiffness. These foam segments also effectively round off the section top and bottom for aesthetic and aerodynamic improvement.

The primary I-beam structure is made up in separate sandwich slabs comprising graphite type-A covers and Nomex core. The web and cap panels are then jointed to form the I-section by graphite pultruded angle members running longitudinally, which are bonded and mechanically attached. The vertical fin is constructed of graphite and is similar to that shown in Figure 2 except that the rear spar is configured as a one-piece banjo-type combined spar and tail-boom end bulkhead. The front spar ends at the intersection with tail-boom skin. The shell is notched locally, and heavy molded graphite angles running from the front spar caps protrude down into the boom and connect onto both the canted bulkhead and the web beam to form a strong front spar attachment to the tail boom.

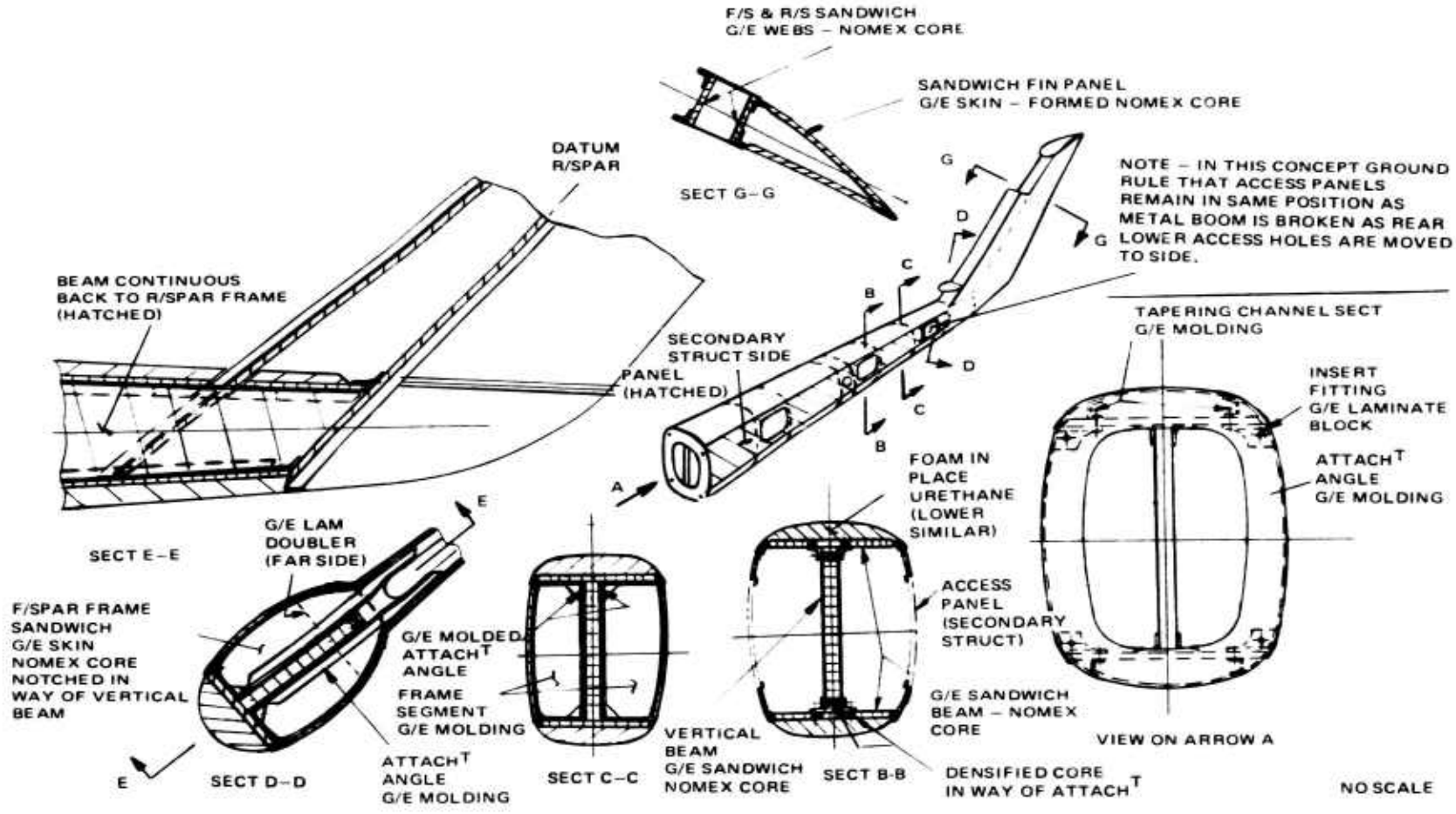

Figure 8. I-Beam Primary Structure-Secondary Side Panels.

Problems - The two rear underside access panels have to be repositioned onto the side due to configuration; this violates the ground rule that access panels remain at the existing AH-1G location. Secondary structure panels substantial enough to carry torsional shears and structures become heavy and inefficient. Also, there are problems with adequately supporting the elevator.

Integrally Molded Waffle Structure (Figure 9)

The tail boom in this configuration is made up of four main panel assemblies: upper, lower, left-hand, and right-hand. Each panel comprises graphite type-A covers bonded to graphite hat section pultrusion stringers. The frames are made by bonding graphite intercostals in line around the inner circumference and by adding a peripheral continuous unistrip around the inner surface to form frame cap continuity.

On assembly, the four panels are bonded along their longitudinal edges by a graphite joint strap. Local frame completion intercostals are then bonded in at four places, and an overlapping length of unicap strap is bonded across the inner frame positions to make the inner cap continuous all around. The canted bulkhead and front spar of the vertical fin are made in one graphite molding with notches to let stringers through. The remainder of the vertical stabilizer is as shown in Figure 2.

The forward and rear bulkheads are of sandwich construction in graphite type-A, and a substantial fingerplate doubler is bonded to the skin at the forward end to assist diffusion of loads into the four main attached fittings. The fittings are titanium and of the "bathtub" type, with a flange configuration to allow them to be mechanically attached to the stringer running on each side in addition to bonding.

Problems - The major detraction with this arrangement is the excessive number of parts which have to be carefully located and bonded together. The fitting of the frame intercostal segments requires that all stringers be accurately located along the total length of the tail boom. Secondary bonding of further intercostal frame inserts and cap continuity strips is another complication. This would not be a suitable design for quantity production methods.

PARAMETER EVALUATION

Table VII lists the four selected parameters, with a definition of the subjects each encompasses and the approved weighting factor.

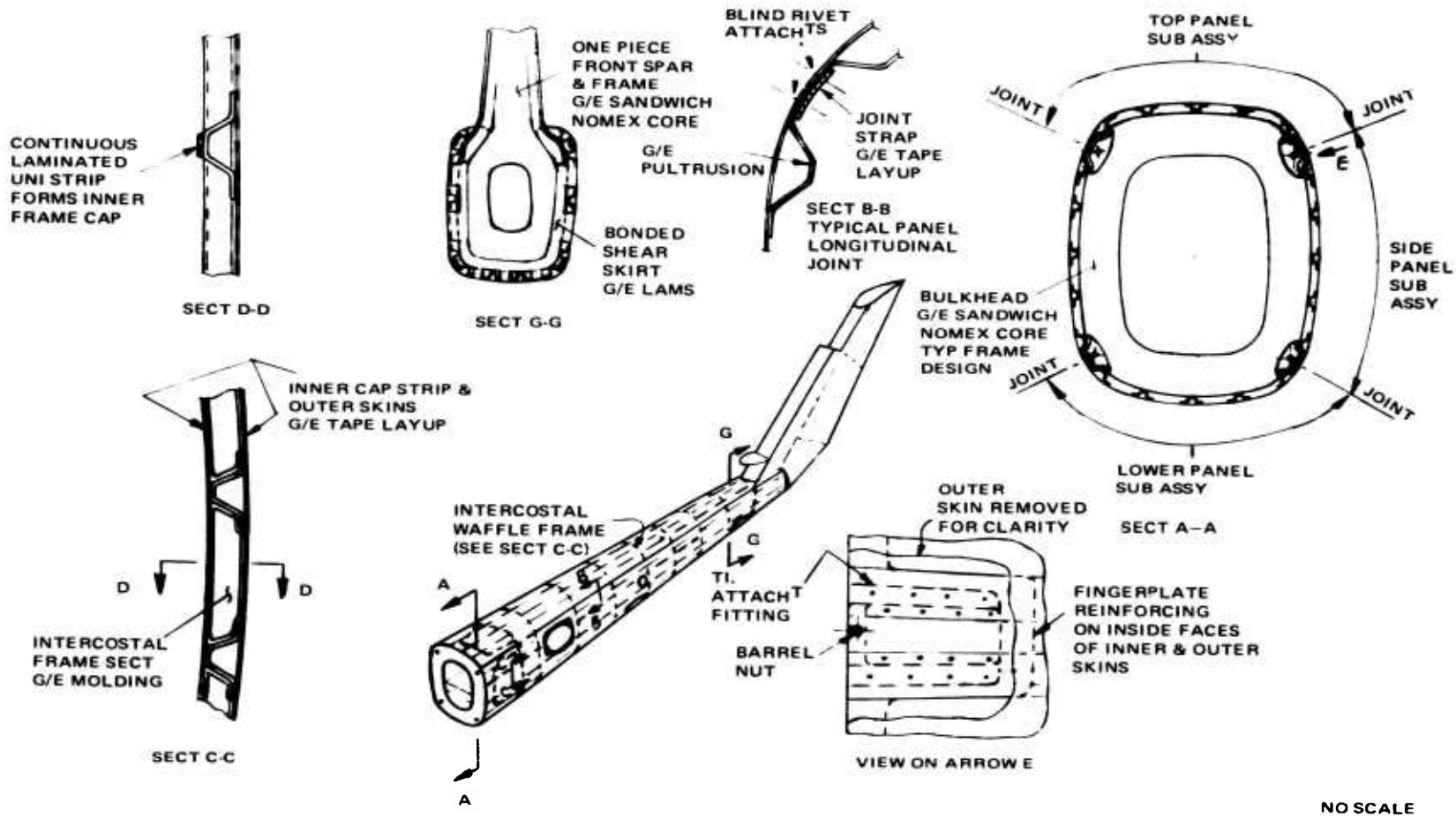

Figure 9. Integrally Molded Waffle Structure.

TABLE VII. COBRA COMPOSITE TAIL-BOOM PARAMETERS FOR PRELIMINARY DESIGN SELECTION

Parameter	Consideration	Weighting Factor
Safety and survivability	Fail-safe structure - gunfire and fatigue Damage tolerance - ballistic - operational - lightning strike - foreign object damage	5
Reliability and maintainability	Structural reliability Repairability Inspectability Interchangeability	4
Manufacturing cost	Nonrecurring costs - plant facilities required (autoclave, tape machines, etc.) - tooling costs - automated processes Recurring costs - ease of production - material cost - labor cost - quality control	2
Design factors	Technical risk Structural efficiency (weight, performance, strength, stiffness) Design simplicity Dynamic response (tuning) Safe life Environmental suitability Radar transparency	3

Table VIII shows the preliminary design selection. The format is arranged so as to appraise the preliminary design concepts against the four basic parameters.

A simple comparative lettering system was used for the rating process. The point value for each letter input was later calculated by applying a standard point value allocated to each letter (see Table VIII, top left-hand) and multiplying by the appropriate weighting factor (ratio) for each. This scoring arrangement ensured reasonable consistency between evaluators and enabled "implications" of the columns to be understood directly from Table VIII.

TABLE VIII. COBRA TAIL-BOOM (COMPOSITE) PRELIMINARY DESIGN SELECTION

Point Rating for Table
(+ or - May Be Added to Any Letter with + = Plus One Point and - = Minus One Point)

	Points
E = Excellent	(10)
VG = Very Good	(8)
G = Good	(6)
F = Fair	(4)
P = Poor	(2)

Ratio	Parameter	Fig. 2 Mandrel Lay-Up With Female Cure Mold	Fig. 3 Clam Shell	Fig. 4 GFW (Graphite Filament Wound)	Fig. 5 Thin Sandwich Shell With Longerons & Frames	Fig. 6 Integrally Molded Skin/Stringer Clamshell	Fig. 7 Monocoque Skin/ Stringer With Foam Core	Fig. 8 I-Beam Primary Structure Secondary Panels	Fig. 9 Integrally Molded Waffle Structure
		Monocoque Sandwich							
5	Fail Safety and Ballistic Tolerance	F	F	F	G	G	F		
4	Reliability and Maintainability	E	VG	E-	G-	F+	VG-	Cancelled	Cancelled
3	Design Factors	G+	G+	G+	F+	G	F-		
2	Manufacturing Costs	G	E	P-	F	P+	P		
	Point Total	91½	91½	80½	73½	72	64½		
	Concept Placings		1		2	3			

PRELIMINARY DESIGN CONCEPTS - REVISIONS

Evaluation of two of the concepts, shown in Figures 8 and 9, was terminated, since they would both obviously fall very low in the ratings and were considered to be unsuitable for this application. Two alternative concepts were added to the evaluation:

- Sandwich shell with rib supports (knitted composite square style sleeves)
- Sandwich shell with corrugated core

Both were found to be somewhat less than viable arrangements when all structural and material ramifications were evaluated. The knitted sleeve system suffered shortcomings because it was not feasible to taper the sleeve width going rearward on the tail-boom shell and still retain constant depth. Another drawback was the lack of desired laminate orientation, which is controlled by the geometry of the knit style, and also loss of basic strength due to weaving laminators out of plane.

The corrugated core system also could not be easily tapered and was found to be relatively inefficient and heavy when compared to other core systems which carried similar loads.

FINAL SCREENING SELECTION

SELECTION OF BEST THREE CONCEPTS BY SPECIALIST RATING

1. The evaluator representing each specific discipline (e.g.,Manufacturing, R&M, etc.) was requested to complete only the parameter line in which he was a specialist. Where more than two evaluators were available, a majority vote was used.

2. When tables were received from the various disciplines, each with one horizontal line of letter ratings, the letters were then converted to a point value.

3. The point value of each concept was then multiplied by the appropriate weighting factor (ratio), which appears in the left-hand column of Table VIII.

4. A master table was prepared which combined these weighted point values; one line from each discipline was used to make up a complete parameter tabulation of specialist evaluations.

5. The point total of each concept was then obtained by adding each column vertically.

6. The concept with the highest point total was the winner.

SELECTION RESULTS

Table VIII shows the final master chart point total for each concept, which indicates that the concepts shown in Figures 2 and 3 were tied for highest score, with the concept shown in Figure 4 having the next highest score. However, as all three were considered similar forms of a monocoque structure, it was decided that only one selection would be made from them.

Using this approach, the results were as follows:

Highest point total -

Figure 3 - Monocoque sandwich clamshell (91-1/2 points)

Second highest point total -

Figure 5 - Thin sandwich shell with longerons and frames (73-1/2 points)

Third highest point total -

Figure 6 - Integrally molded skin/stringer clamshell (72 points)

CONCLUSIONS OF PARAMETRIC STUDY

The winning concept came out clearly ahead of the second and third place concepts, which emerged close to each other in points total. From the various preliminary design trade-off studies based on parameters with weighting factors as outlined in Table VIII, it can be concluded that the most advantageous structural design for the Cobra AH-1G tail section when fabricated in advanced composite materials should be a semimonocoque sandwich clamshell tail boom with a sandwich construction integral fin using similar material. It is further concluded that a high-modulus-material, graphite type-A should be utilized for all primary structures, including skins, and that Nomex should be used as the honeycomb core. Secondary structures should be of a cheaper material, such as fiberglass with compatible resin system.

DESIGN DEVELOPMENT STUDIES

EVALUATION AND DESIGN CONSIDERATIONS FOR THE THREE SELECTED CONCEPTS

The three designs were refined to the extent that comparative values of weight, structural efficiency, material cost, maintenance, dynamic response, service-incurred damage, manufacturing cost, ballistic resistance, and structural service performance could be derived for the tail section.

The three structural arrangements were identified as follows:

Concept 1 - Monocoque sandwich clamshell (Figure 10) based on winning concept originally delineated in Figure 3.

Concept 2 - Thin sandwich shell with longerons and frames (Figure 11) based on the second-place concept originally delineated in Figure 5.

Concept 3 - Integrally molded skin/stringer clamshell (Figure 12) based on the third-place concept originally delineated in Figure 6.

At this stage, prior to commencing actual design and analysis, a comprehensive review of practical advanced composite materials suitable for tail-boom structural application was carried out. All aspects of the materials were investigated at this time, such as material physical properties, general characteristics, suitable adhesive systems, weight and cost, compatibility with other materials in hybrid arrangements, ballistic tolerance, low-energy impact qualities, and thermal and chemical stability.

During the evaluation and rating period, the supporting stress group was preparing material allowable data and conducting preliminary strength and stiffness checks of viable concepts and was also evaluating the existing Cobra AH-1G loads documents.

In conjunction with stress, the material system for each concept was confirmed or modified from that shown on the preliminary drawings, and a tentative adhesive and cure cycle plan evolved.

Table IX lists the advanced composite materials evaluated together with some pertinent comments.

Figure 13 shows strength and modulus of type-A graphite compared to other grade graphite and composite materials.

Also at this time an overall review of honeycomb cores was made, and latest developments and fabricating techniques pertaining to Nomex core were discussed with the suppliers. These investigations subsequently confirmed Boeing's intention to use Nomex honeycomb core in all tail section sandwich applications. The advantages of the Nomex core are as follows:

- Nomex made in designation HRH10 is a high-temperature nylon fiber/phenolic resin honeycomb; and being plastic rather than metal, it is not subject to corrosion, which is a serious problem with metal honeycomb core systems.

- Tail-boom shell and fin torque box and trailing-edge shear loads are not particularly high, and Nomex HRH10, despite its low shear modulus, is suitable for this application.

- Nomex is a more flexible material to handle and form than metal honeycomb. By heating in an oven up to 600°F, it may be readily draped into various straight-line element configurations.

- Nomex and graphite are compatible materials forming a chemically inert system.

- Nomex is readily bonded to graphite material using tried and tested epoxy adhesive systems, affording excellent bond strength and durability.

- This core has demonstrated excellent capability to provide greater tolerances, in that local yielding occurs instead of core crippling as occurs in aluminum core when tolerances are slightly oversize.

- Nomex core demonstrated resilience to impact and does not crush locally as does aluminum core when indented by impact.

The basic objectives for all concepts are stated below:

- Match Cobra stiffness requirements.

- Do not exceed existing (metal) Cobra tail section weight.

- Match all existing Cobra interface points without compromising composite structural efficiency.

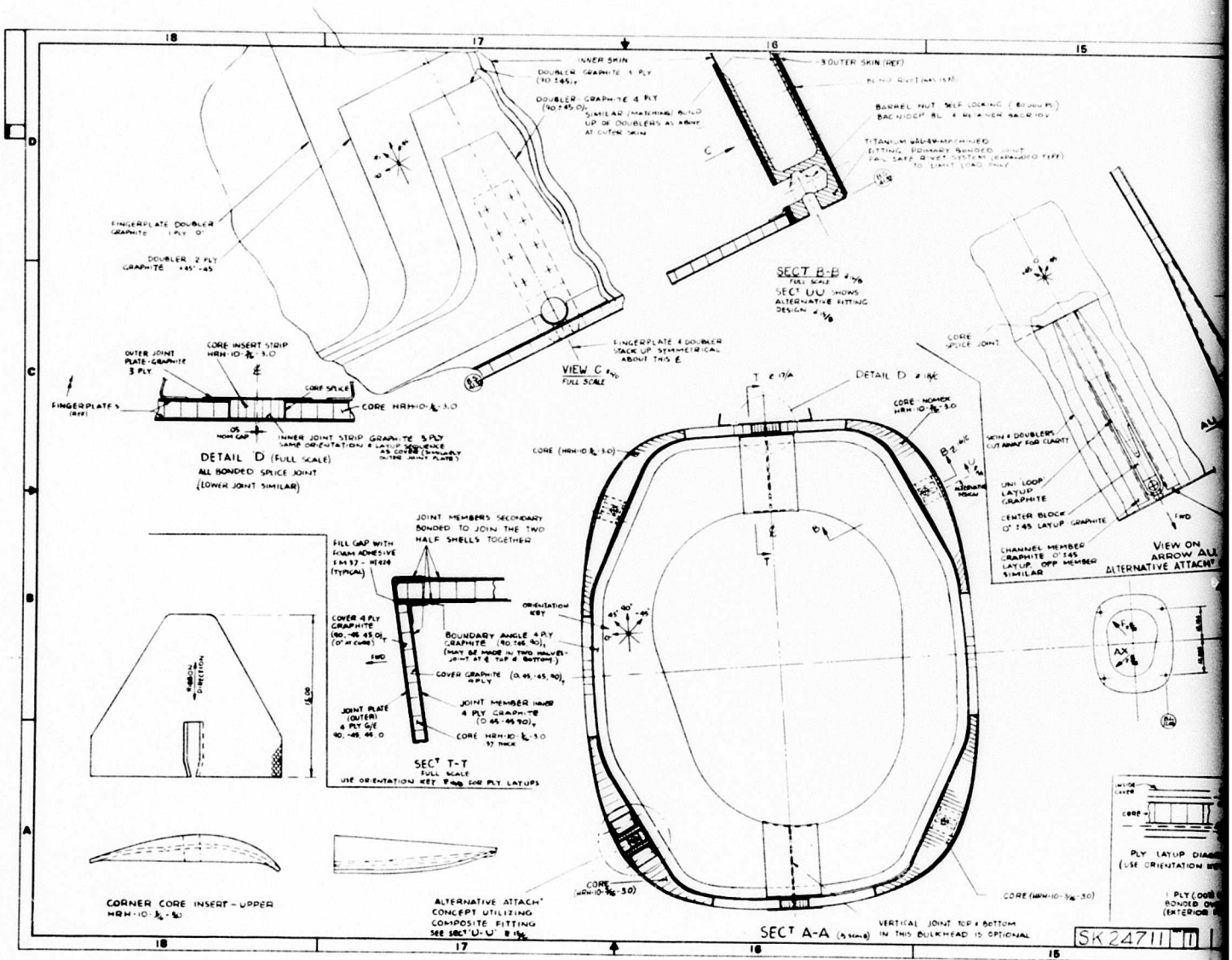

Figure 10. Concept 1 Monocoque-Sandwich Clamshell.

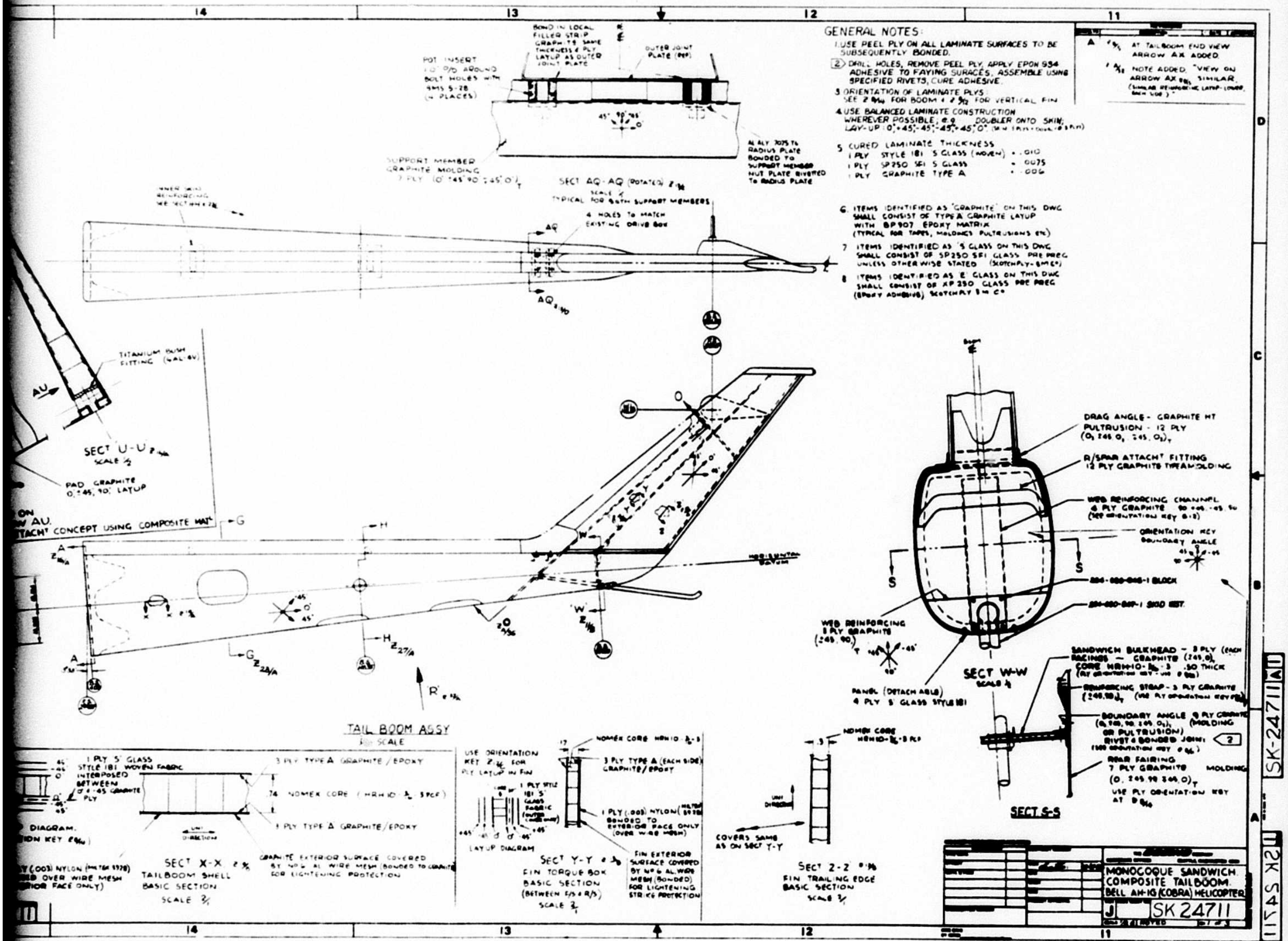
GENERAL NOTES:
1. USE PEEL PLY ON ALL LAMINATE SURFACES TO BE SUBSEQUENTLY BONDED.
2 DRILL HOLES, REMOVE PEEL PLY, APPLY EPON 934 ADHESIVE TO FAYING SURFACES, ASSEMBLE USING SPECIFIED RIVETS, CURE ADHESIVE.
3 ORIENTATION OF LAMINATE PLYS: SEE FOR BOOM & FOR VERTICAL FIN
4 USE BALANCED LAMINATE CONSTRUCTION WHEREVER POSSIBLE, e.g. DOUBLER ONTO SKIN; LAY-UP: 0°, +45°, -45°, -45°, +45°, 0°
5 CURED LAMINATE THICKNESS
1 PLY STYLE 181 S GLASS (WOVEN) = .010
1 PLY SP250 SF1 S GLASS = .0075
1 PLY GRAPHITE TYPE A = .006
6. ITEMS IDENTIFIED AS 'GRAPHITE' ON THIS DWG SHALL CONSIST OF TYPE A GRAPHITE LAYUP WITH BP907 EPOXY MATRIX (TYPICAL FOR TAPES, MOLDINGS PULTRUSIONS ETC)
7 ITEMS IDENTIFIED AS 'S GLASS' ON THIS DWG SHALL CONSIST OF SP250 SF1 GLASS PRE PREG UNLESS OTHERWISE STATED (SCOTCHPLY-3M Co)
8 ITEMS IDENTIFIED AS 'E' GLASS ON THIS DWG SHALL CONSIST OF XP250 GLASS PRE PREG (EPOXY ADHESIVE) SCOTCHPLY 3M Co
A AT TAILBOOM END VIEW ARROW AX ADDED.
NOTE ADDED. "VIEW ON ARROW AX SIMILAR."
SECT AQ-AQ (ROTATED)
TYPICAL FOR BOTH SUPPORT MEMBERS
4 HOLES TO MATCH EXISTING DRIVE BOX
SECT U-U
PAD GRAPHITE 0, ±45, 90, LATUP
TITANIUM BUSH FITTING
ATTACH CONCEPT USING COMPOSITE HAT
TAIL BOOM ASSY
DRAG ANGLE - GRAPHITE HT PULTRUSION - 12 PLY
R/SPAR ATTACH FITTING 12 PLY GRAPHITE TYPE A MOLDING
WEB REINFORCING CHANNEL 4 PLY GRAPHITE
ORIENTATION KEY BOUNDARY ANGLE
WEB REINFORCING 3 PLY GRAPHITE
PANEL (DETACHABLE) 4 PLY S GLASS STYLE 181
SECT W-W
SANDWICH BULKHEAD - 3 PLY (EACH FACINGS) - GRAPHITE
REINFORCING STRAP - 3 PLY GRAPHITE
BOUNDARY ANGLE 9 PLY GRAPHITE (MOLDING OR PULTRUSION)
RIVET & BONDED JOINT
REAR FAIRING 7 PLY GRAPHITE MOLDING
USE PLY ORIENTATION KEY
SECT S-S
SECT X-X
TAILBOOM SHELL BASIC SECTION
3 PLY TYPE A GRAPHITE/EPOXY
NOMEX CORE (HRH10 3/16 3PCF)
GRAPHITE EXTERIOR SURFACE COVERED BY NO. 6 AL. WIRE MESH (BONDED TO GRAPHITE) FOR LIGHTENING PROTECTION
SECT Y-Y
FIN TORQUE BOX BASIC SECTION (BETWEEN F/S & R/S)
LAYUP DIAGRAM
FIN EXTERIOR SURFACE COVERED BY NO. 6 AL. WIRE MESH (BONDED) FOR LIGHTENING STRIKE PROTECTION
COVERS SAME AS ON SECT Y-Y
SECT Z-Z
FIN TRAILING EDGE BASIC SECTION
MONOCOQUE SANDWICH COMPOSITE TAILBOOM. BELL AH-1G (COBRA) HELICOPTER
J
SK 24711

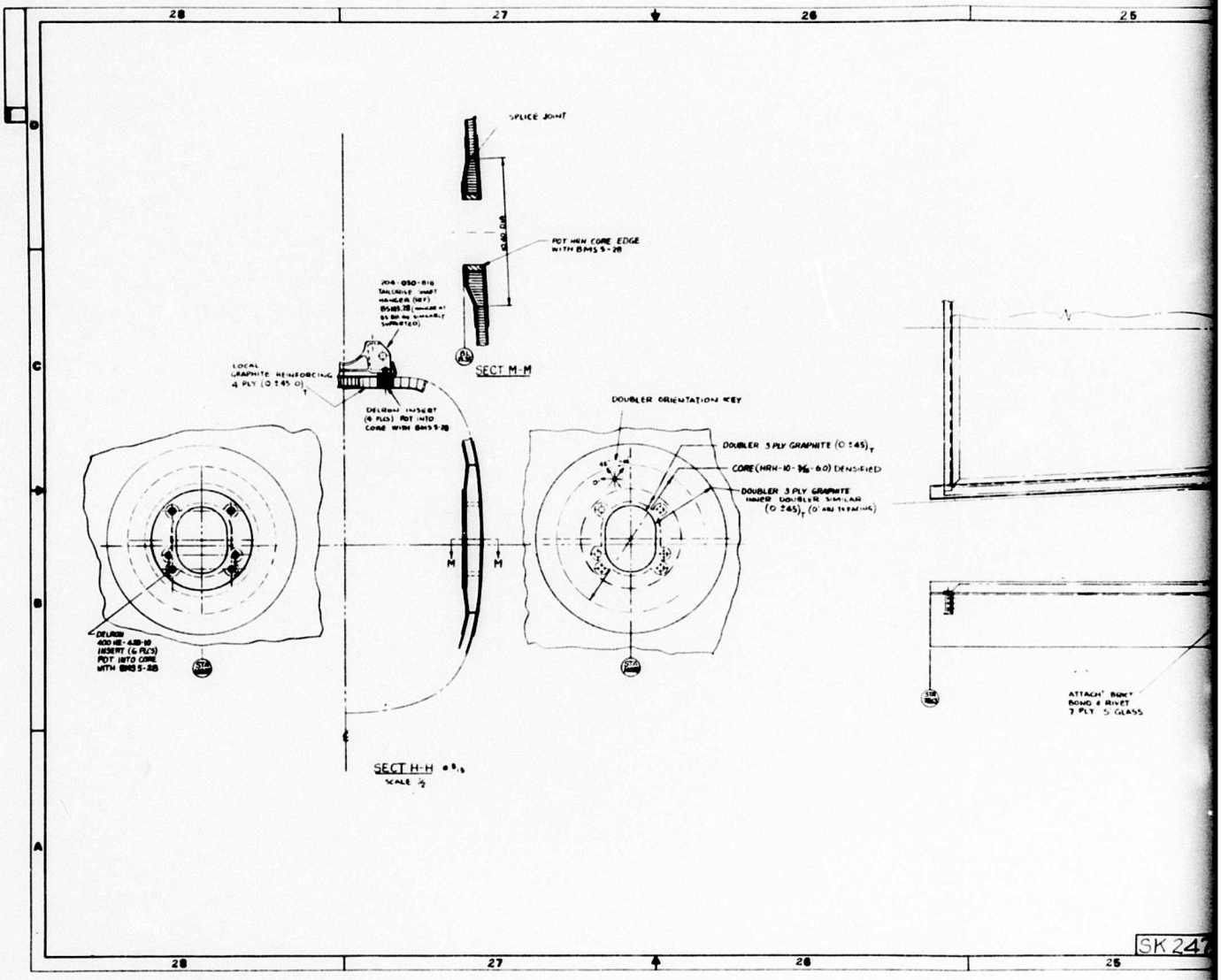

Preceding page blank

Figure 10. Continued.

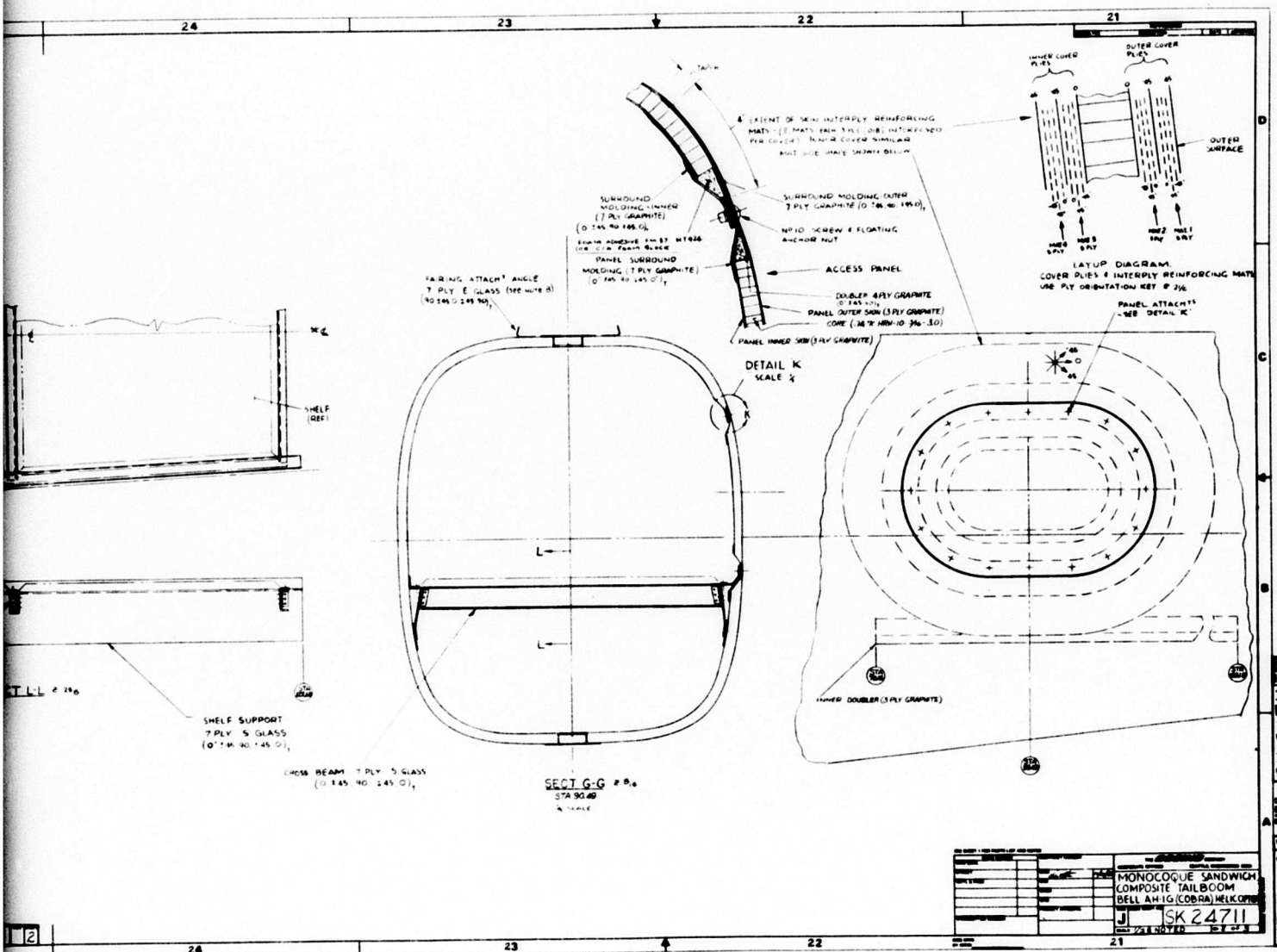
24
23
22
21
SURROUND MOLDING-INNER (7 PLY GRAPHITE)
PANEL SURROUND MOLDING (7 PLY GRAPHITE)
SURROUND MOLDING-OUTER 7 PLY GRAPHITE
NP10 SCREW & FLOATING ANCHOR NUT
ACCESS PANEL
DOUBLER 4 PLY GRAPHITE
PANEL OUTER SKIN (3 PLY GRAPHITE)
CORE (.78"P HRH-10 3/16-3.0)
PANEL INNER SKIN (3 PLY GRAPHITE)
FAIRING ATTACH ANGLE 7 PLY E GLASS (SEE NOTE 8)
DETAIL K
SCALE X
PANEL ATTACH — SEE DETAIL K
INNER COVER PLIES
OUTER COVER PLIES
OUTER SURFACE
LAYUP DIAGRAM
COVER PLIES & INTERPLY REINFORCING MATL
USE PLY ORIENTATION KEY P 2/6
INNER DOUBLER (3 PLY GRAPHITE)
SHELF (REF)
SHELF SUPPORT 7 PLY S GLASS
CROSS BEAM 7 PLY S GLASS
SECT G-G
STA 90.49
MONOCOQUE SANDWICH COMPOSITE TAILBOOM
BELL AH-1G (COBRA) HELICOPTER
SK 24711
SK24711

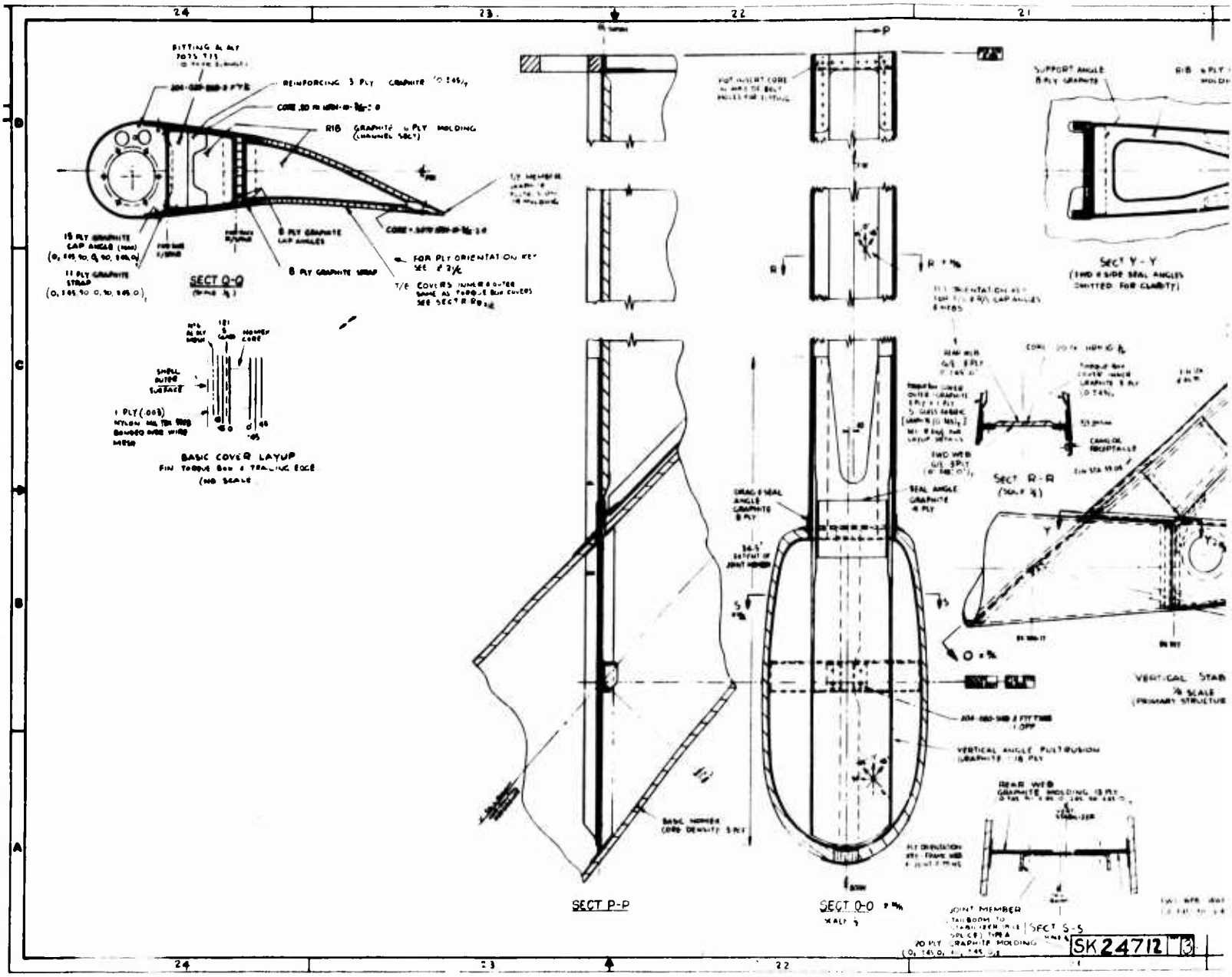

Preceding page blank

Figure 10. Continued.

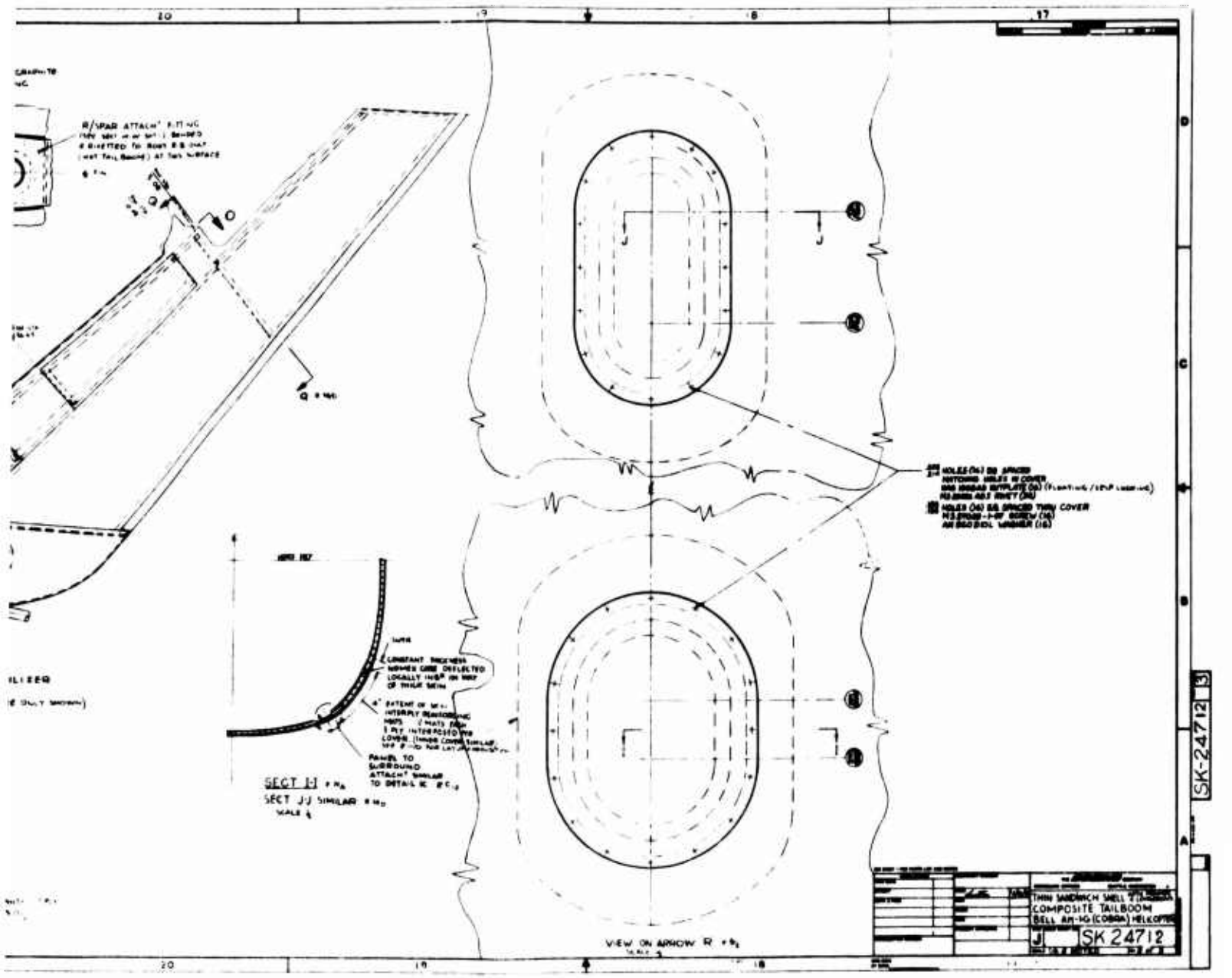
SECT J-J
SECT JJ SIMILAR
VIEW ON ARROW R
THIN SANDWICH SHELL
COMPOSITE TAILBOOM
BELL AH-1G (COBRA) HELICOPTER
J
SK 24712
SK-24712

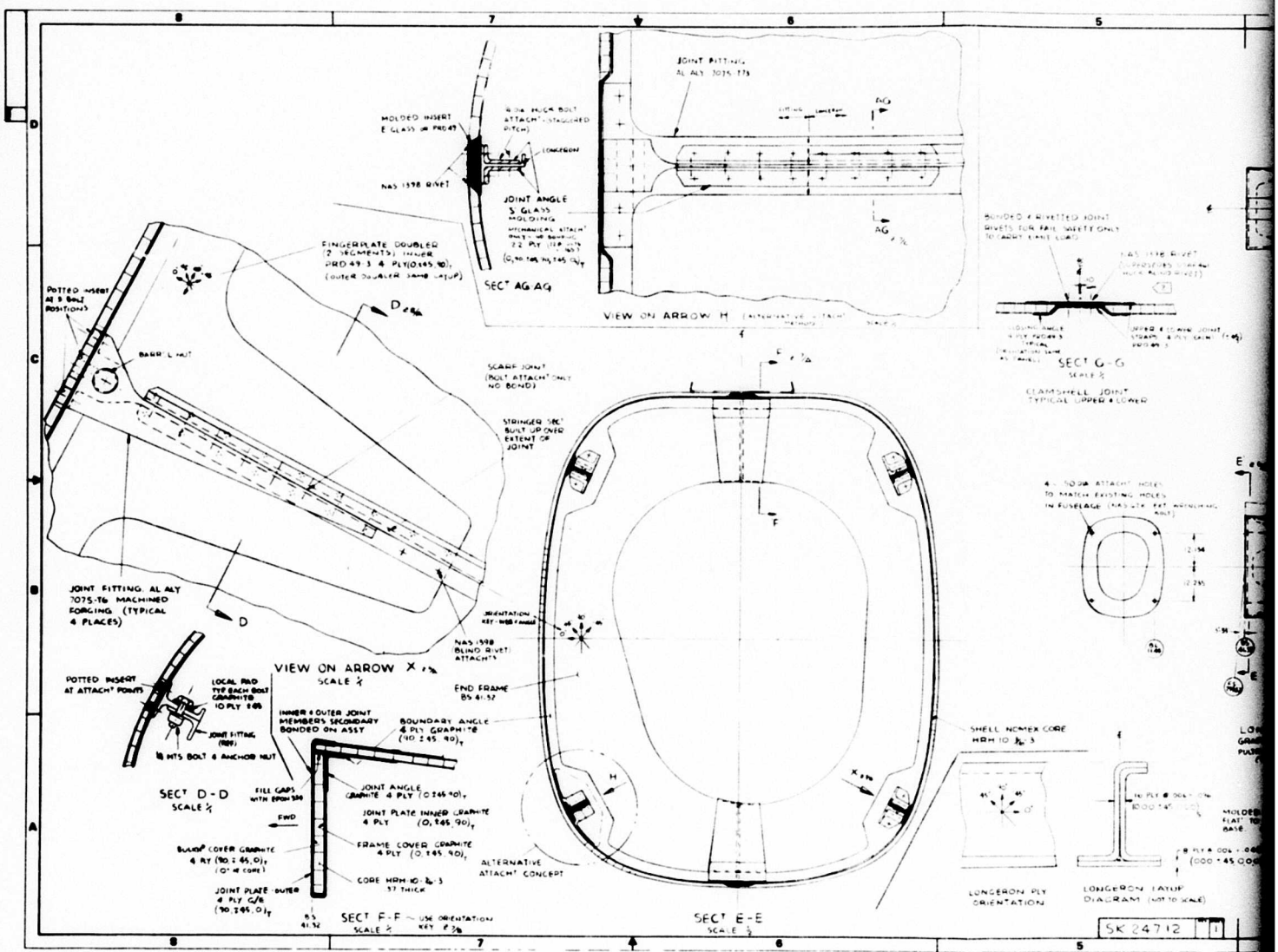

Preceding page blank

Figure 11. Concept 2 Thin Sandwich Shell With Longerons and Frames.

GENERAL NOTES

1. USE PEEL PLY ON ALL LAMINATE SURFACES TO BE SUBSEQUENTLY BONDED
2. PLY ORIENTATION — 0° IS PARALLEL TO AXIS OF BOOM
3. USE BALANCED LAMINATE LAYUP AS NOTATED IN MATERIAL CALL UP
4. ITEMS IDENTIFIED AS GRAPHITE ON THIS DWG SHALL CONSIST OF TYPE A GRAPHITE LAMINATES WITH BP907 EPOXY MATRIX (G/E)
5. ITEMS IDENTIFIED AS PRD49-3 ON THIS DWG SHALL CONSIST OF PRD49-3 LAMINATES WITH BP907 EPOXY MATRIX
6. ITEMS IDENTIFIED AS 'S' GLASS SHALL CONSIST OF XP250 GLASS PRE PREG (EPOXY)

PLAN VIEW
SCALE 1/10

SECT A-A
SCALE 1/2

SECT B-B
SCALE 1/2

SECT C-C
SCALE 1/2

SECT U-U
SCALE 1/2

TYPICAL SHELL LAYUP & MASTER STRINGER ARRANGEMENT

			THIN SANDWICH SHELL & LONGERON COMPOSITE TAILBOOM BELL AH1G COBRA HELICOPTER
			J SK 24712

SK 24712

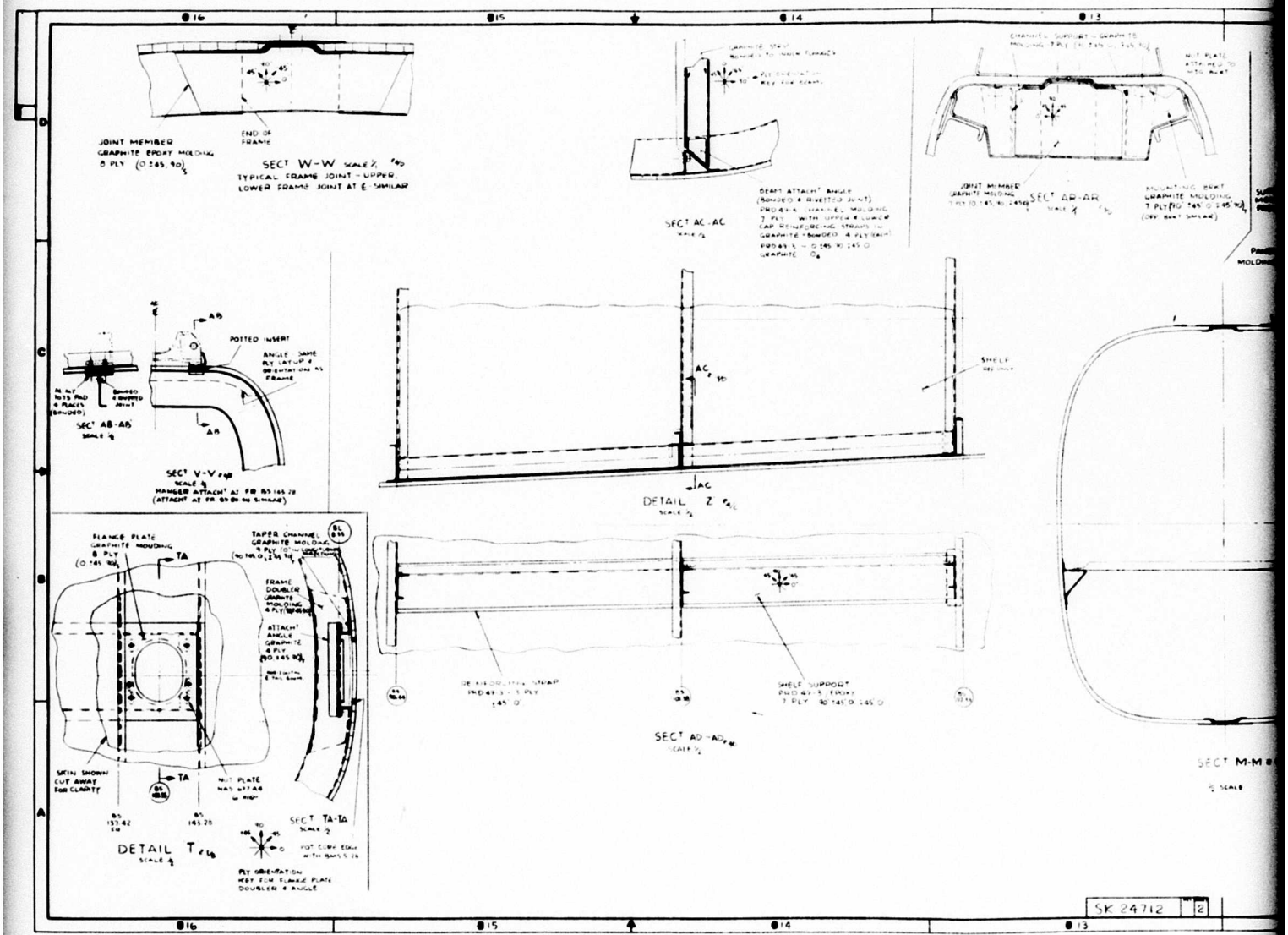

Preceding page blank

Figure 11. Continued.

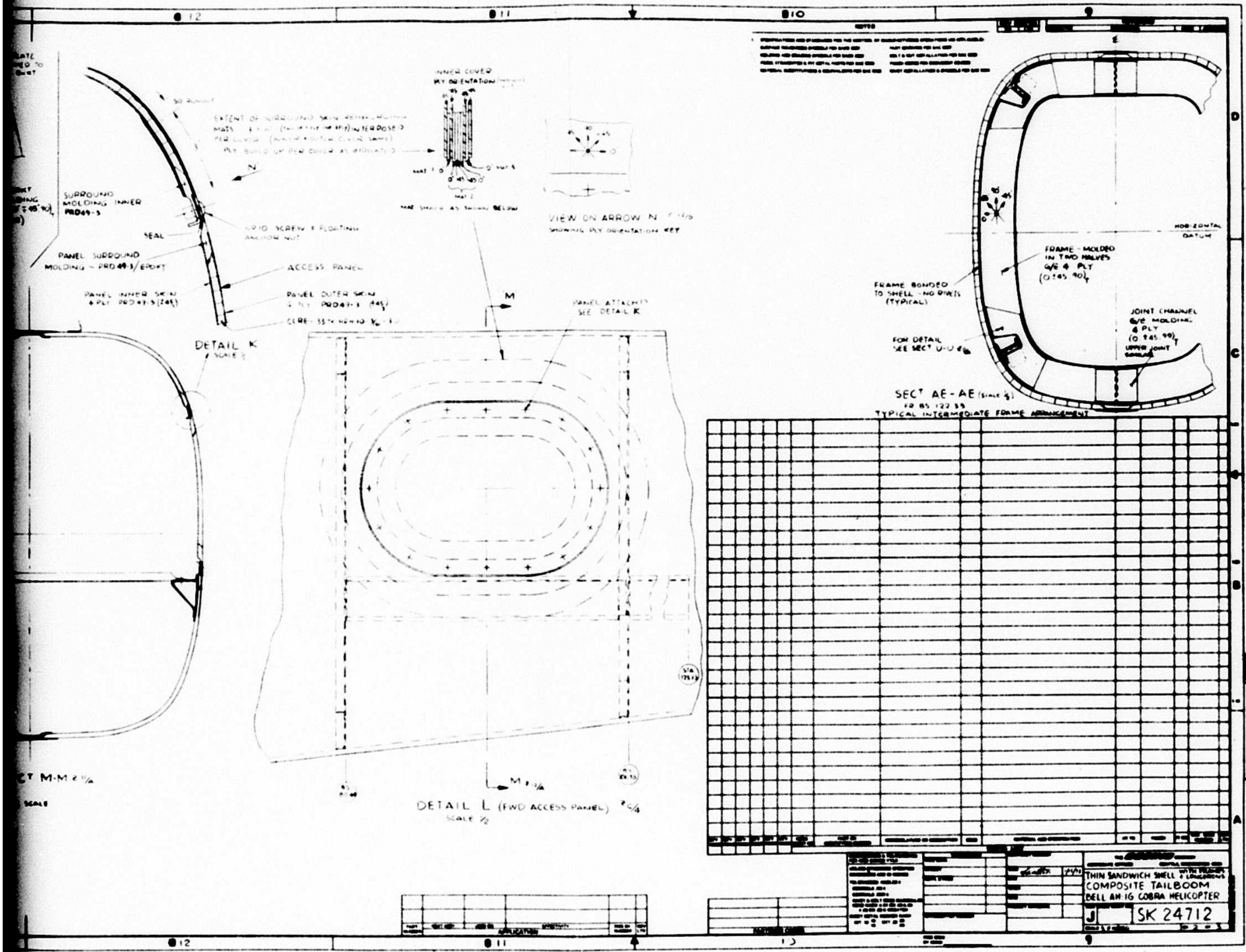
SURROUND MOLDING INNER PRD49-3
SEAL
PANEL SURROUND MOLDING ~ PRD49-3/EPOXY
PANEL INNER SKIN
ACCESS PANEL
PANEL OUTER SKIN
DETAIL K
INNER COVER
VIEW ON ARROW N
SHOWING PLY ORIENTATION KEY
PANEL ATTACH
SEE DETAIL K
DETAIL L (FWD ACCESS PANEL)
SCALE 1/2
FRAME - MOLDED IN TWO HALVES G/E 4 PLY
FRAME BONDED TO SHELL - NO RIVETS (TYPICAL)
FOR DETAIL SEE SECT U-U
JOINT CHANNEL G/E MOLDING 4 PLY
UPPER JOINT
HORIZONTAL DATUM
SECT AE-AE
TYPICAL INTERMEDIATE FRAME ARRANGEMENT
THIN SANDWICH SHELL
COMPOSITE TAILBOOM
BELL AH-1G COBRA HELICOPTER
SK 24712

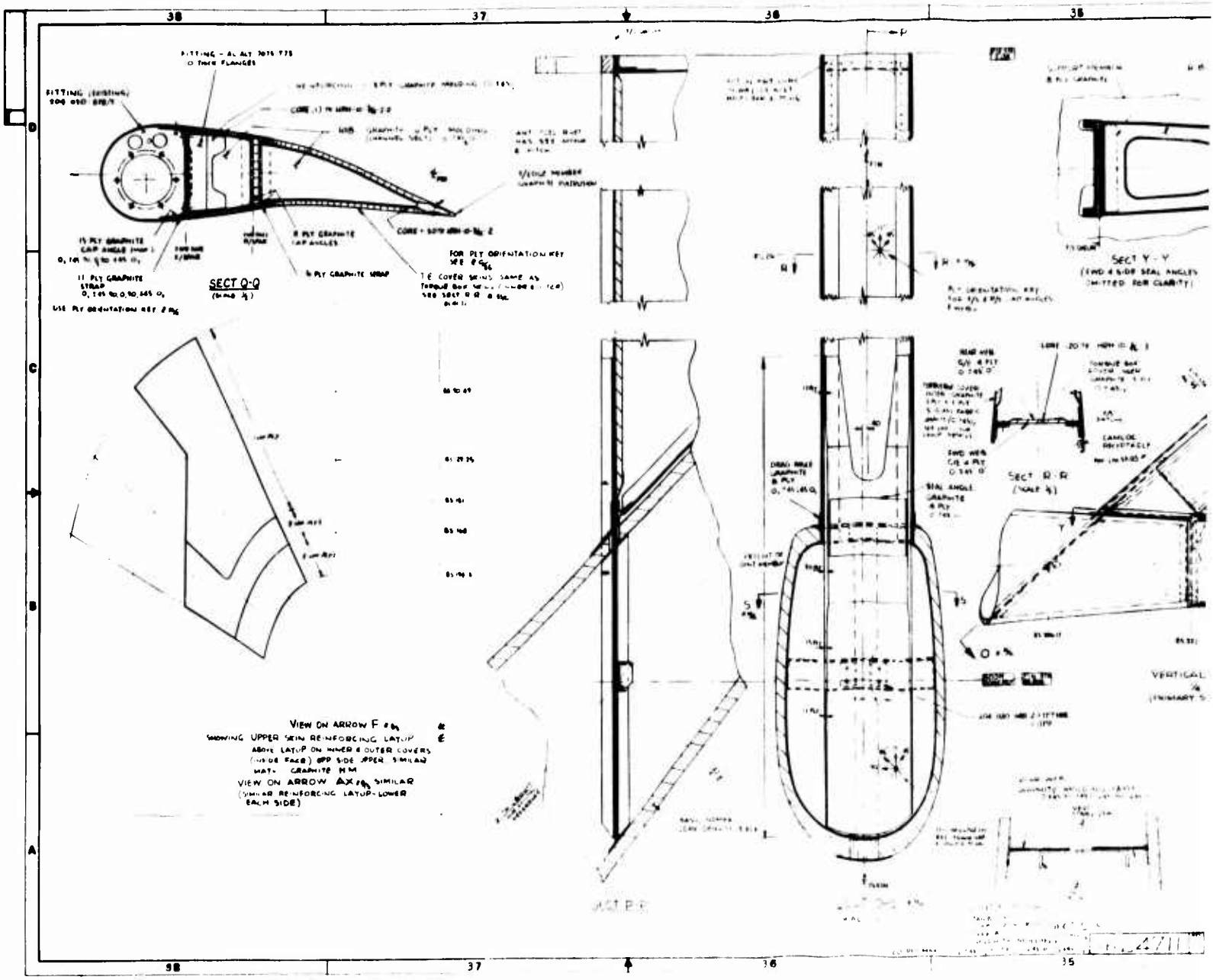

Preceding page blank

Figure 11. Continued.

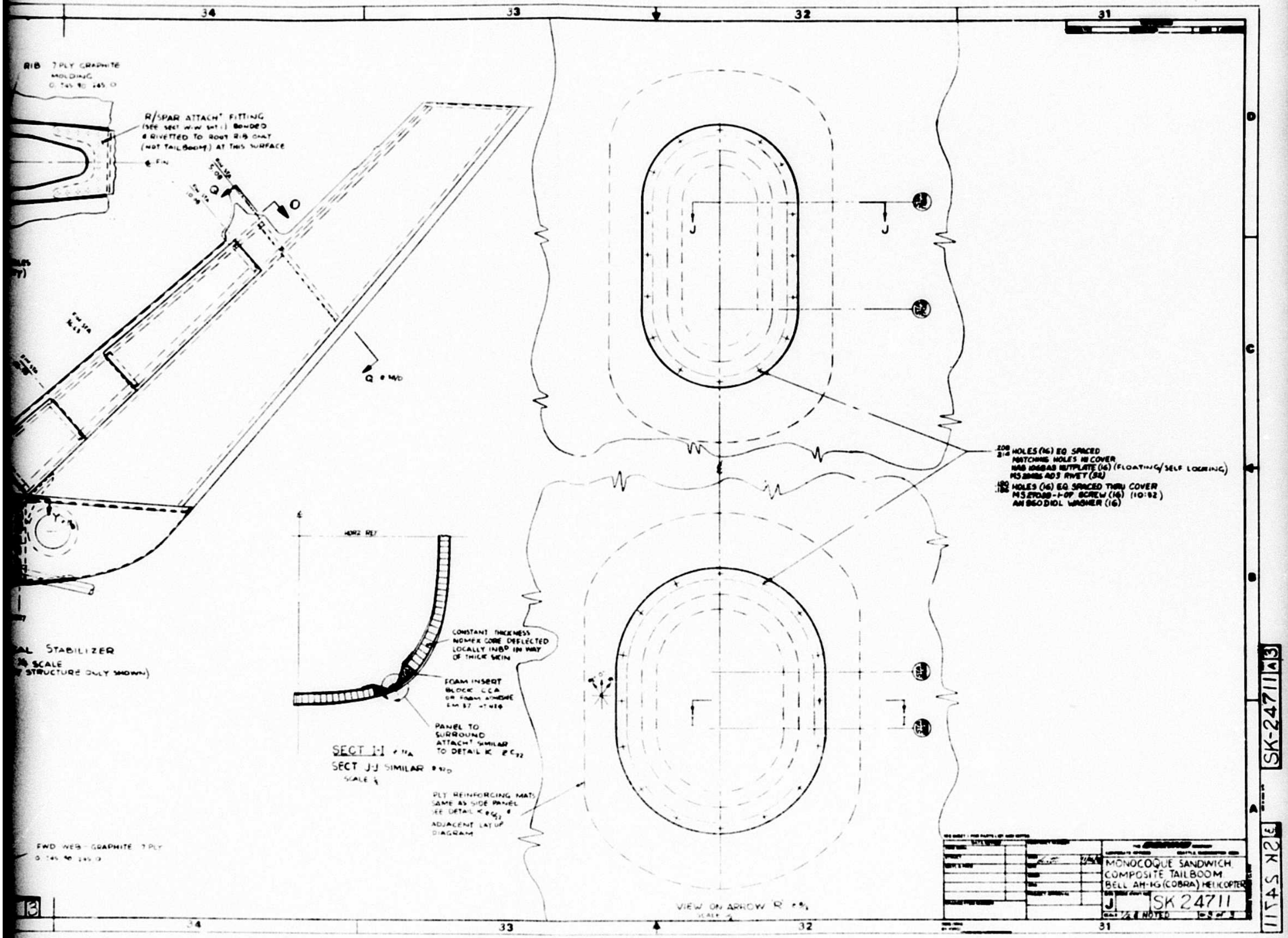

RIB 7 PLY GRAPHITE MOLDING
R/SPAR ATTACH' FITTING (SEE SECT W-W SHT 1) BONDED & RIVETTED TO ROOT RIB ONLY (NOT TAILBOOM) AT THIS SURFACE
STABILIZER
STRUCTURE ONLY SHOWN
CONSTANT THICKNESS NOMEX CORE DEFLECTED LOCALLY INBD IN WAY OF THICK SKIN
FOAM INSERT
PANEL TO SURROUND ATTACH' SIMILAR TO DETAIL K
SECT I-I
SECT J-J SIMILAR
PLY REINFORCING MATS SAME AS SIDE PANEL SEE DETAIL K
ADJACENT LAYUP DIAGRAM
FWD WEB - GRAPHITE 7 PLY
HOLES (16) EQ SPACED MATCHING HOLES IN COVER
HOLES (16) EQ SPACED THRU COVER
AN960D10L WASHER (16)
VIEW ON ARROW 'R'
MONOCOQUE SANDWICH COMPOSITE TAILBOOM BELL AH-1G (COBRA) HELICOPTER
SK 24711
SK-24711

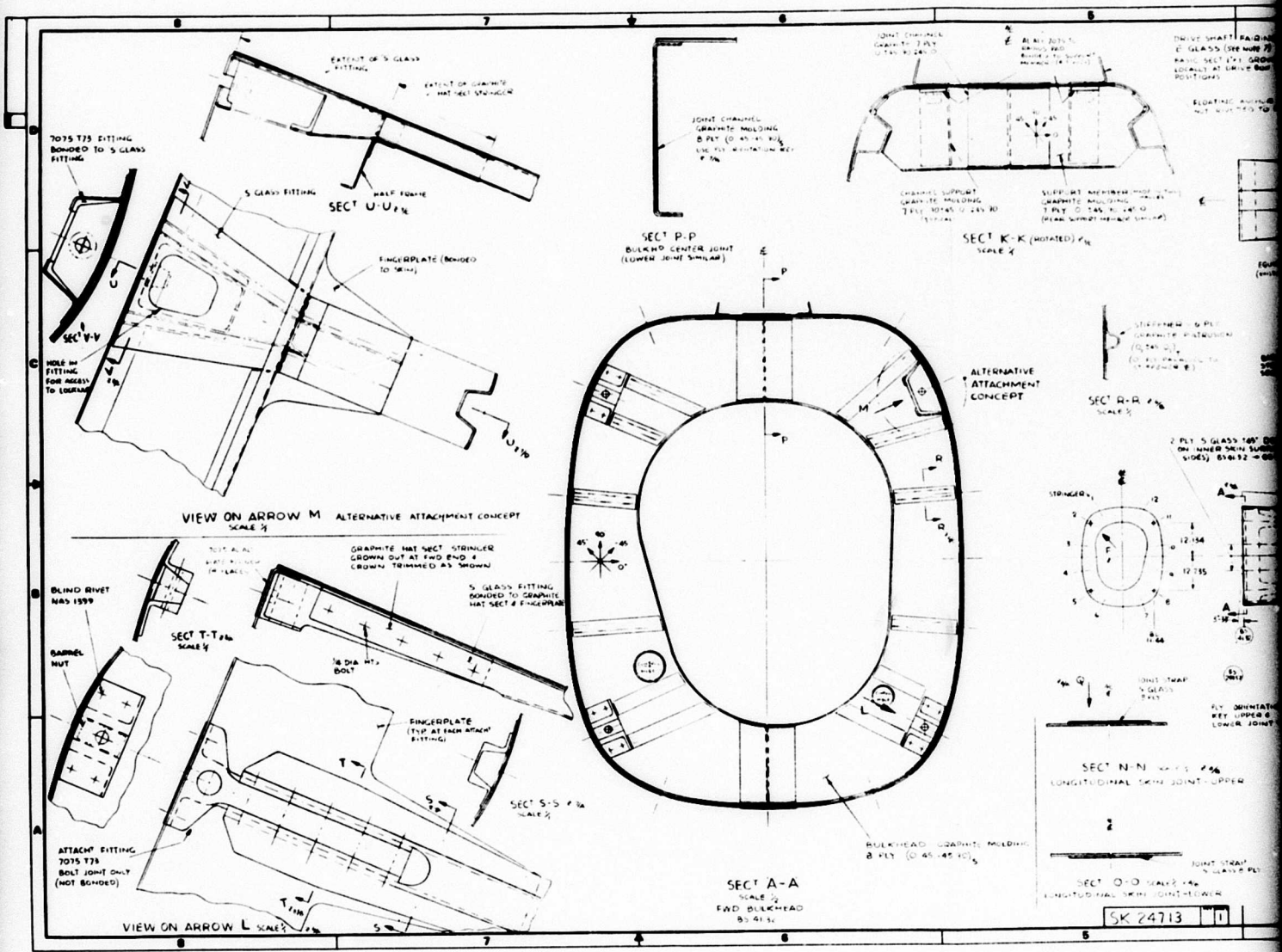

Figure 12. Concept 3 Integrally Molded Skin/Stringer Clamshell.

Preceding page blank

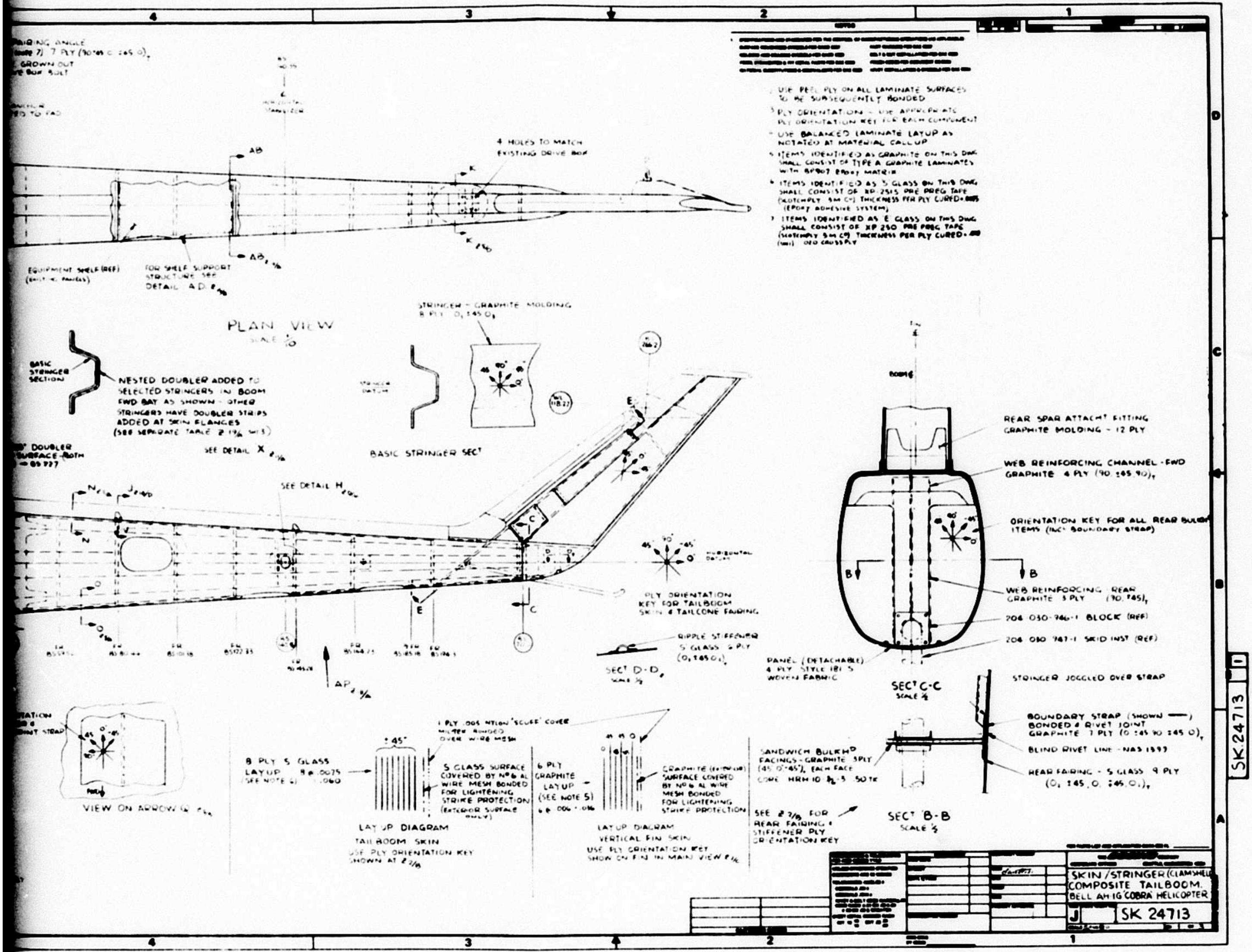

USE PEEL PLY ON ALL LAMINATE SURFACES TO BE SUBSEQUENTLY BONDED
PLY ORIENTATION - USE APPROPRIATE PLY ORIENTATION KEY FOR EACH COMPONENT
USE BALANCED LAMINATE LAYUP AS NOTATED AT MATERIAL CALLUP
ITEMS IDENTIFIED AS GRAPHITE ON THIS DWG SHALL CONSIST OF TYPE A GRAPHITE LAMINATES WITH BP907 EPOXY MATRIX
ITEMS IDENTIFIED AS S GLASS ON THIS DWG SHALL CONSIST OF XP 251S PRE PREG TAPE (SCOTCHPLY 3M CO) THICKNESS PER PLY CURED
ITEMS IDENTIFIED AS E GLASS ON THIS DWG SHALL CONSIST OF XP 250 PRE PREG TAPE (SCOTCHPLY 3M CO) THICKNESS PER PLY CURED
4 HOLES TO MATCH EXISTING DRIVE BOX
EQUIPMENT SHELF (REF)
FOR SHELF SUPPORT STRUCTURE SEE DETAIL AD
PLAN VIEW
STRINGER - GRAPHITE MOLDING 8 PLY (0, ±45 0)
BASIC STRINGER SECTION
NESTED DOUBLER ADDED TO SELECTED STRINGERS IN BOOM FWD BAY AS SHOWN - OTHER STRINGERS HAVE DOUBLER STRIPS ADDED AT SKIN FLANGES (SEE SEPARATE TABLE)
BASIC STRINGER SECT
SEE DETAIL X
SEE DETAIL H
PLY ORIENTATION KEY FOR TAILBOOM SKIN & TAILCONE FAIRING
RIPPLE STIFFENER S GLASS 6 PLY (0, ±45 0)
SECT D-D
REAR SPAR ATTACH FITTING GRAPHITE MOLDING - 12 PLY
WEB REINFORCING CHANNEL - FWD GRAPHITE 4 PLY (90, ±45, 90)
ORIENTATION KEY FOR ALL REAR BULKD ITEMS (INC BOUNDARY STRAP)
WEB REINFORCING - REAR GRAPHITE 3 PLY (90, ±45)
204 030 946-1 BLOCK (REF)
204 030 947-1 SKID INST (REF)
PANEL (DETACHABLE) 4 PLY STYLE 181 S WOVEN FABRIC
SECT C-C
STRINGER JOGGLED OVER STRAP
BOUNDARY STRAP (SHOWN) BONDED & RIVET JOINT GRAPHITE 7 PLY (0, ±45, 90, ±45, 0)
BLIND RIVET LINE - NAS 1397
REAR FAIRING - S GLASS 9 PLY (0, ±45, 0, ±45, 0)
SANDWICH BULKHD FACINGS - GRAPHITE 3 PLY (45, 0, -45), EACH FACE CORE HRH 10
SEE 2/6 FOR REAR FAIRING & STIFFENER PLY ORIENTATION KEY
SECT B-B
VIEW ON ARROW
8 PLY S GLASS LAYUP (SEE NOTE 6)
1 PLY .005 NYLON 'SCUFF' COVER
S GLASS SURFACE COVERED BY No 6 AL WIRE MESH BONDED FOR LIGHTENING STRIKE PROTECTION (EXTERIOR SURFACE ONLY)
LAY UP DIAGRAM TAILBOOM SKIN
USE PLY ORIENTATION KEY SHOWN AT 2/6
6 PLY GRAPHITE LAYUP (SEE NOTE 5)
GRAPHITE (EXTERIOR) SURFACE COVERED BY No 6 AL WIRE MESH BONDED FOR LIGHTENING STRIKE PROTECTION
LAY UP DIAGRAM VERTICAL FIN SKIN
USE PLY ORIENTATION KEY SHOWN ON FIN IN MAIN VIEW
SKIN/STRINGER (CLAMSHELL) COMPOSITE TAILBOOM. BELL AH-1G 'COBRA' HELICOPTER
SK 24713

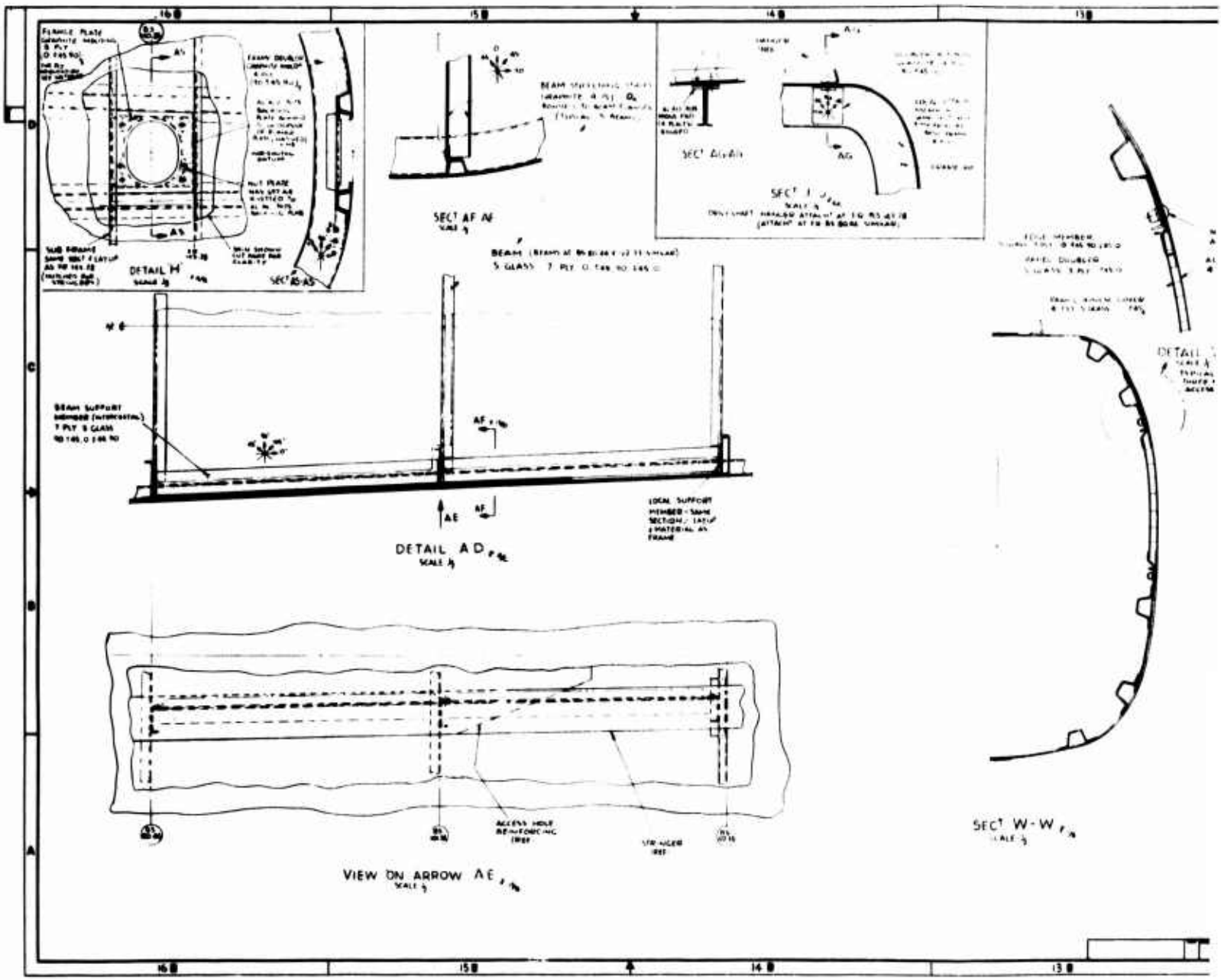

Figure 12. Continued.

Preceding page blank

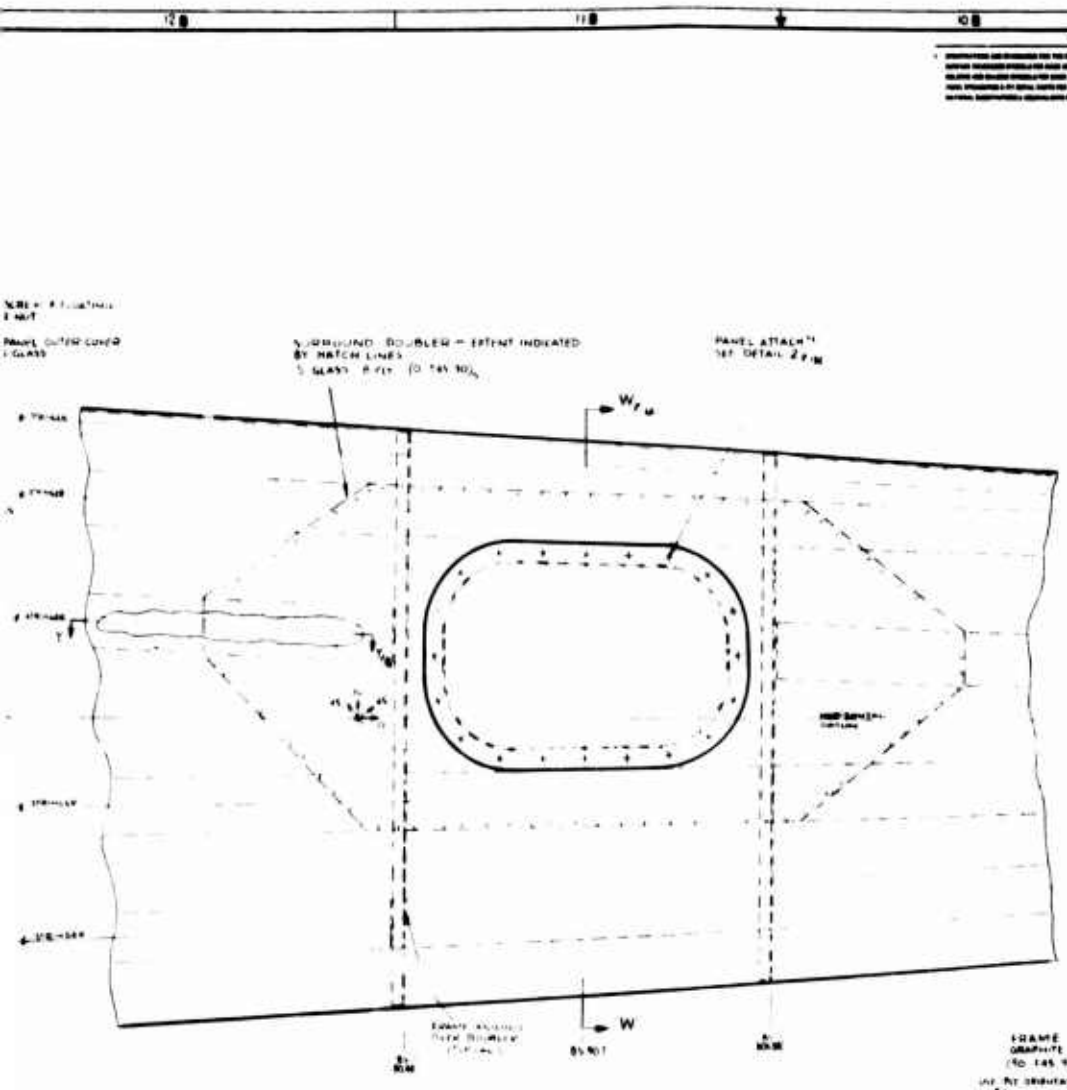

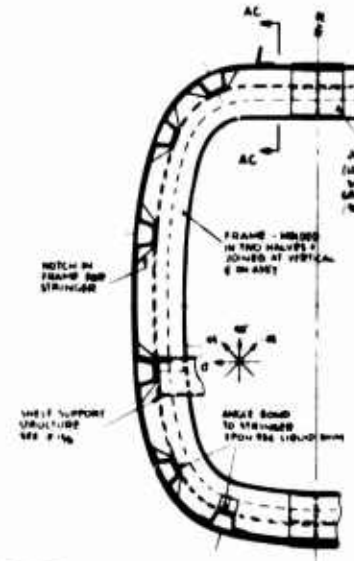

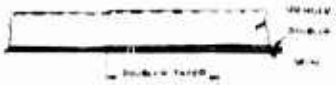

SECT AB - AB

SECT AC - AC

SECT Y - Y

DETAIL X

SKIN STRINGER (CLAMSHELL) COMPOSITE TAILBOOM, BELL AH-1G COBRA HELICOPTER

J SK24713

SK24713

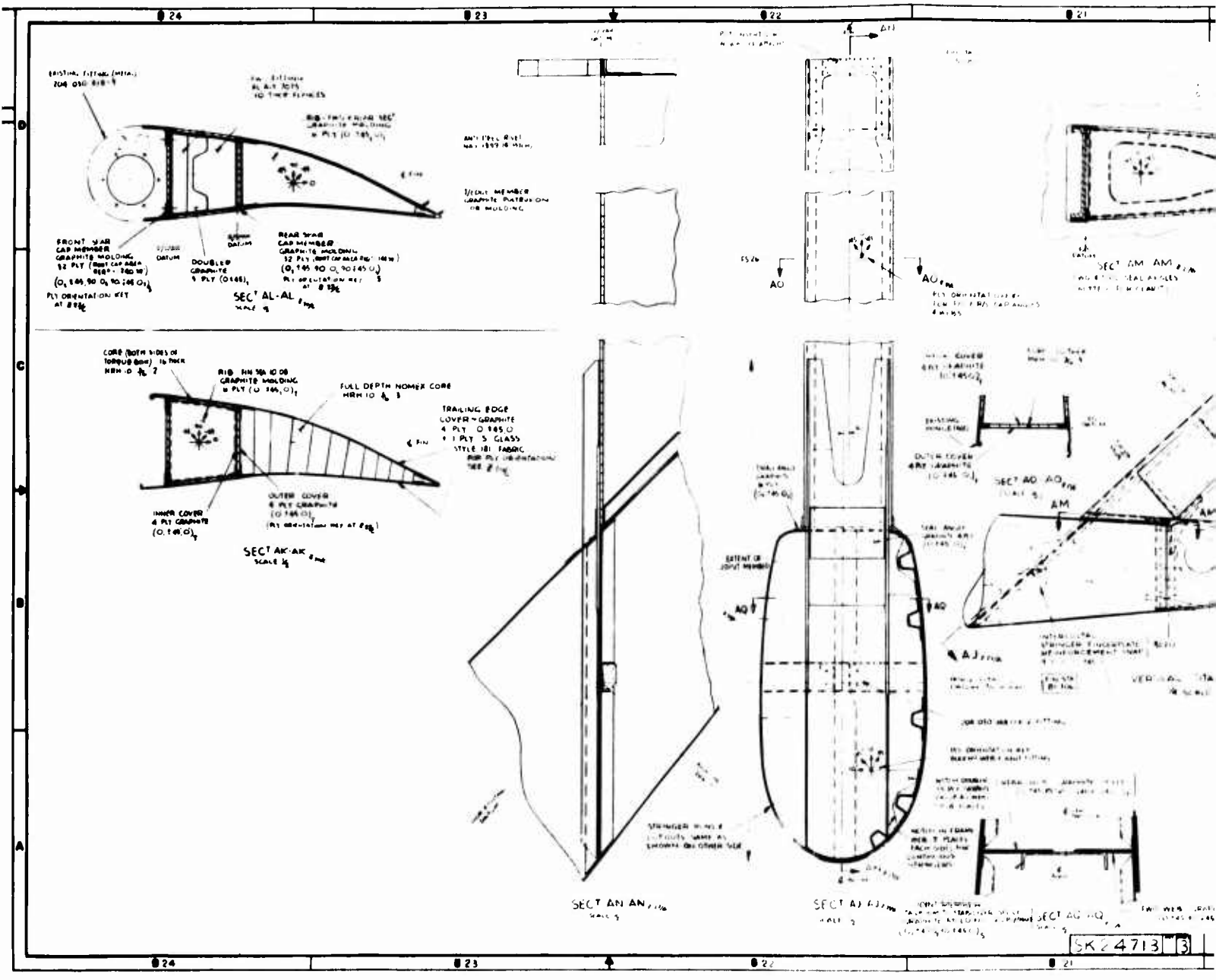

Figure 12. Continued.

Preceding page blank

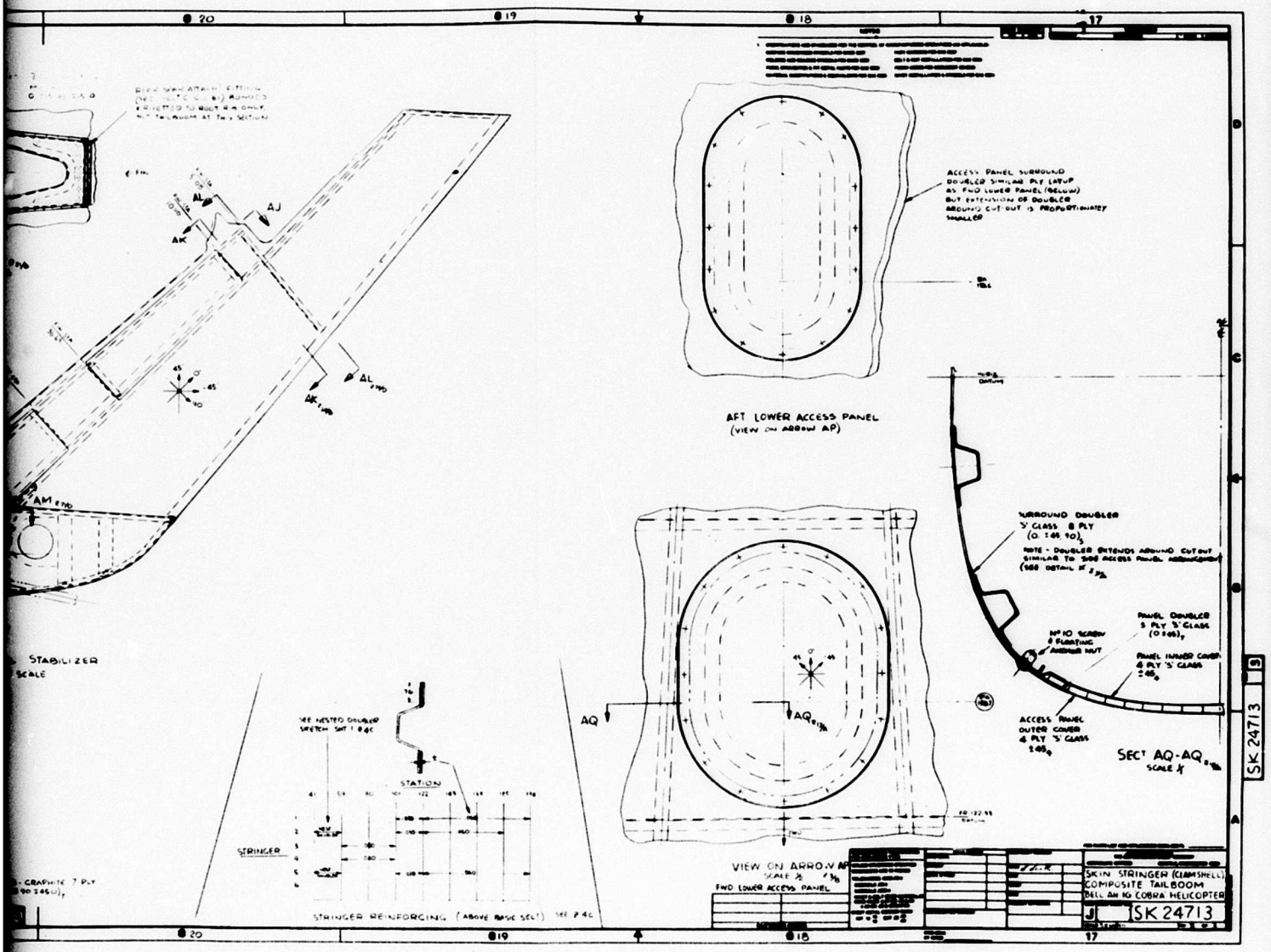
20
19
18
17
AJ
AK
AL
AM
AQ
45
0
-45
90
ACCESS PANEL SURROUND DOUBLER SIMILAR PLY LAY-UP AS FWD LOWER PANEL (BELOW) BUT EXTENSION OF DOUBLER AROUND CUT-OUT IS PROPORTIONATELY SMALLER
AFT LOWER ACCESS PANEL
(VIEW ON ARROW AP)
STABILIZER
SCALE
SEE NESTED DOUBLER SKETCH SHT 1 #4C
STATION
STRINGER
STRINGER REINFORCING (ABOVE BASIC SECT) SEE P 4C
VIEW ON ARROW AP
SCALE
FWD LOWER ACCESS PANEL
SECT AQ-AQ
SCALE
SKIN STRINGER (CLAMSHELL) COMPOSITE TAILBOOM
BELL AH 1G COBRA HELICOPTER
SK 24713
J

TABLE IX. ADVANCED COMPOSITE MATERIALS EVALUATED FOR APPLICATION TO COBRA AH-1G COMPOSITE TAIL SECTION

Material	Comment
Graphite HT	High strength and stiffness. Boeing Vertol has considerable experience with designing and fabricating in this material.
Graphite HM	High stiffness - relatively brittle.
Graphite Type-A	Economical price. Medium modulus and strength. Less susceptible to low-velocity impact damage than graphite HT or HM.
Boron	High-cost material. Stiffest material. Good data points available. Handling and machining difficulties.
PRD 49	High modulus. High tensile strength. Low compressive strength. Good impact resistance. Low density. Lower dialetric constant than E glass. Easily handled - as fiberglass. Recent breakthrough in cost on fabric materials, approximately $27/lb as compared to previous $50/lb.
S Glass	High tensile stress but relatively low modulus. Degraded by E glass. Ends must be carefully sealed to prevent ingress of fluid by capillary action and subsequent corrosion of fibers.
E Glass	Lower strength and modulus than S glass. Cheapest composite material.

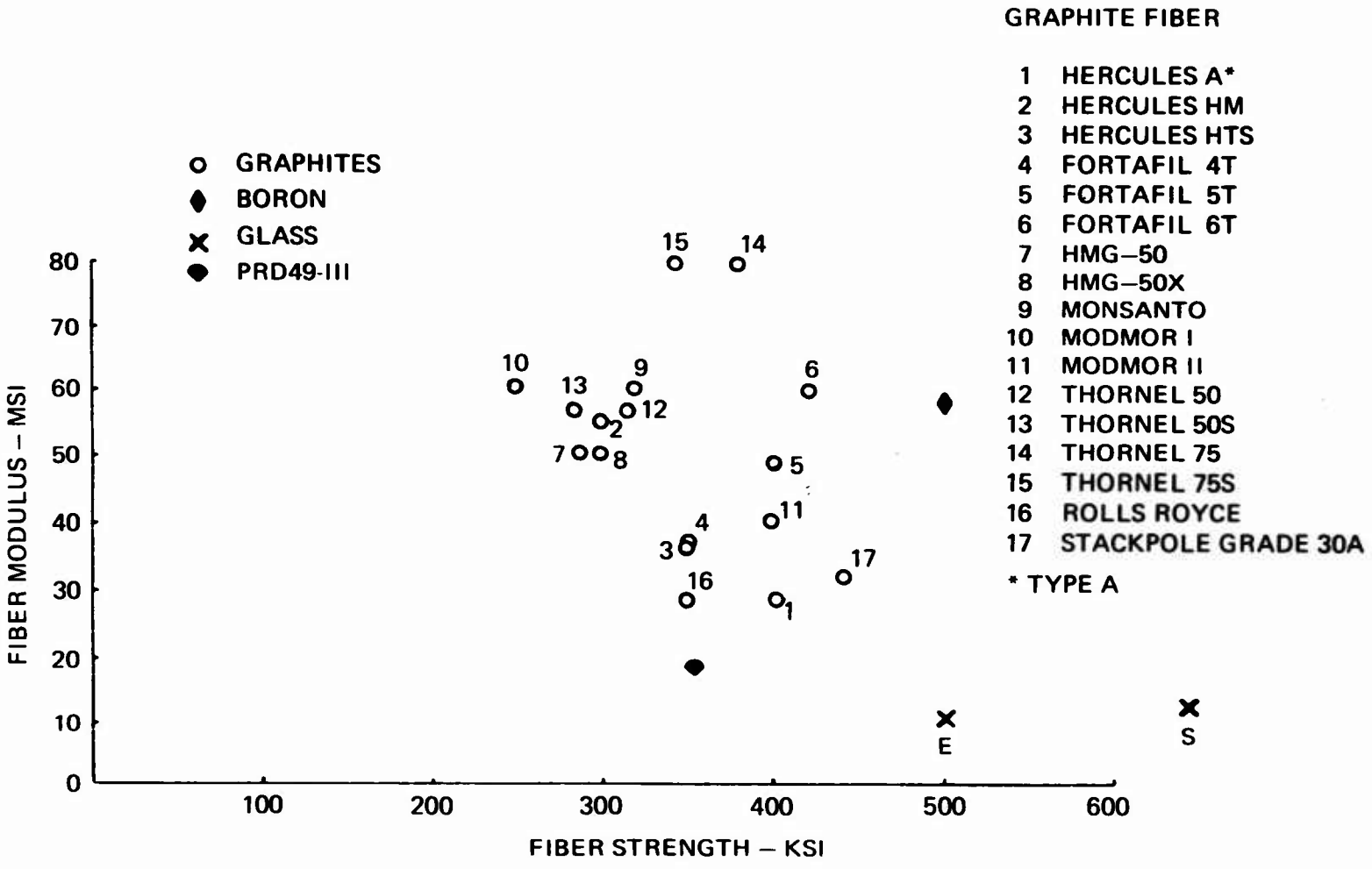

Figure 13. Strength and Modulus for Various Reinforcing Fibers.

- Incorporate design features into structure which specifically relate to leading parameter requirements (e.g., ballistic tolerance, fail safety, etc.).

- Develop concepts and techniques leading to the design of a simple tail section which is practical to build, is a low-risk concept, and is quantity production orientated; at selected positions, introduce higher risk unique items which could easily be replaced by state-of-the-art items in the event of unforeseen design or manufacturing problems.

- Design and analyze structure on all three concepts in enough depth to obtain realistic weight, cost, survivability, and complexity factors.

The composite material selections for the Cobra tail-boom concepts chosen are listed below:

1. Monocoque sandwich clamshell - honeycomb sandwich construction. No frames or stringers.
   Graphite type-A - primary structure
   S-glass - secondary structure and outside protective cover ply
   Core material - Nomex

2. Thin sandwich shell with four longerons and frames - thin honeycomb sandwich skins with frames and longerons.
   Cover material - PRD 49-3 over Nomex core
   PRD 49-3 - secondary structure
   Graphite type-A - frames and longerons
   Vertical stabilizer - all graphite type-A

3. Integrally molded skin/stringer clamshell
   Cover material - S-glass
   Frames and stringers - (Primary structure) - graphite type-A
   Secondary structure - S-glass
   Vertical stabilizer - all graphite type-A

USE OF EXISTING AH-1G HARDWARE

Existing AH-1G operational hardware will be fitted to the composite tail boom in a manner similar to the existing metal tail boom.

Mechanical items such as drive shafts and hanger fittings will be mounted and aligned in the same way as the installation into the metal tail section, using shims for vertical alignment and accurate attachment hole positioning in the composite structure for lateral and longitudinal alignment.

LIGHTNING PROTECTION

In general, the all-metal-skinned aircraft is safe because the metal acts as a Faraday cage, and the current can be conducted along the aircraft surface without affecting either the skin or the internal components. However, the use of composite structures and bonded joints introduces problems.

The component itself is more susceptible to damage, and the lack of a complete Faraday cage increases the vulnerability of the onboard electrical and electronic equipment to the transient voltages induced in the circuitry by the lightning flash. When such structures with no lightning protection are subjected to high-amperage strokes, corona discharge, and streamers, extensive structural damage could occur; and with current surges occurring inside the tail boom, the wiring and electronic gear could be damaged.

There are compelling reasons for protecting the composite tail section, and two practical methods are available:

- Total shielding of the tail section wetted area by an aluminum alloy mesh or grid system, with adequate grounding strips to the forward metal fuselage.

- Aluminum film coating.

The aluminum flame spray system appears to be the simpler solution; however, there are doubts as to the efficiency and durability of this material and how thick the coating should be. Therefore, it has been determined to proceed with a mesh or grid system using information gathered from such current investigations as reported by McDonnell-Douglas.*

Figure 14 shows the protection afforded to boron/epoxy laminate by various aluminum meshes and foils. For the total wetted area of the tail section, approximately 97 square feet, it can be seen that a 120-mesh aluminum weighing 4 pounds will protect in excess of limit load against a 200,000-amp strike.

It is considered that all three concept structures should be protected using the mesh system with adequate integrated earthing cables back to the metal fuselage structure. A nominal weight of 5 pounds has been allowed in each estimate for this arrangement.

*SEVENTH INTERIM REPORT, McDonnell-Douglas Corporation, Air Force Contract F33615-71-C-1414.

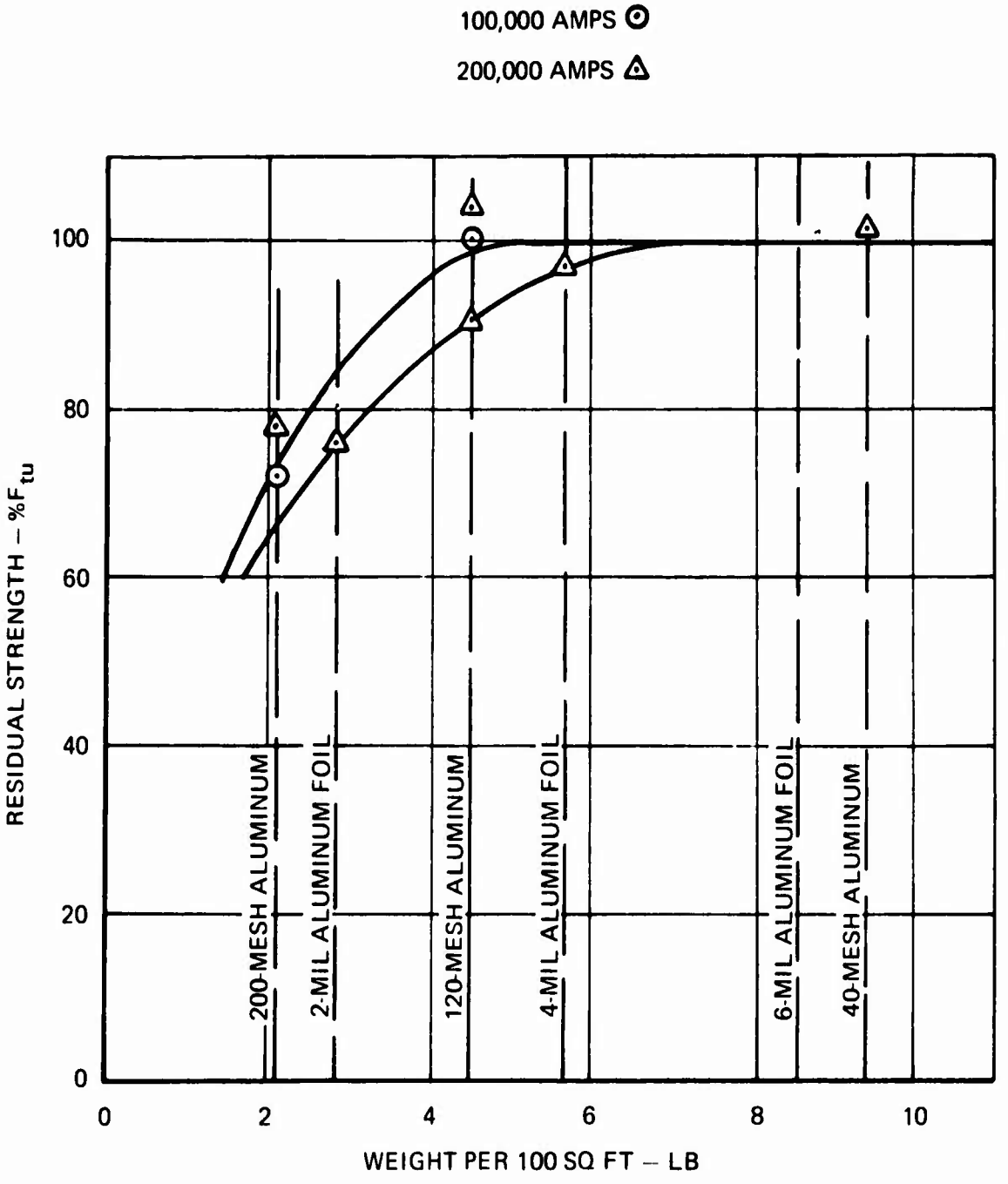

Figure 14. Residual Strength Versus Coating Weight for Conductive Coatings Evaluated on Boron/ Epoxy Laminate.

COBRA TAIL SECTION WEIGHT

Actual weight of the Cobra tail section (metal) on loan to Boeing Vertol is 185.6 pounds.

Weight includes:

- Tail boom and vertical fin (primary structure)
- Tail drive shaft hanger fittings (2)*
- Upper fin drive box support fitting (1)*
- Control brackets*

Weight does not include:

- Avionics, avionics shelves, electrics and other loose equipment
- Tail drive shaft and drive shaft fairing
- Fin leading-edge drive shaft and fairing
- Angle box and angle box fairing
- Tail rotor drive box, rotor blades and fairing

---

*For comparison purposes, subtract the estimated weight of such mechanical parts common to metal and composite tail-boom designs. Estimated total weight of the above items = 15.6 lb.

Actual tail-boom (metal) weight	= 185.6 lb
Less asterisked items (total)	= 15.6 lb
Tail-boom airframe weight for comparison purposes	170.0 lb

Composite Concept 1 weight = 145 lb - saving = $\frac{25}{170}$ = 15%

Composite Concept 2 weight = 154 lb - saving = $\frac{16}{170}$ = 10%

Composite Concept 3 weight = 170 lb - saving = 0 = 0%

WEIGHT OF THE THREE SELECTED CONCEPTS

The weight breakdowns for the selected concepts are shown in Tables X, XI and XII. Weights were based on a stress sized shell (as against a trend curve) with sizing of primary structure to preliminary design levels. Secondary structure was directly estimated from the drawing only (not stress sized).

It is emphasized that these design concept drawings are not to production standard and mainly cover primary structure, with some representative secondary structure only to afford some measure of complexity.

A lump estimate for the secondary structure not shown on each concept drawing is contained under the Miscellaneous Brackets and Fixtures entry.

TABLE X. MONOCOQUE SANDWICH CLAMSHELL WEIGHT ESTIMATE

	Lb
Tail-boom shell (includes all reinforcings, access panels, inserts, protective covers)	87.0
Fwd and rear bulkheads (3 plus 2 respectively)	5.0
Tail-cone fairing	2.0
Miscellaneous internal brackets and fixtures	8.0
Fwd main attach fittings (4)	4.0
Canted bulkhead	3.0
Shelf beams and brackets	4.0
Joint plate (canted bulkhead/ fin) and drag angles	2.0
Vertical stabilizer complete	25.0
Lightning strike mesh	5.0
Total	145.0

TABLE XI. THIN SANDWICH SHELL WITH LONGERONS AND FRAMES - WEIGHT ESTIMATE

	Lb
Tail-boom shell (includes all reinforcings, access panels, inserts)	91.0
Fwd and rear bulkheads (3 plus 2 respectively)	5.0
Tail-cone fairing	3.0
Miscellaneous internal brackets and fixtures	10.0
Fwd main attach fittings (4)	3.0
Canted bulkhead	3.0
Shelf beams and brackets	2.0
Joint plate (canted bulkhead/fin) and drag angles	2.0
Vertical stabilizer complete	25.0
Lightning strike mesh	5.0
Ring frames (7)	5.0
Total	154.0

TABLE XII. INTEGRALLY MOLDED SKIN/STRINGER CLAMSHELL - WEIGHT ESTIMATE

	Lb
Tail-boom shell (includes all reinforcings, access panels, etc.)	109.0
Fwd and rear bulkheads (2.5 plus 1.5)	4.0
Tail-cone fairing	3.5
Miscellaneous internal brackets and fixtures	9.0
Fwd main attach fittings (4)	3.0
Canted bulkhead	3.0
Shelf beams and brackets	2.5
Joint plate (canted bulkhead/fin) and drag angles	2.0
Vertical stabilizer complete	25.0
Lightning strike mesh	5.0
Intermediate frames (7)	4.0
Total	170.0

TECHNOLOGY SUMMARY

The basic technology objectives for the design of the composite tail section structure were as follows:

- Selection, evaluation, and efficient application of composite materials resulting in an optimum strength/weight design.
- Vertical and lateral bending stiffness of a composite structure to match that of the Cobra tail boom.
- Torsional stiffness of the composite structure also to match that of the Cobra tail boom.
- Selection of efficient load paths, especially suitable to composite materials.

The critical external loads applied on the tail boom are bending combined with transverse and torsional shears. For a composite structure, the most efficient lay-up is a fiber orientation parallel (0^o) to the load direction for axial stresses, and $\pm 45^o$ fiber orientation with respect to shear load. Therefore, for the honeycomb clamshell boom structure, Concept 1, a minimum lay-up configuration of $0^o/\pm 45^o$ per facing was established. This provided longitudinal (0^o) laminates for the boom bending stresses and stiffness, and crossplied ($\pm 45^o$) laminates for shear stresses and torsional stiffness. For the initial design and material evaluation of the honeycomb clamshell configuration, Concept 1, GR/EP (HT) was the first material selected for the shell facings, and Hexcel Nomex HRH-10 for the core, with a 3-pound-per-cubic-foot (pcf) density. Stress analysis of the most critical boom panel loaded in combined compression and shear showed that a sandwich using a three-ply GR/EP (HT) facing material, $0^o/\pm 45^o$ lay-up, .018 in. thick, with a .70-in. core thickness was required. The fin honeycomb sandwich skin panels using the same facing materials and lay-up required a core density of 2 pcf, and a thickness of .16 in. and .29 in. for the forward and aft panels, respectively.

A quasi-isotropic facing laminate was also investigated using a $0^o/\pm 45^o/90^o$ GR/EP (HT) material, .024 in. thick. The critical panel for this configuration required a core thickness of approximately .60 in. However, a weight comparison indicated a facing weight increase of .0966 pound per square foot (psf) and a core weight decrease of only .0250 psf. This was considered to be undesirable from a weight standpoint.

The final material investigated for the clamshell design was GR/EP (Type A), intermediate strength, since it has a relatively greater resistance to impact. The boom and fin sandwich facing considered was a three-ply $0^o/\pm 45^o$ lay-up. For the most

critically loaded boom panel, the resulting sandwich core thickness was .74 in. - 5 percent greater than that required for the HT facing. Similarly, the vertical fin skin panel core thickness also increased, but a lesser average amount of 4 percent - .17 in. and .30 in. for the forward and aft panels, respectively.

The tail-boom vertical and lateral bending stiffnesses, and torsional stiffness determined for the clamshell design using GR/EP (HT) and (Type A) facings showed good correlation with the design requirement. However, the lateral bending stiffness as calculated was somewhat less than that given in the Cobra design requirement. Therefore, to improve this stiffness, doublers of unidirectional GR/EP (HM) material and varying plies were added at selected circumferential and longitudinal locations. The resulting bending stiffness computations showed that the lateral bending stiffness now slightly exceeded that requirement. Adjustments can be made to fine-tune the structure by moving the doublers from their present locations to more advantageous points along the circumference and by adding or subtracting plies as desired to finally match the basic curve.

A single ply of 181E glass cloth was added to the outer facing lay-up to improve the overall damage tolerance. This design feature is discussed in detail in the design section. The resulting vertical and lateral bending stiffness curves for the boom showing the effect of this additional one-ply cloth are also included.

The second design evaluation, Concept 2, was selected to be a hybrid structure using PRD 49-3 honeycomb skin panels and GR/EP (Type A) longerons. Four longerons provide the primary boom bending strength. The primary purpose of the PRD honeycomb skin is to react the applied shears. However, these panels also partially react the bending moments, the stresses being applied on the panels in proportion to the elastic moduli of the two materials. After investigating several longeron lay-up combinations, the configuration was finalized using 75 percent unidirectional and 25 percent of $\pm 45^{o}$ plies, for a total of sixteen plies, .096-in. thick. This resulted in ample longeron compression strength as well as the elastic modulus necessary to match the stiffness design requirement. The honeycomb skin panel configuration was $\pm 45^{o}$ (four plies) of PRD 49-3 facings, .024-in. thick each, with .33-in.-thick Hexcel Nomex HRH-10 core of 3 pcf density.

The vertical and lateral bending stiffnesses as calculated for Concept 2 showed that both stiffnesses very nearly match the Cobra design requirement. If additional fine tuning is desired, unidirectional plies of GR/EP may be added to the longerons, or unidirectional plies of PRD may be added to the

skin panels as required. The torsional stiffness also closely matched the design requirement.

The third concept is of a skin/stringer configuration, using a total of twelve stringers and thin skin shear webs. This was the optimum number of stringers for Concept No. 3, giving good bending and stiffness material distribution and shear panel size for adequate skin shear buckling allowables. The material selected for the stringer was GR/EP (Type A); glass epoxy was selected for the skins. Skin thickness requirements to match the torsional stiffness of the existing boom were determined considering $\pm 45^{o}$ 1002S-glass or $\pm 45^{o}$ XP251S-glass epoxy laminates. Comparison showed that the XP251S material resulted in a lighter skin weight due to a greater modulus of rigidity with respect to the 1002S-glass epoxy. The final skin material selected was eight plies ($\pm 45^{o}_{4}$) of XP251S-glass, .060-in. thick (total). The basic stringer section established was of a hat section configuration, using a GR/EP (Type A) material with a $0^{o}_{3}/\pm 45^{o}/0^{o}_{3}$ lay-up, a distribution of 75 percent unidirectional, and 25 percent $\pm 45^{o}$ plies, for a thickness of .043 in. This resulted in an optimum combination of stringer area, compression strength, and elastic modulus similar to Concept 2. In the region of high compression stresses, laminated doublers (five- and ten-ply, .030-in. and .060-in. thick respectively) were added to the hat section flanges to increase both the stringer section area and the crippling allowable. The skin panels were designed to be shear resistant, nonbuckling, at limit loads.

The vertical and lateral bending stiffnesses for Concept 3 were determined using only the GR/EP (Type A) stringers for boom cross-section bending material. The XP251S-glass skin was considered to be ineffective in bending. In this design, due to the discontinuity of the lower stringers in the region of the cutouts, laminated doublers were also added to the stringer flanges at selected locations to match the Cobra vertical bending stiffness. The resulting calculations showed that both the vertical and lateral bending stiffnesses closely matched the design requirement. The torsional stiffness also showed good correlation with this requirement.

STRUCTURAL DESIGN CRITERIA

The tail-boom shell and vertical fin structures for Concepts 1, 2, and 3 meet the following design criteria:

- Structural strength to react the applied loads taken from Reference (1)

- Tail-boom bending and torsional stiffness requirement for adequate dynamic response

- Factors of safety:

  - Limit Factor of Safety = 1.0

  - Ultimate Factor of Safety = 1.5

- Honeycomb panels and shell failure criteria:

  - No compression and shear buckling at ultimate loads

  - No local instability failures at ultimate loads

- Thin skin, composite lay-up failure criteria:

  - No buckling at limit shear loads

  - No failure at ultimate shear loads

LOADS

Shears, axial loads, and bending and torsional moments applied at the AH-1G (Cobra) tail-boom reference axis are determined from data given in Reference 1, Section 4, for the most highly loaded flight conditions. These critical conditions are:

Condition VB Yaw, +15° Recover
Condition VB Yaw, -15° Recover
Condition XIV, Tail-Down Landing

The sign convention for loads, moments, and coordinates used herein is shown in Figure 15.

The geometry and station location of the tail boom and vertical fin are shown in Figure 16.

Vertical and lateral shears and bending moments, torsional moments, and axial loads for these critical conditions are shown in Figures 17 and 18, and these are the limit unless otherwise noted.

The critical tail boom to fuselage attachment fitting loads as determined in Reference 1 are included in Table XIII and Figure 19.

Limit vertical fin loads are given in Reference 1, Section 5. The critical limit fin spanwise shear, spanwise, chordwise, and torsional moment diagrams are shown in Figures 20 and 21.

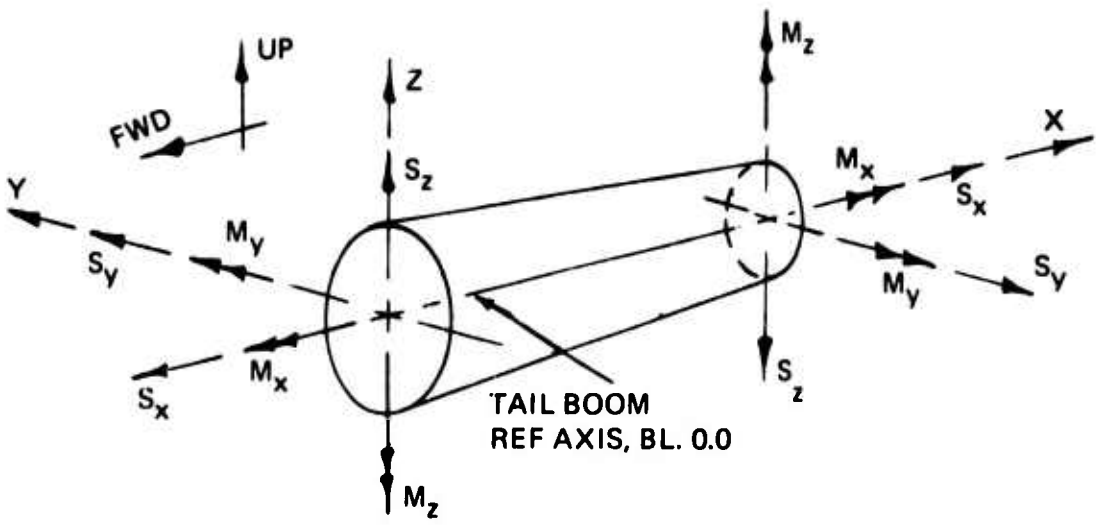

Figure 15. Sign Convention.

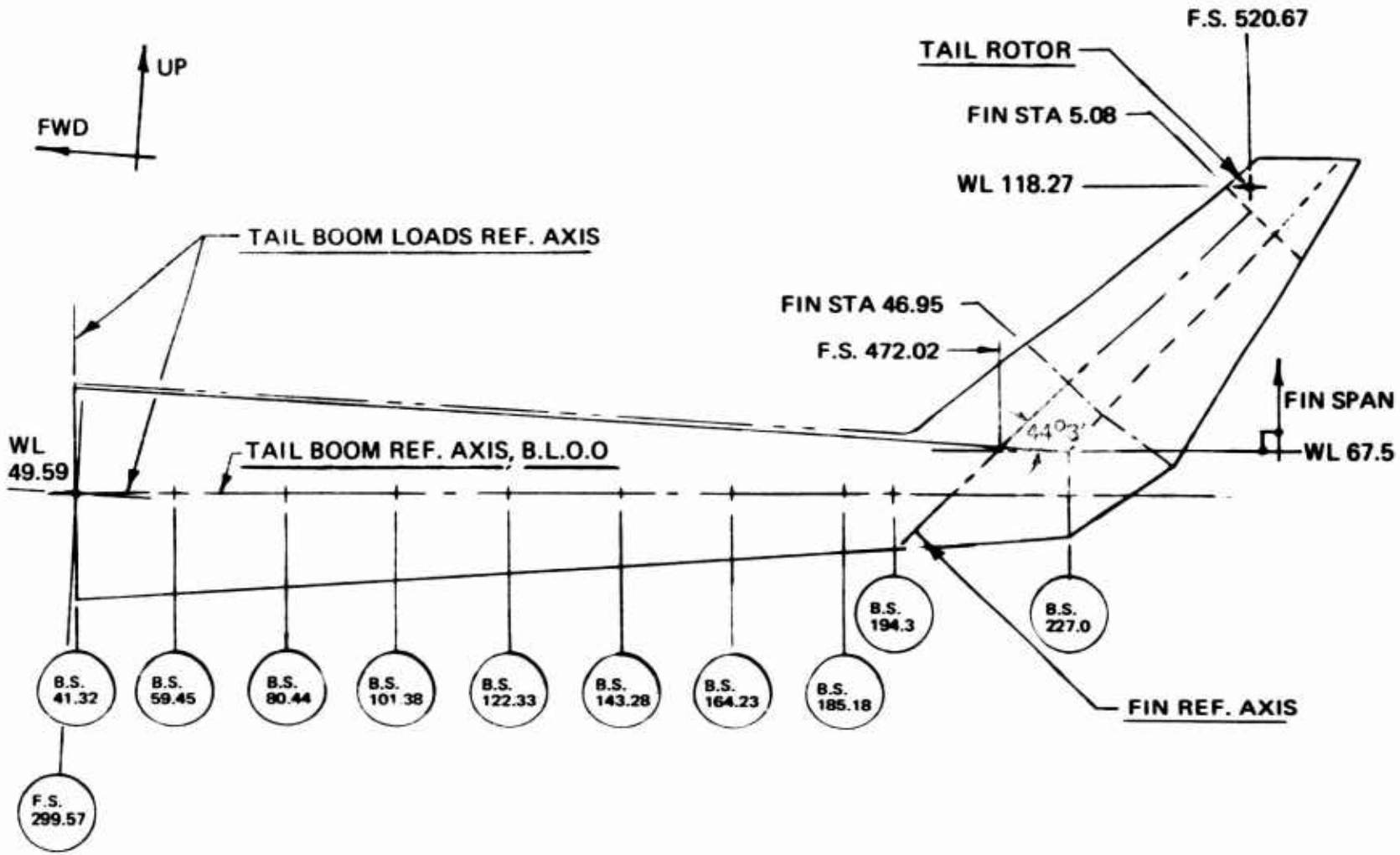

Figure 16. Geometry and Station Location, Tail Boom and Vertical Fin.

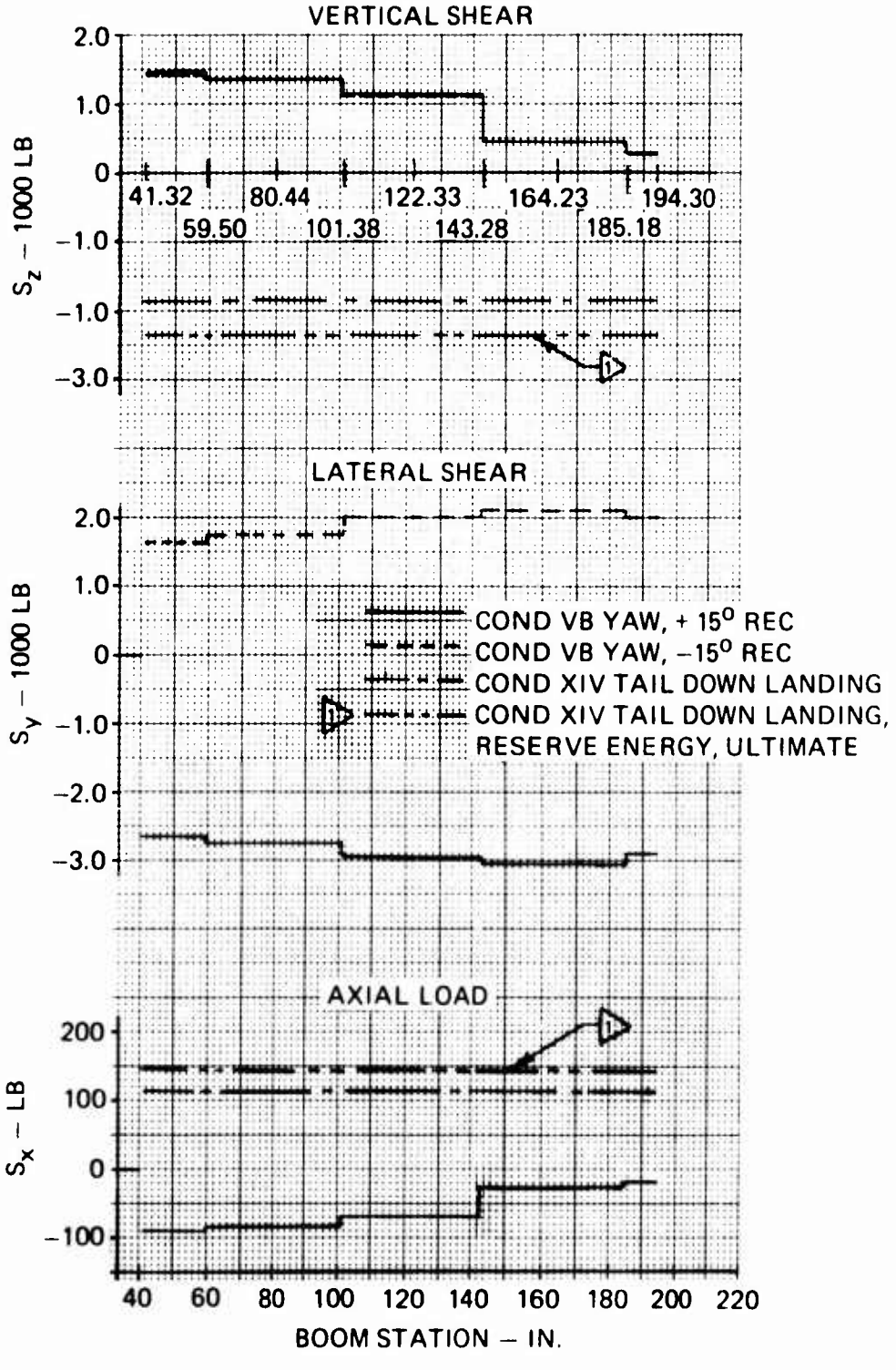

Figure 17. Tail-Boom Structural Strength.

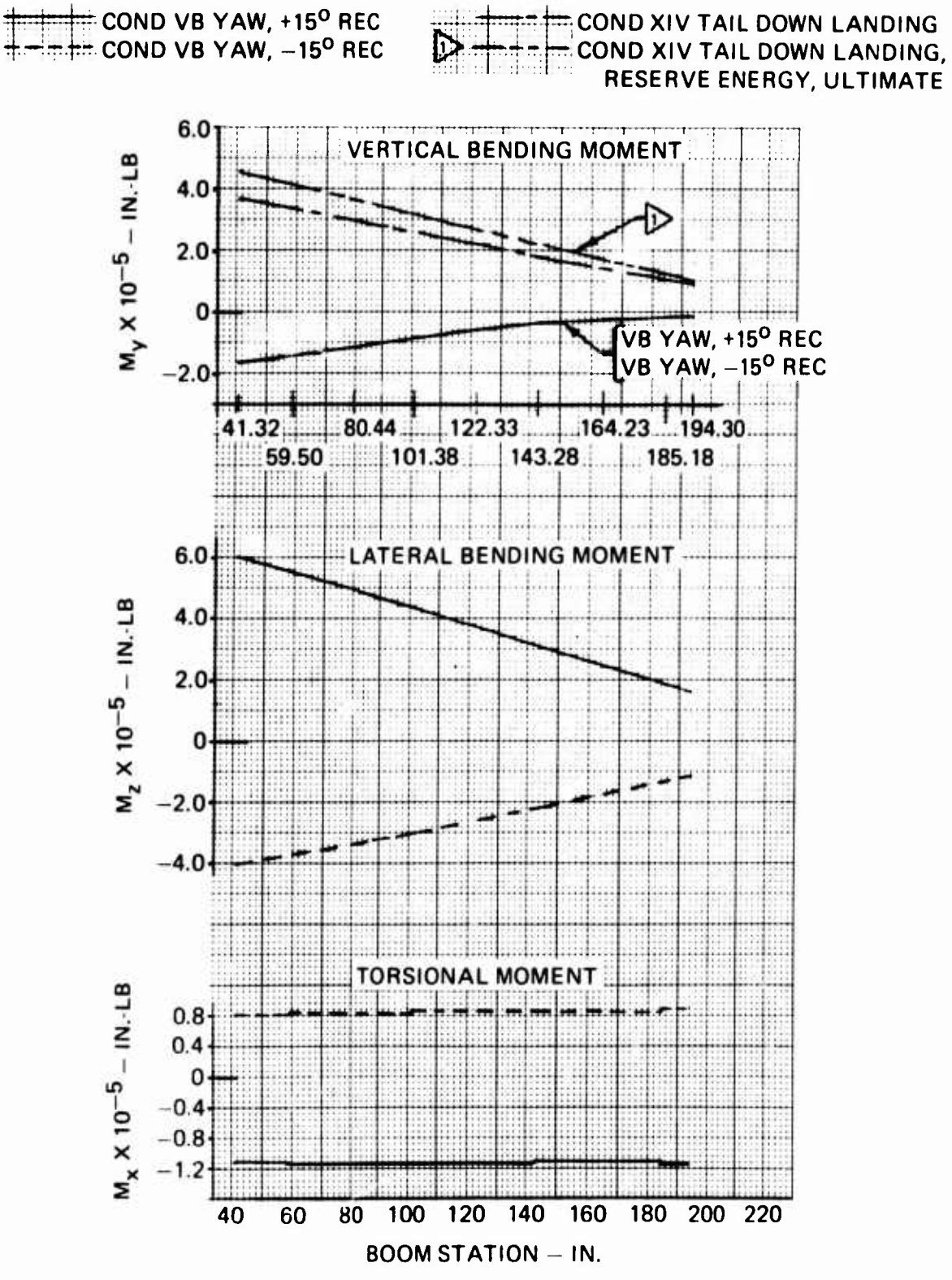

Figure 18. Tail-Boom Bending and Stiffness.

TABLE XIII. ATTACHMENT FITTING AXIAL LOADS, ULTIMATE*				
Fitting	Tension Load (lb)	Condition	Compression Load (lb)	Condition
Upper Right	15687	VB Yaw, -15° Recover	-11802	VB Yaw, +15° Recover
Lower Right	10086	VB Yaw, -15° Recover	-26278	VB Yaw, +15° Recover
Upper Left	21824	VB Yaw, +15° Recover	-5735	VB Yaw, -15° Recover
Lower Left	16122	VB Yaw, +15° Recover	-20171	VB Yaw, -15° Recover

Reference (1), Page 4.136.

*Limit Load x 1.5 = Ultimate Load
Factor of Safety = 1.5

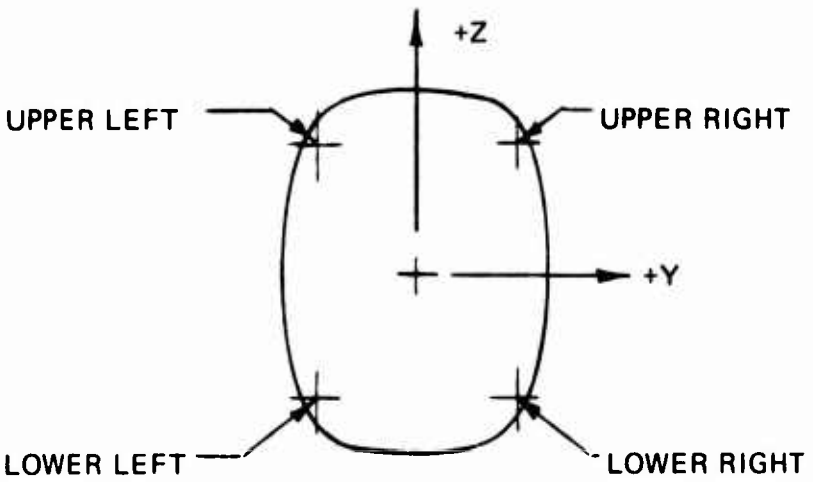

Figure 19. Attachment Fittings Designation.

DYNAMICS

Due to the amplification of the dynamic loads on the tail boom and fuselage, it is essential that the vibratory mode of the boom remain the same. Thus, consistent mass distribution and bending and torsional stiffnesses are required to maintain current natural frequencies. Therefore, the stiffnesses shown in Figure 22 form part of the design requirement. This stiffness data is taken from Reference (1). The lateral and vertical bending stiffness properties presented in Reference (1) are the effective properties corresponding to limit load conditions.

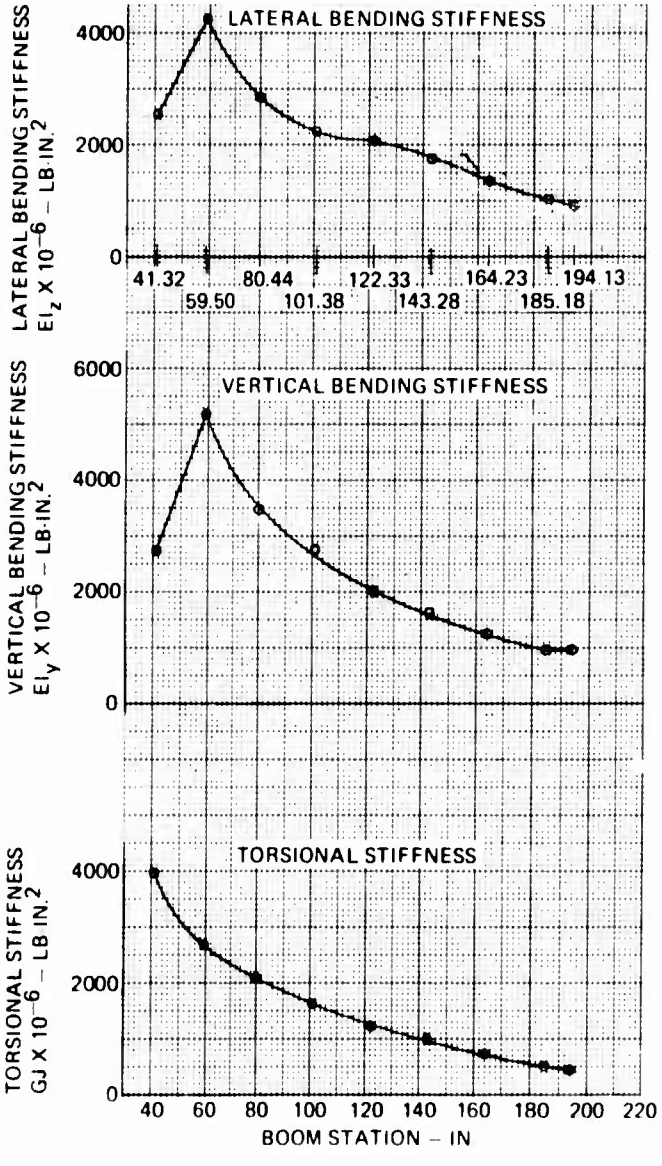

Figure 22. Lateral, Vertical, and Torsional Stiffnesses of Bell Structure.

TABLE XIII. ATTACHMENT FITTING AXIAL LOADS, ULTIMATE*				
Fitting	Tension Load (lb)	Condition	Compression Load (lb)	Condition
Upper Right	15687	VB Yaw, -15° Recover	-11802	VB Yaw, +15° Recover
Lower Right	10086	VB Yaw, -15° Recover	-26278	VB Yaw, +15° Recover
Upper Left	21824	VB Yaw, +15° Recover	-5735	VB Yaw, -15° Recover
Lower Left	16122	VB Yaw, +15° Recover	-20171	VB Yaw, -15° Recover

Reference (1), Page 4.136.

*Limit Load x 1.5 = Ultimate Load
Factor of Safety = 1.5

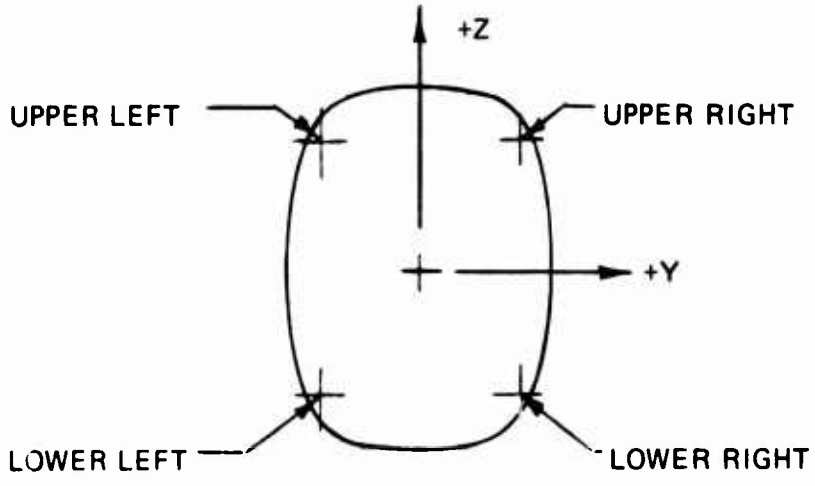

Figure 19. Attachment Fittings Designation.

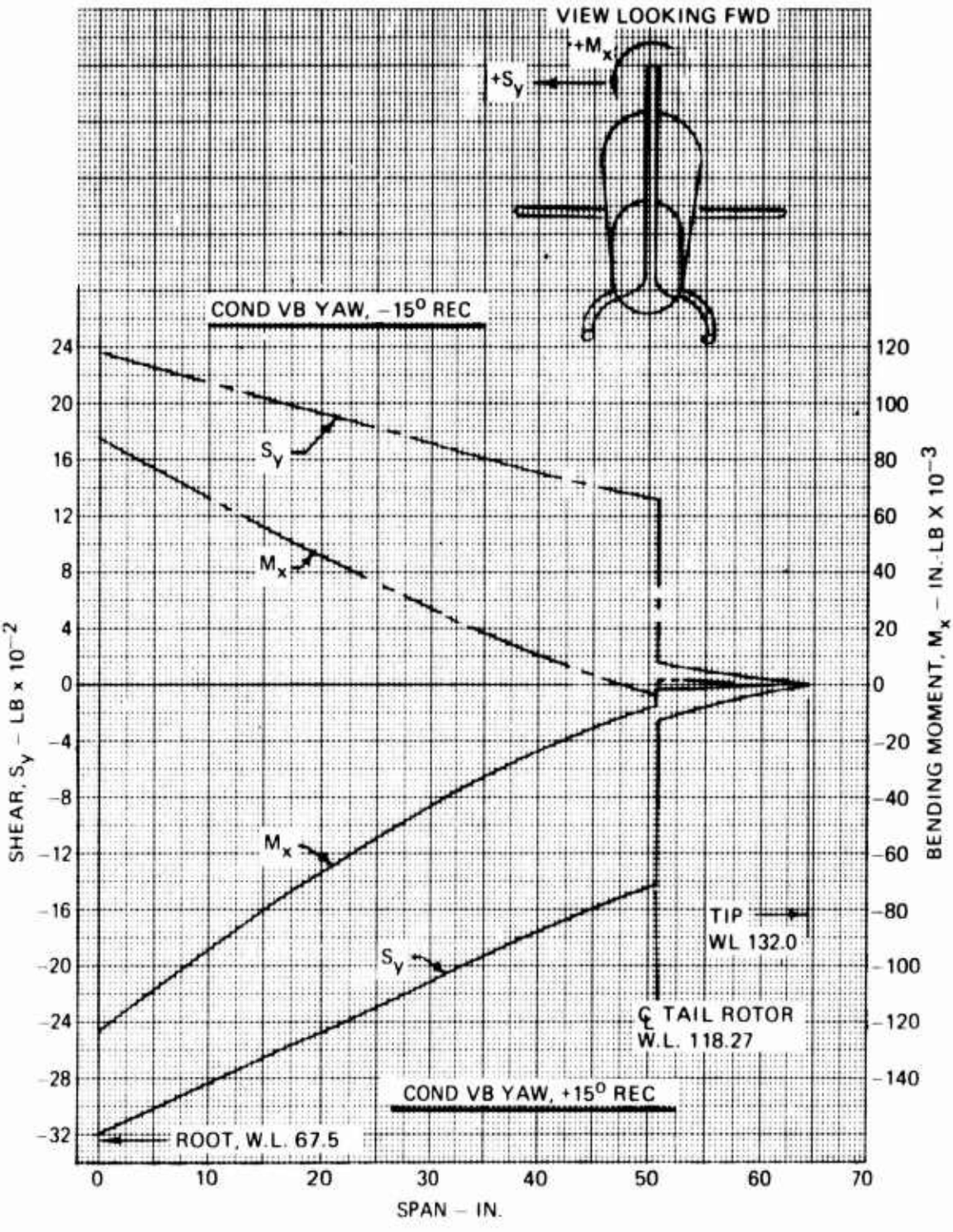

Figure 20. Vertical Fin Spanwise Shear and Bending Moment.

DYNAMICS

Due to the amplification of the dynamic loads on the tail boom and fuselage, it is essential that the vibratory mode of the boom remain the same. Thus, consistent mass distribution and bending and torsional stiffnesses are required to maintain current natural frequencies. Therefore, the stiffnesses shown in Figure 22 form part of the design requirement. This stiffness data is taken from Reference (1). The lateral and vertical bending stiffness properties presented in Reference (1) are the effective properties corresponding to limit load conditions.

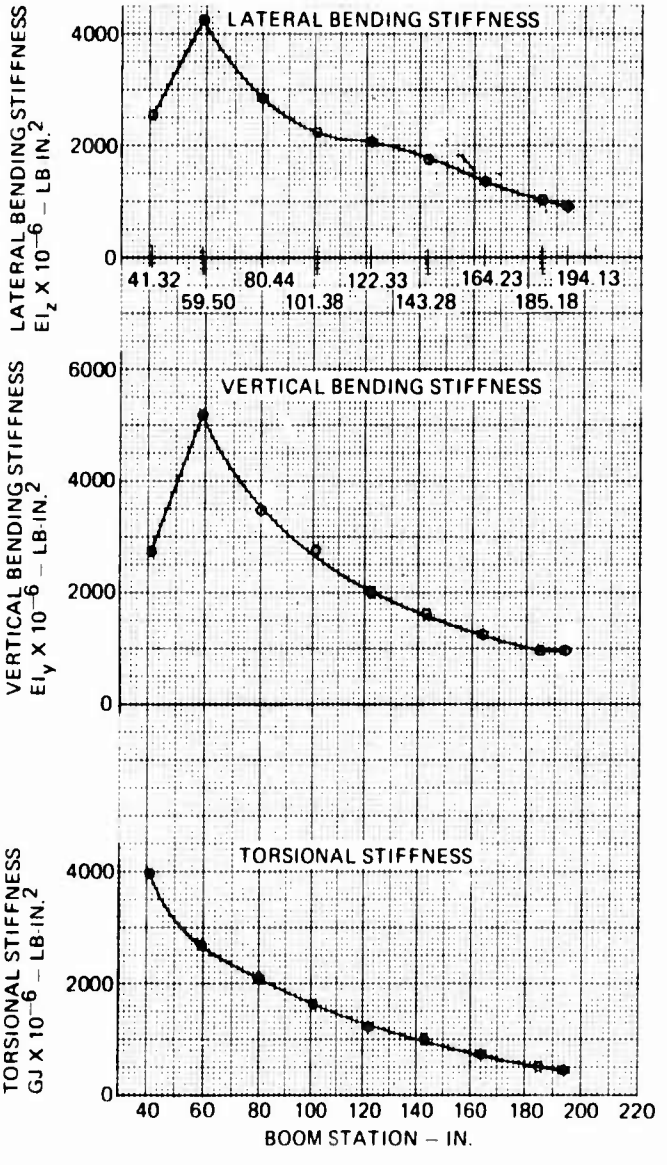

Figure 22. Lateral, Vertical, and Torsional Stiffnesses of Bell Structure.

MATERIAL ALLOWABLES

The allowable mechanical properties of the materials used in the design of Concepts 1, 2, and 3 are given in Tables XIV through XIX.

TABLE XIV. GRAPHITE/EPOXY LAMINATE ALLOWABLES

Description	Intermediate Strength GR/EP (Type A) V_f = 0.60				High-Modulus GR/EP (HM) V_f = 0.60
	Unidirectional	Cross-plied Laminates			Unidirectional
		Fiber Orientation			
	Reference (2) Table 1.2.1-IV	0°:33% ±45°:67%	0°:75% ±45°:25%	Reference (2) Figure No.	Reference (2) Table 1.2.1-III
F_{tux} (L) (KSI)	160.0	69.0	128.0	1.2.2-34	110.0
F_{tuy} (T) (KSI)	7.5	25.0	17.0	1.2.2-34	4.0
F_{cux} (L) (KSI)	160.0	70.0	128.0	1.2.2-36	100.0
F_{cuy} (T) (KSI)	25.0	39.0	29.0	1.2.2-36	20.0
Shear Strength					
F_{su} * (KSI)	10.0	36.0	18.0	1.2.2-38	9.0
F_{isu} ** (KSI)	13.0	13.0	13.0	--	10.0
E_x (L) (MSI)	17.0	7.3	13.2	1.2.2-39	25.0
E_y (T) (MSI)	1.7	3.4	2.4	1.2.2-39	1.7
G_{xy} (LT) (MSI)	0.65	3.23	1.6	1.2.2-41	0.65
μ_{xy} (L)	0.21	0.69	0.49	1.2.2-42	0.30
μ_{yx} (T)	0.021	0.31	0.089	1.2.2-42	0.020

*In-Plane
**Interlaminar

TABLE XV. PDR 49-III/BP907 LAMINATE ALLOWABLES

	Fiber Orientation						V_f (%)
	0^o		$\pm 45^o$		90^o		
F_{tu} (KSI)	160.0	(c,e)	17.6	(d)	2.1	(c)	58
F_{cu} (KSI)	32.0	(e)	17.6	(d)	15.5	(f)	58
Shear Strength							
F_{su} (a) (KSI)	6.0	(c)	6.0	(c)	6.0	(c)	58
F_{isu} (b) (KSI)	5.5	(c)	20.0	(g)	5.5	(c)	58
E (MSI)	12.6	(c,e)	1.0	(d)	0.766	(c)	58
G (MSI)	0.4	(c)	2.8	(e)	0.4	(c)	58
μ	0.325	(c)	0.8	(h)	0.03	(h)	--

(a) In-Plane
(b) Interlaminar
(c) Data taken from Reference (3).
(d) Data taken from Reference (4).
(e) Data taken from Boeing Vertol Co. preliminary design allowables data sheet.
(f) Calculated from DuPont Co. test data, M-3 Allowable, V_f = 50%.
(g) Calculated from DuPont Co. test data, same as (f), but for PRD-49-III with SP-306 ("Scotchply SP-306 PRD 49-III Tape"); allowable for C_V = 8%, V_f = 60%.
(h) Estimated values.

TABLE XVI. $\pm 45^o$ XP251S FIBERGLASS LAMINATE ALLOWABLES*

F_{tu}	(KSI)	22.6
Shear Strength		
F_{su} (In-Plane)	(KSI)	42.2
F_{isu} (Interlaminar)	(KSI)	9.0
E	(MSI)	2.40
G	(MSI)	2.21
μ		0.63

*Reference (5)

TABLE XVII. MECHANICAL PROPERTIES OF HEXCEL HRH-10 NYLON FIBER/PHENOLIC RESIN HONEYCOMB*

Hexcel Honeycomb Designation	Compressive		Plate Shear			
			L Direction		W Direction	
	Strength (PSI)	Modulus (KSI)	Strength (PSI)	Modulus (KSI)	Strength (PSI)	Modulus (KSI)
	Min.	Typ.	Min.	Typ.	Min.	Typ.
HRH-10-3/16-2.0	105	11	72	4.2	40	2.2
HRH-10-3/16-3.0	270	20	135	7.0	67	3.5

*Ref. (6)

TABLE XVIII. MECHANICAL PROPERTIES OF STRUCTURAL ADHESIVES

Supplier Product Designation	Supplier	Lap Shear Strength (PSI)
AF-126	3M Company	3000*
EA934	Hysol, Div. Dexter Corp.	2500**

*Ref. (7)
**Ref. (8)

TABLE XIX. E-720E/7781(ECDE-1/0-550) CLOTH ALLOWABLES*

	Warp Direction: 0^{o}	Fill Direction: 90^{o}
F_{tu} (KSI)	60.4	49.0
F_{cu} (KSI)	64.8	50.2
E (MSI)	3.12	2.82
G (MSI)	0.75	0.75

*Ref. (11)

FABRICATION CONCEPTS

Concept 1 was selected as a base-line design for the fabrication cost trade-off study. Detailed fabrication sequences were conceived, specific component tools were designed, and all assembly operations were detailed. Tooling and fabrication costs were then estimated using current techniques and the above operations analysis. Standard learning curves were then applied to arrive at the production cost figures used in the Math Model. Operations common to all three concepts upon which design changes had no impact, such as lightning protection, painting, gearboxes and drive shaft installations, were not included in the trade-off study.

The tooling and fabrication planning developed for Concept 1 was then modified as required on a detail basis to complete the cost estimates for Concepts 2 and 3. A summary of the factors which controlled the fabrication and tooling costs is shown in Table XX, followed by a detail fabrication and tooling description for Concept 1.

MANUFACTURING APPROACH

Concept 1, monocoque sandwich clamshell, was selected as the base-line design for a detailed manufacturing cost producibility study. Concept 1 represented the structural configuration which required the fewest component parts, tools and fabrication and assembly operations. Type-A graphite was recommended since, in addition to its high strength and stiffness characteristics, it currently has the largest share of the current graphite market, the lowest current cost, and the most favorable projected future cost trend.

A core of DuPont Nomex was selected as a result of design impact considerations, relative insensitivity to shop handling damage and contamination, even though its initial cost is higher and its fabrication forming operations are more difficult than those for aluminum core.

TOOLING CONCEPTS

Female right- and left-hand tooling was selected to form the basic airframe structural components which were to be subsequently joined by two longitudinal splices (Figure 23).

TABLE XX. COBRA COMPOSITE TAIL-BOOM FABRICATION TOOLING COST STUDY

Operation	Concept No. 1 Monocoque Sandwich Clamshell	Concept No. 2 Thin Sandwich Shell With Longerons	Concept No. 3 Integrally Molded Skin Stringer Shell
Lay-up complexity	1	2	3
Component machining	1	3	2
Tool complexity	1	2	3
Prefabricated components	1	2	3
Assembly ease	1	2	3
Automation adaptability	3	2	1
Inspectability	1	2	3
Reproducibility	1	2	3

Legend

1 indicates minimum operations/complexity
3 indicates maximum operations/complexity

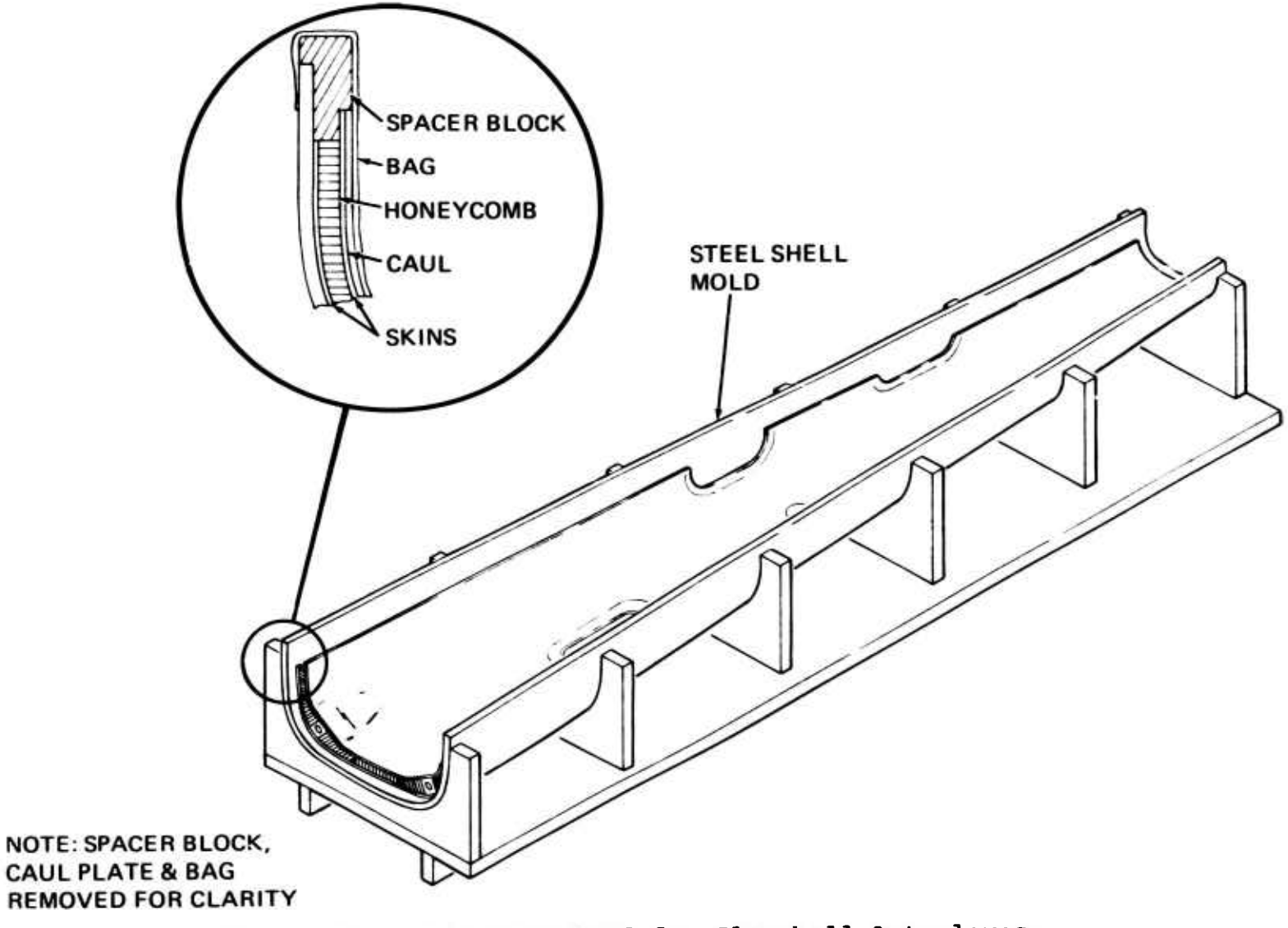

Figure 23. Tail-Boom Mold for Clamshell Autoclaves.

Thin-gauge low-carbon steel was selected for the tooling material, and autoclave curing techniques were selected such that rapid heat-up and cool-down rates could be achieved, with multiple tools stacked in the autoclave to match increased production rates. This concept results in the lowest unit tooling cost, because it makes maximum use of currently available autoclave systems widely available in the industry.

In contrast, self-contained internally heated and cooled pressurized tooling is far more expensive than thin-shell autoclave tools, and the addition of increased rate tools is also more costly.

CORE CONFIGURATION

Due to the small radii of the aft tail-boom area, preforming of the Nomex core is required. This is a difficult operation requiring close control of time and temperature, and considerable area shrinkage of the core occurs during this process. For this reason, the raw core blanks would be formed first and subsequently trimmed and spliced. Square edges would be used whenever possible in the design to maintain tool and core machining simplicity.

MATERIALS, RESINS, ADHESIVES

The materials selected for construction of the fuselage components have been utilized in other Boeing Vertol programs, and no new processes or fabrication techniques would be required.

The fibers would be impregnated with an epoxy novalac resin system supplied by American Cyanamid, and coded BP907. This resin has been selected from among the many available candidates for the following reasons:

- Previously used in high-modulus rotor blade flight evaluation programs.
- Demonstrated good impact resistance due to high elongation and toughness.
- Amenable to precast film or solvent dispersed fiber prepregging processes.
- Excellent structural properties over the required service temperature range.
- Demonstrated long-term field service history.
- Good tack and drape characteristics.
- Excellent work life and storage stability.

- Demonstrated compatibility with co-cure concepts and single-stage sandwich structure bonding processes developed by Boeing Vertol.

- Has moderate curing temperatures, can endure multiple cure cycles, and requires no post cure.

- Moderate cost and industry-wide availability.

ADHESIVE SYSTEMS

Two adhesive systems were selected for use in the airframe structural fabrication. Both of these systems have been used in flight-tested composite structures for the fabrication of sandwich panels and bonded structural joints. The sealing material selected has demonstrated its suitability for use by many years of service in commercial and military aircraft.

The basic adhesive film used to bond the graphite face sheets to the honeycomb is a moderate-temperature-curing epoxy film adhesive fully qualified to military bonding specifications; also, it has demonstrated its ability to form a tough peel-resistant bond to honeycomb when co-cured with BP907 graphite prepreg.

The second stage and final assembly component joints should use ambient-temperature-curing epoxy-based mastic adhesive systems. These adhesive systems are in production use within the Boeing Vertol Company and have been used extensively in the construction of composite structures.

One such system has a relatively high modulus, making it compatible with graphite structures. It has excellent property retention over the temperature range expected, and the capability to retain good structural properties at temperatures well above 250°F. This high-temperature strength retention is essential in case elevated-temperature-cured repair techniques are required during the evaluation or as a result of in-service damage.

The sealing requirements are limited for the design selected; however, a maximum structural panel environmental seal requirement can be maintained throughout component design, fabrication and assembly to prevent panel altitude breathing and subsequent moisture entry and panel degradation. Assembly joints, fastener areas and panel edges are to be sealed with a polysulfide elastomeric material fully qualified to Boeing specifications and military specification MIL-S-8802.

A single-stage sandwich bonding process in which structural sandwich composite laminates are cured and simultaneously adhesively bonded to a honeycomb core was selected from the

basic panel fabrication. The use of this "co-cure" system allows the completion of an entire one-half of the fuselage structure with a single process cure cycle. This results in a minimum fabrication cost for a composite component because of the reduced number of autoclave cycles, and service performance has shown increased structural reliability and environmental resistances over multi-stage assembly systems.

STRUCTURAL SHELL ASSEMBLY

The main structural shell of the tail boom is fabricated in steel sheet metal female molds (Figure 23). Each half is fabricated in a single cure cycle in its own mold and then joined in an assembly jig (Figure 24), using ambient temperature mastic adhesives and precured splice plates. Strap clamps are to be used to pull the boom halves together in the assembly jig. Air bags between a collapsible mandrel and the splice joint are to pressure the bond area. A separate but similar mandrel should be used between the fin front spar fuselage web and the rear bulkhead, which can be removed through the gap in the spar web.

The structural joint concept developed allows the installation of the few required bulkheads at the same time that the two shell halves are joined. The various detail internal components such as control system fair leads, bell crank brackets, and supporting structure for the electronics shelves would be installed in the shell halves before assembly bonding. This concept, again, keeps assembly tooling costs to a minimum.

The front and rear bulkheads are to be made on simple flat-plate type tooling by the co-cure process and can include bonding of any angle attachments simultaneously.

The various fittings, angles, channels, etc., should be made on simple male or female tools by hand lay-up. Many of these could be made in production by a pultrusion process.

The side hatch cover is to be made in the proper half of the clamshell mold the same as the boom shell to assure a close matchup. The bottom hatch covers will require separate, simple tools.

VERTICAL FIN

Fabrication of the vertical fin starts with the front and rear spars, which are made on simple flat plates with side guides (Figure 25). The assembly is bagged and autoclave cured. Front spar angles can be attached simultaneously with the spar molding.

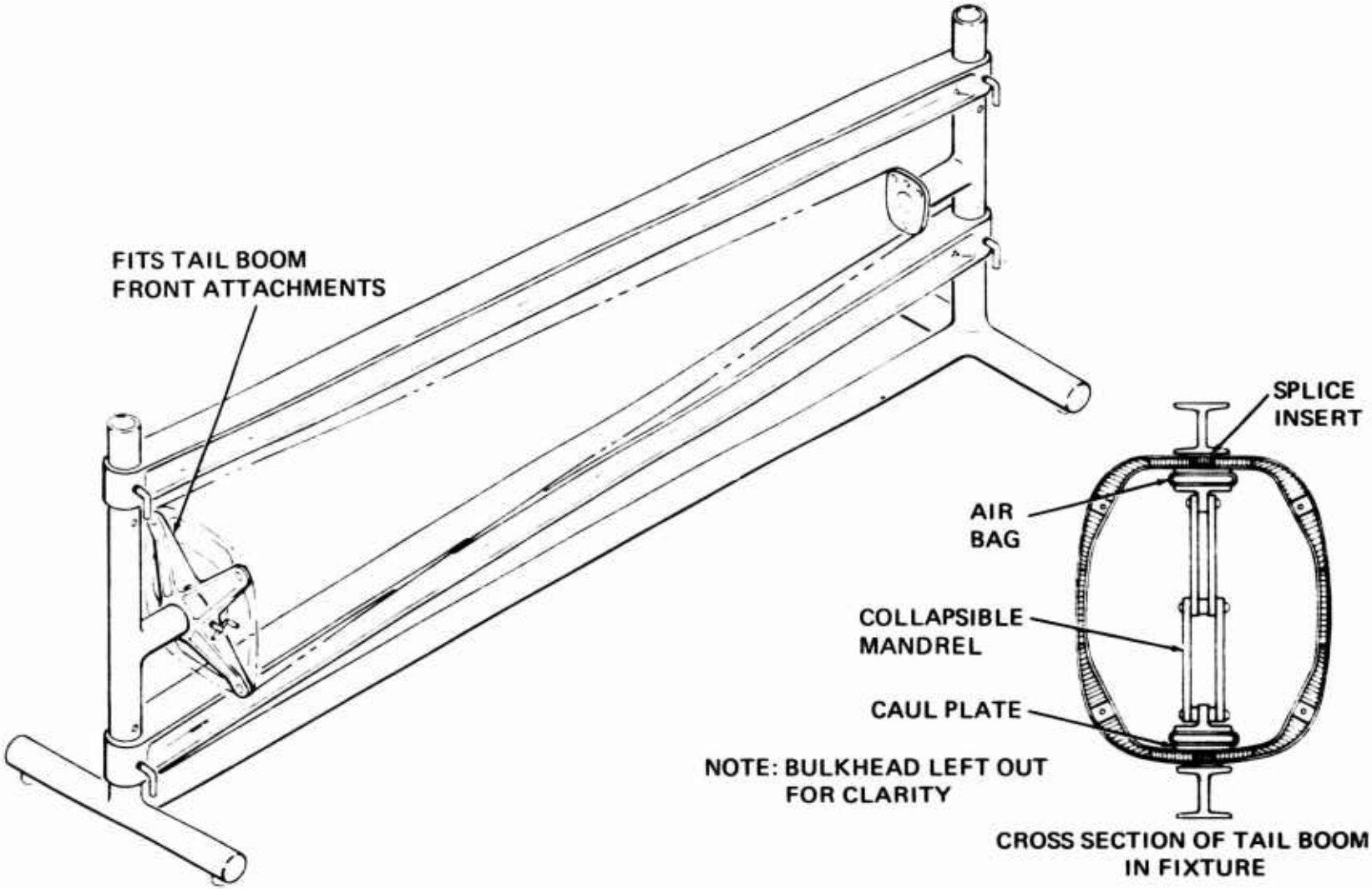

Figure 24. Assembly Fixture for Tail Boom.

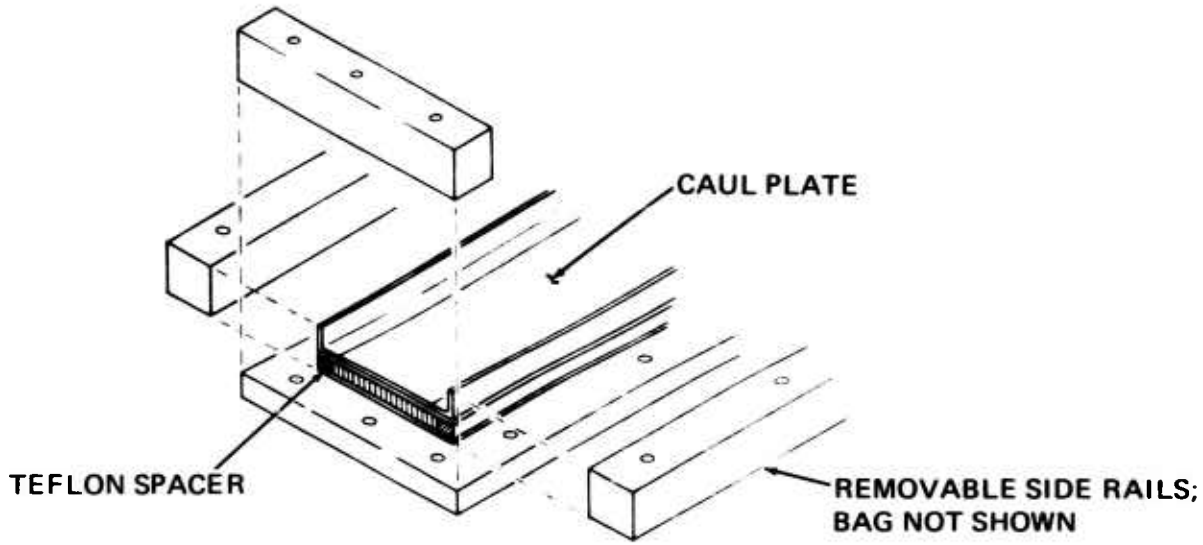

Figure 25. Fabrication of Vertical Fin Front Spar.

The torque box sides are made in the female shell mold with suitable inserts, as are the removable inspection plates, and all are made by the co-cure process.

The torque box is assembled with the corner angles, adhesive, pressure bag and inspection plates in place and positioned in the female mold, with inserts as shown in Figure 26. Moderate pressure is applied to the internal bag to assure proper matching of the torque box to the mold. After adhesive cure, the box is removed from the mold, leaving the bag temporarily in place.

The aft trailing-edge section of the fin can be made two ways. Assuming a fully machined honeycomb core, the raw skin laminate and a layer of sheet adhesive can be placed in the lower mold half; the honeycomb and a leading-edge spacer block are next positioned along with the trailing-edge wedge as a means of anchoring the trailing edge of the honeycomb. The top layer of adhesive and skins is finally laid up on the honeycomb. A top caul plate is added, and the assembly is bagged and autoclave cured in one shot. An alternate approach is to use unmachined honeycomb, but of a uniform wedge shape, and to bag this down to the first skins and adhesive, cure, and then machine the opposite side of the honeycomb. The final skin is added and cured in the lower mold with a caul plate. The latter method simplifies honeycomb machining but adds an extra autoclave operation. Both methods have been used at Boeing Vertol.

The trailing-edge section of the fin would be joined to the torque box with adhesive, positioned in the lower half of the mold, a caul plate added, and the assembly bagged. Cold cure can be under vacuum pressure with the torque box internal bag balancing the external pressure. Hot bonding of this joint is also feasible.

After removal of the torque box bag, the ribs can be bonded in and the outboard fitting and other details added.

BOOM AND FIN ASSEMBLY

The tail boom and the fin would be positioned in a suitable alignment fixture (Figure 27). After alignment, the necessary holes are to be drilled, the fin removed and all prebonding cleaning carried out.

After applying adhesive, the fin is to be repositioned in the jig. Secondary fasteners will apply pressure to the joints and the primary fasteners added at the trailing-edge spar fitting. The tail cone is to be bonded in place along with secondary fasteners.

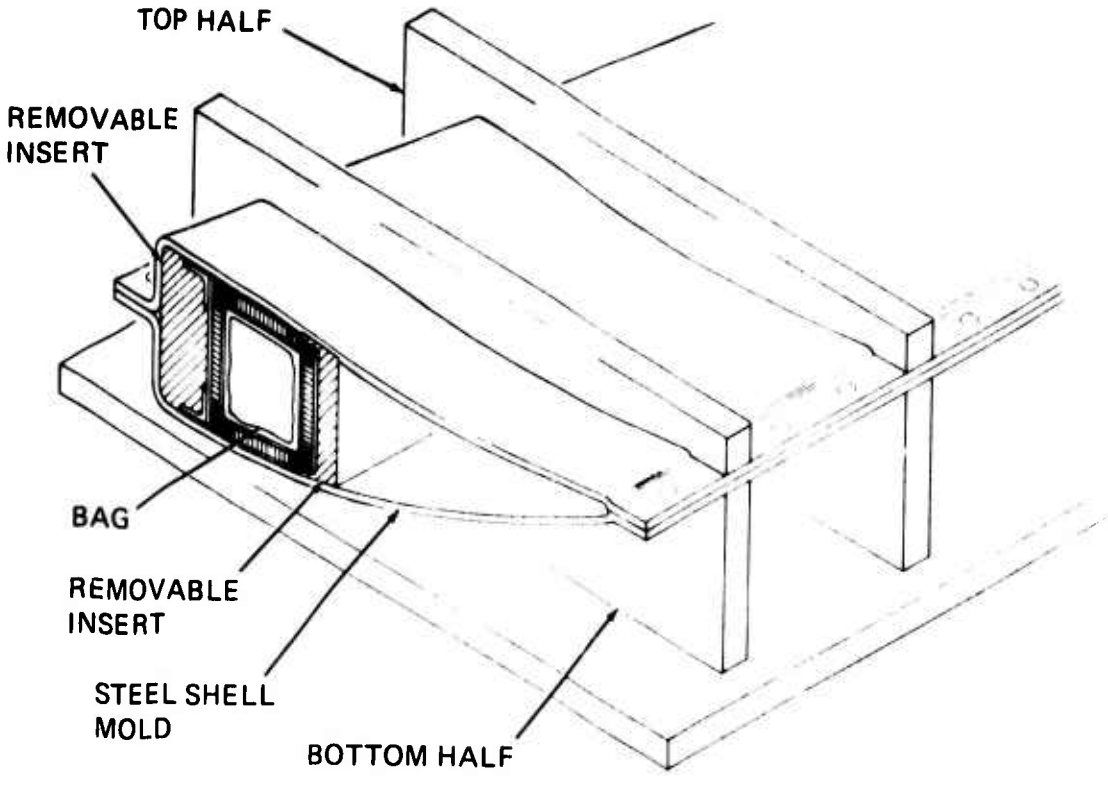

Figure 26. Fabrication of Vertical Fin Torque Box.

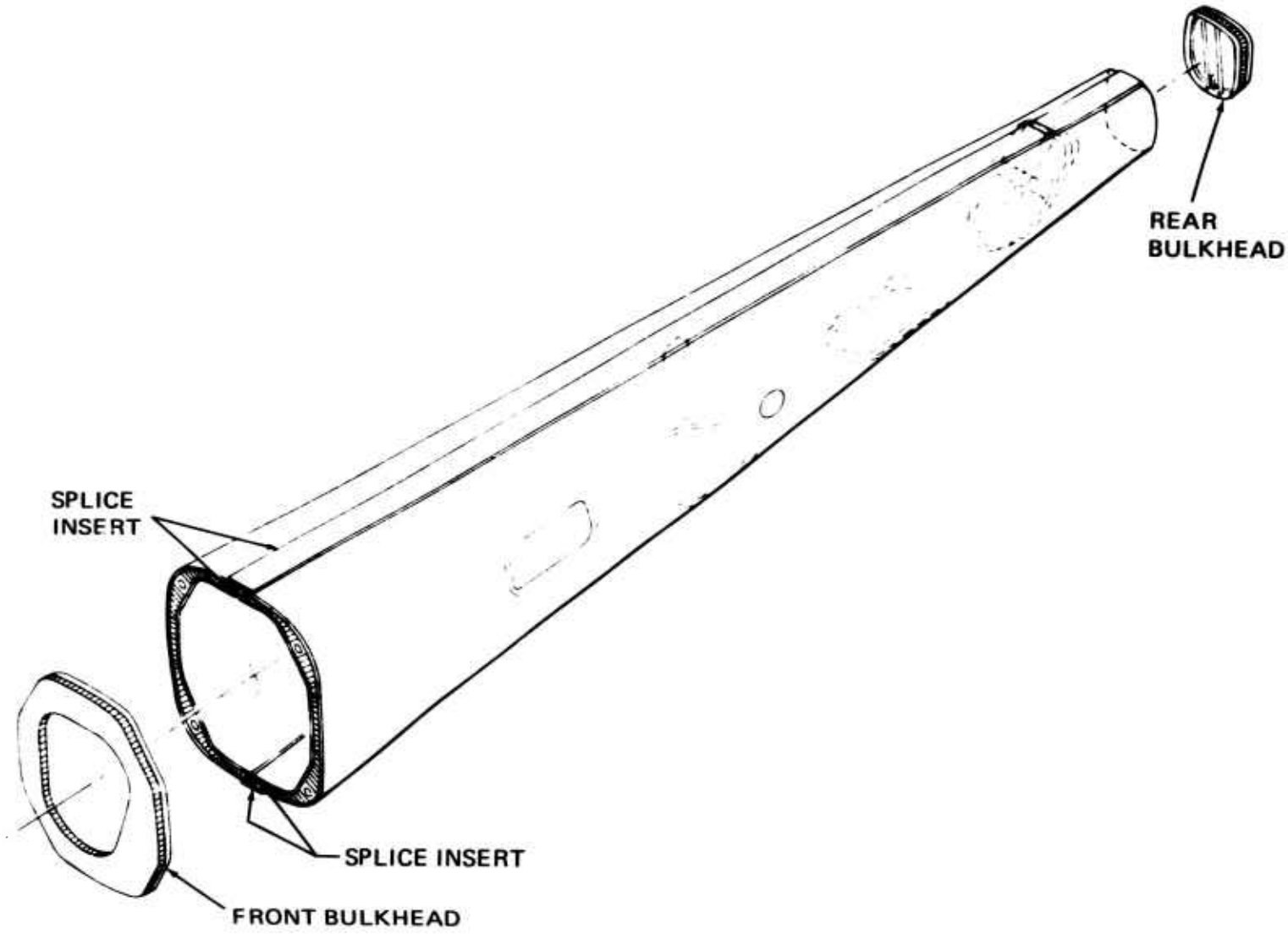

Figure 27. Tail-Boom Assembly.

STRUCTURAL CONFIGURATION OF CONCEPT 1, MONOCOQUE SANDWICH CLAMSHELL

TAIL SECTION

The tail section comprising the tail-boom shell, with integrated vertical fin and tail-cone fairing, is shown in Figure 10 and is the same envelope as the existing Cobra AH-1G tail section. It is a functional, damage-resistant, structurally efficient design using advanced concepts and composite materials throughout. The proposed arrangement is exceptionally simple, affording minimum parts count with low cost, and is oriented toward quantity production fabrication processes.

The design logic pertaining to this particular concept is based on the following:

- Placed first in the parametric trade-off study out of a possible eight configurations

- Simplest design to make, with the least number of parts, and facilitates mass production techniques

- Lightest weight of all the concepts; pure monocoque, all-bending and shear loads taken by shell, no stabilizing frames required

- Utilizes predominantly graphite type-A material

    1. Readily available in production quantity

    2. State-of-the-art material and numerous data points and test samples available

    3. Low priced

    4. Excellent strength and stiffness characteristics

    5. Superior fatigue qualities compared to most metals

- Problem of susceptibility of graphite to low-velocity damage overcome by the use of woven glass ply discretely placed in shell cover lay-up and a thin outer scuff ply. Samples have survived a 2-inch-diameter 1-pound ball drop from approximately 30 feet.

TAIL BOOM

The primary structure is designed as a semimonocoque composite sandwich concept with minimal bulkheads situated at the forward

and rear ends of the shell, with a third bulkhead canted to line up with the vertical stabilizer front spar. The tail boom is a straight-line element configuration and consists of graphite type-A inner and outer skins sandwiching a Nomex core. A unique feature of the proposed design is the fine-tuning capability, whereby critical bending stiffness modes can be accurately tailored to satisfy dynamic response requirements by the discrete placement of graphite HM reinforcing doublers longitudinally at four quadrants on the inner skin. At the forward end of the shell, a lay-up of predominately 90-degree and ±45-degree ply circumferential doublers on the inner and outer skins performs the dual role of shear-diffusing concentrated loads from the four main fuselage attachments into the shell, and boosting shell peripheral bending stiffness to suitably react the moment generated due to the unavoidable offset of the fitting bolt center from the sandwich shell centroid. (See Figure 28.)

The tail-boom structure incorporates three large access panels of identical size, located in the same positions as on the original metal version. The panels are fastened with bolts and anchor nuts and are constructed in sandwich form similar to the basic shell. These panels are considered to be load-carrying, but in order to ensure against local stress concentrations in the skins surrounding the panel, a system of "doily" configuration reinforcing mats with multi-oriented layups is built into the surrounding area, being interposed between the shell skin plies during initial lay-up. (See Figure 29.)

The forward and rear bulkheads are of sandwich construction with graphite type-A covers over Nomex core. The canted bulkhead, in order to satisfy interface requirements with fin front spar and tail bumper anchorage, is designed in graphite type-A as a conventional web-and-flange bulkhead but is split in two halves to enable a half segment to be easily and accurately assembled in each clamshell prior to joining the halves. The forward bulkhead has a large access hole in its center which matches the existing Cobra AH-1G bulkhead. At the four main bolt attachment positions, the honeycomb bulkhead is recessed locally to allow the attachment fitting forward end to nest up to the bulkhead web.

FUSELAGE/TAIL-BOOM ATTACHMENT

The tail boom will be structurally attached to the fuselage at the four existing bolt positions on the rear fuselage frame of the Cobra AH-1G.

The two types of attachments (see Figure 10) are a metal insert and an integral loop-wound composite.

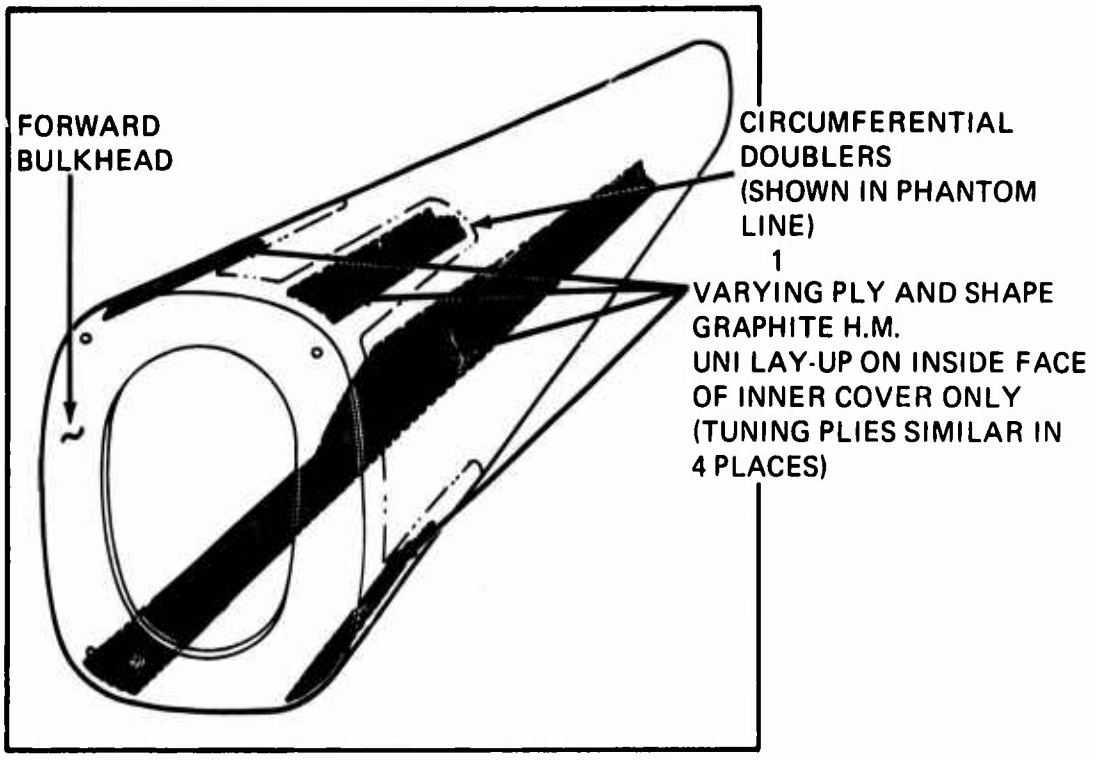

Figure 28. Structural Tuning System and Circumferential Doublers.

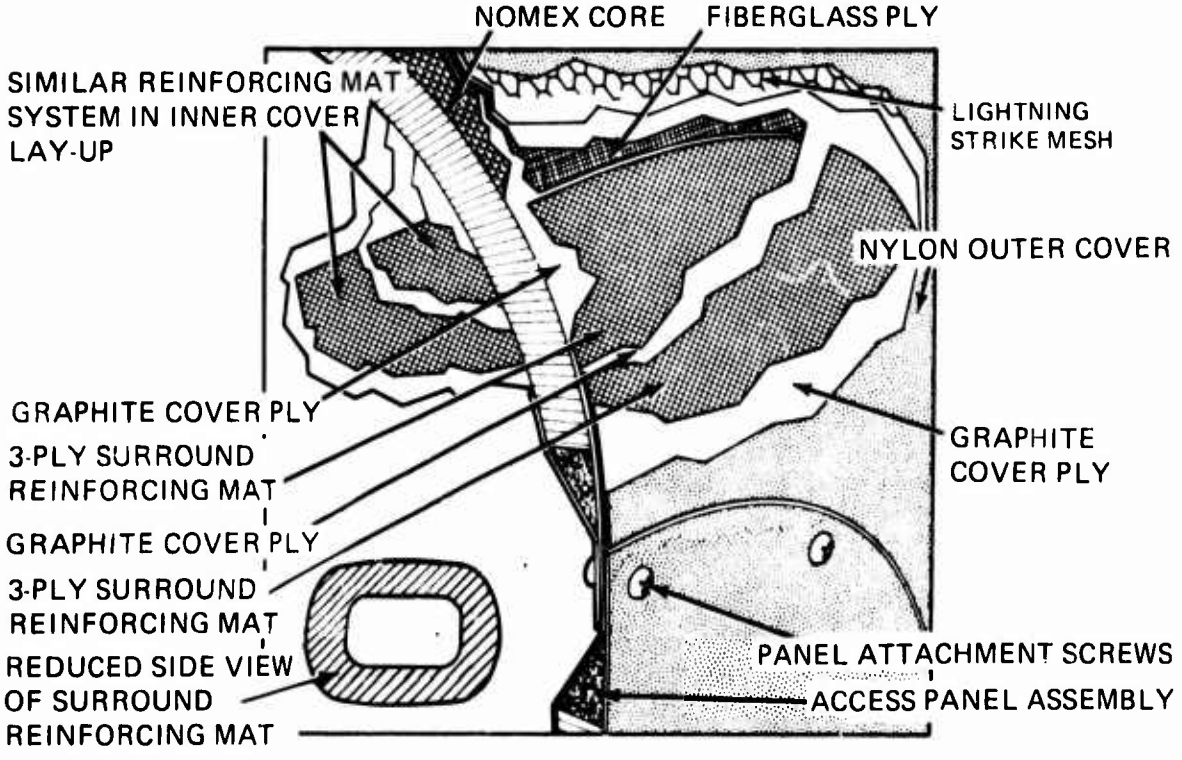

Figure 29. Access Panel Surrounding Reinforcement.

1. Metal Insert

This is designed as a titanium machined fitting consisting, at its forward end, of a block bored to take a barrel nut with, to the rearward, two flat grown-out legs that locate against the inner and outer cover reinforcings. The Nomex core, which is increased in thickness over the general area of the attachment, is removed locally in way of the fitting. Primary attachment of the fitting is by bonding at inner and outer reinforcings and at the bulkhead, but mechanical attachments are also added for fail-safe designs to carry up to limit load in the event of major bond failure. However, the fitting is integral with the sandwich shell and cannot be removed once assembled.

2. Integral Loop-Wound Composite

This is a more advanced design (see Figure 30) which is lighter than the metal/fiberglass arrangement and promises to be a less fatigue-prone joint. This fitting, like the metal insert, cannot be removed once assembled.

Each loop fitting is integrated into the shell at a locally thickened segment with tapered fiberglass channels bonded onto each side of the fitting to transfer loads into the graphite skins of the shell, again via the more forgiving medium of a fiberglass member.

The actual loop fitting is made up of a number of unidirectional tapes bonded together in an elongated horseshoe configuration that loops over and bonds to a titanium bush fitting, which accommodates a barrel nut. This fitting locates at the loop end of the lay-up with a bush protruding through the composite material for the main bolt attachment. The fitting is flat at its rear end so as to bear against a bonded inner block of composite material of varying orientation, which is capable of reacting compression loads from the fitting. A titanium bearing pad at the front of the loop completes what is considered to be a primary bonded subassembly.

After bonded installation of the loop fittings for fail-safe purposes, a system of blind rivet attachments is incorporated through the sandwich skins into the channel flanges on each side capable of carrying up to the limit load in the event of major bond failure.

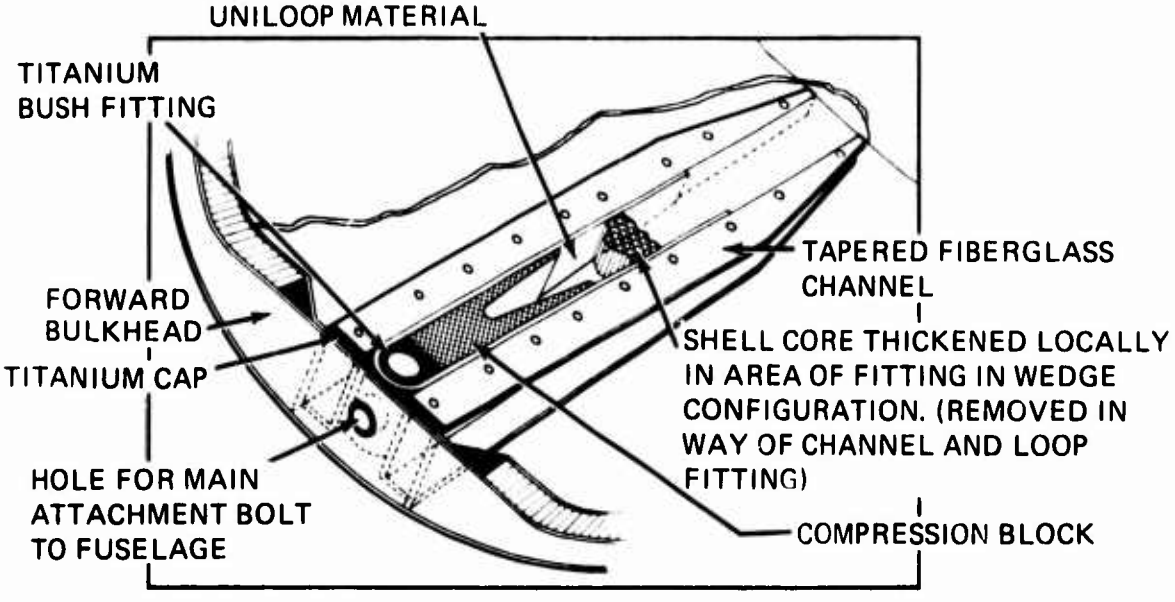

Figure 30. Main Attachment Fitting, Composite Integral Loop-Wound Concept.

The secondary structure proposed in the tail boom comprises the following:

1. Avionics shelf support structure, BS80 to BS122, consisting of longitudinal members bonded to the shell on each side and cross-beam channels, all of fiberglass construction (SP250 SF 1 system). (See Figure 31.)

2. Avionics support structure, BS41-32 - BS67 (for mounting of transponder, etc.). It is proposed to utilize the existing metal support structure and to modify the beam ends to make suitable bonded and mechanically fastened connections to the shell inner surface.

3. Elevator control rod support brackets. Independent rigidized brackets in S-Glass SP250 SF 1 material bonded to the inner shell simulating existing brackets grown from the frame are proposed. These are located at four positions on the left side of the shell, with two holes accurately located for fitting the existing bolt on guide fittings. (See Figure 32.)

4. Tail rotor control rod support brackets. Brackets similar to those described in 3 are located in three positions and again have two holes located for mounting the existing guide fittings.

5. Elevator support structure. The honeycomb core is increased in thickness locally, and a slotted hole is introduced in the shell similar to the existing metal arrangement. The periphery of the hole is consolidated with pot filler, and a graphite doubler system is added to the exterior surface and also the inside face of the inner cover. Delron inserts are let into the shell and set in position with pot filler at six places to match the elevator support assembly bracket. Existing elevator support brackets then bond directly on to the shell via Delron inserts. (See Figure 33.)

6. Drive shaft hanger attachment. Anchorage for the four attachment screws locating the lower section of the hanger fitting is made by locating Delron inserts into hardpoints built into the shell by pot filler disks, replacing honeycomb core in way of the attachment hole. Existing hanger fittings and shim blocks are used but longer attachment screws are required. (See Figure 34.)

7. Intermediate gearbox mounting. Delron inserts in pot filler similar to the hanger attachment are located at four places matching the gearbox attachments. Fiberglass backing members bonded to the inside surface of

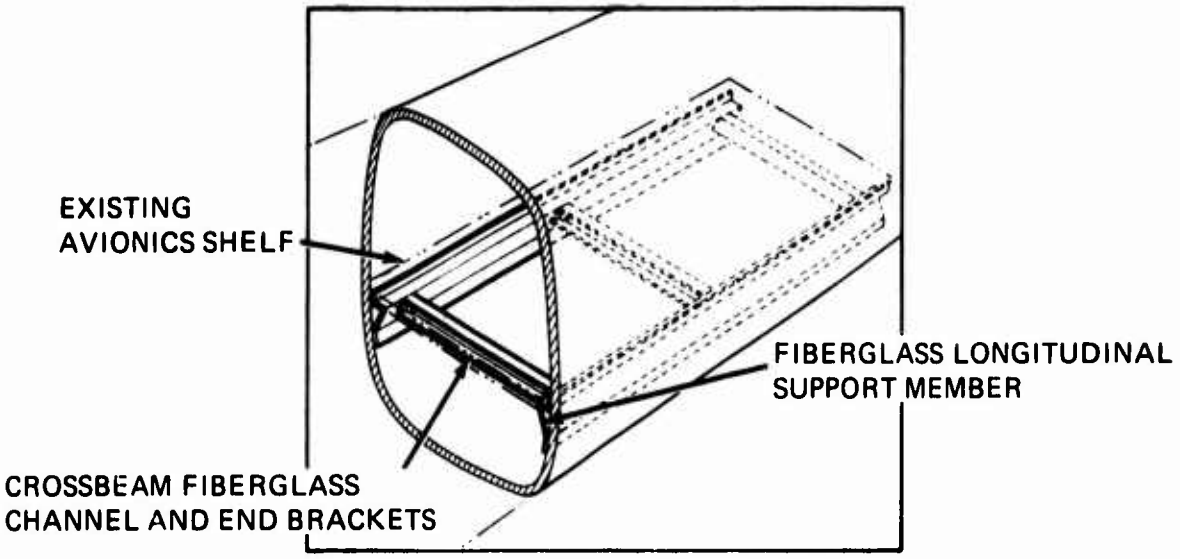

Figure 31. Avionics Shelf Support Structure.

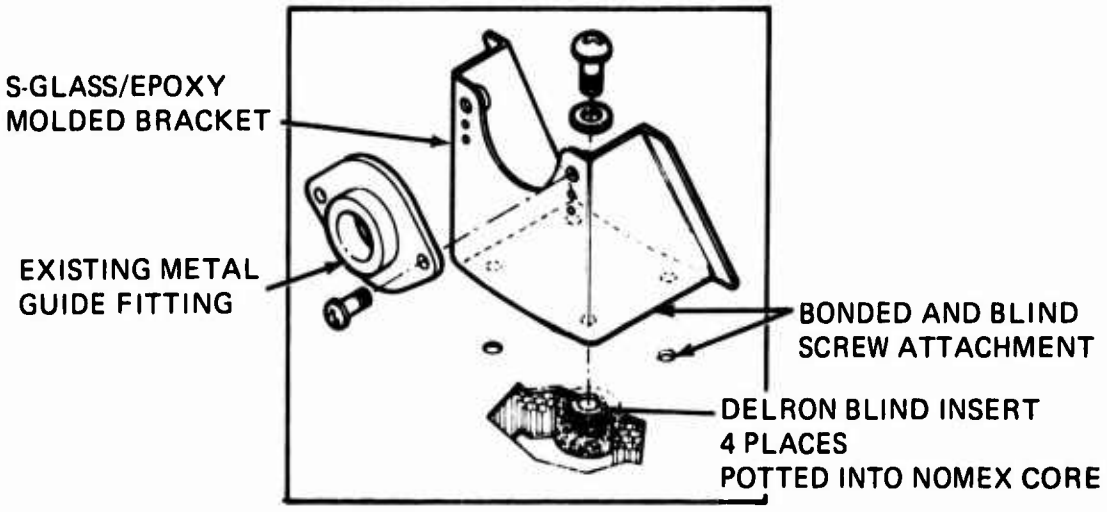

Figure 32. Elevator and Tail Rotor Control Rod Support Bracket (Typical).

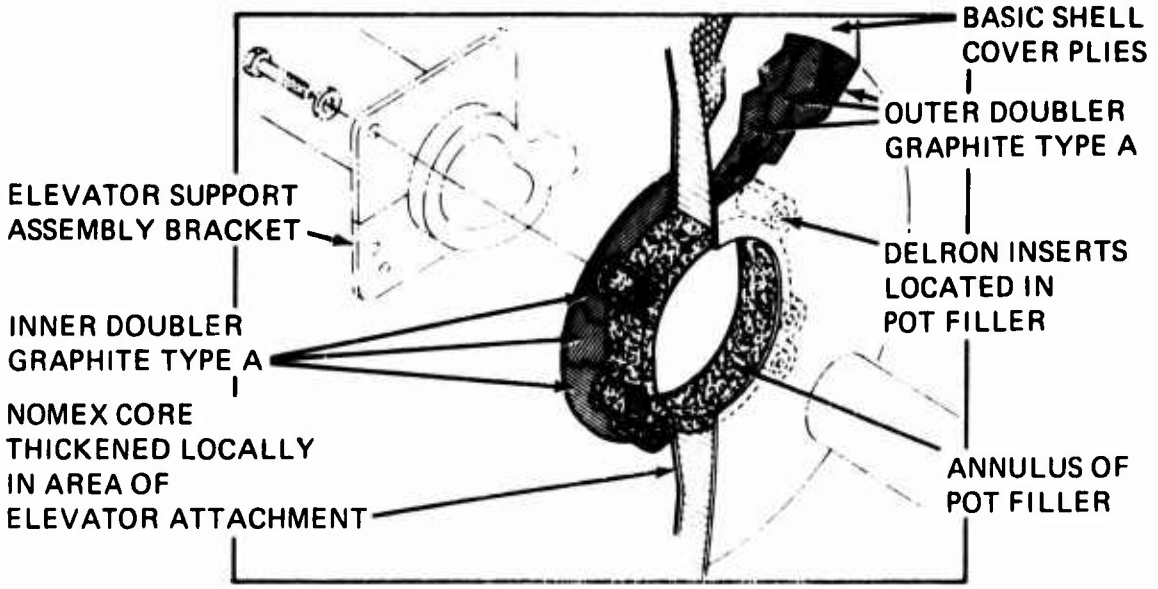

Figure 33. Elevator Support Structure.

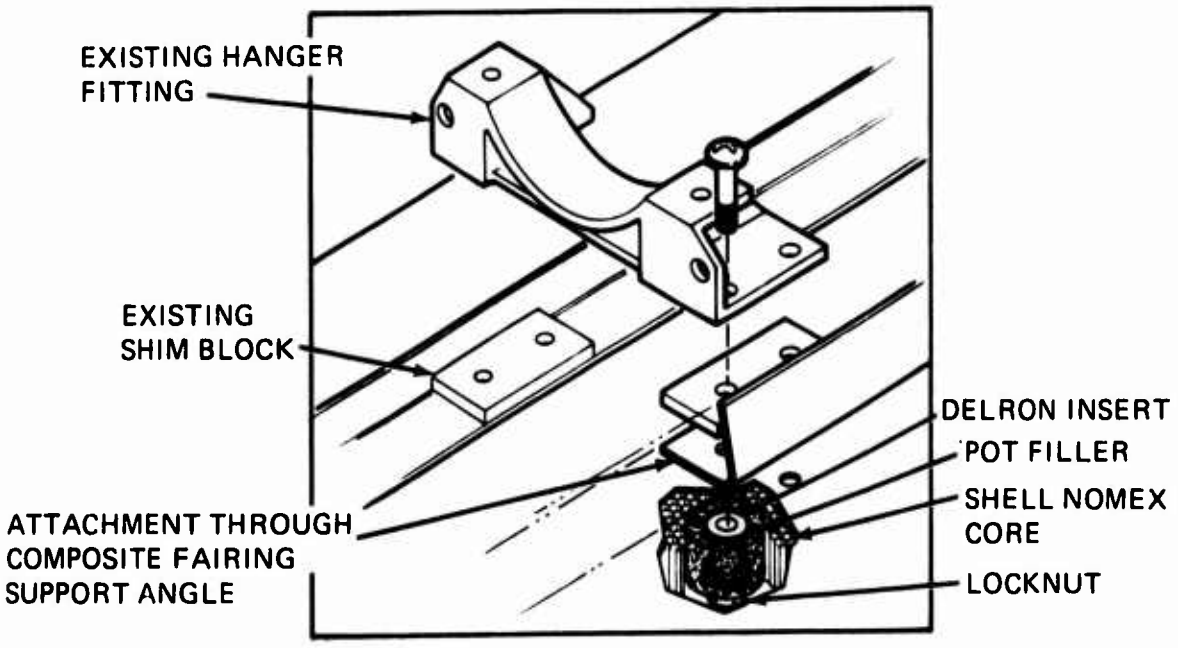

Figure 34. Drive Shaft Hanger Attachment.

the shell pick up gearbox bolt holes and consolidate the mounting. (See Figure 35.)

8. Handling tube assembly. Existing tube assembly will be mounted to the tail-boom shell in a manner similar to the drive shaft hanger attachment. Four bolthole attachments are provided in the shell using the Delron insert and pot filler by the method described in item 6 above.

9. Tail rotor control quadrant mounting member. This assembly is proposed as an S-glass molding stiffened at selected positions by the addition of graphite type-A unilaminates. The attachment to the shell will be similar to the drive shaft hanger with attachment holes provided in the shell, using Delron insert and pot filler by the method as described in item 6 above.

10. Access in tail-boom rear bay. A load-carrying access panel is provided in the side of the tail-boom at the rear end, midway between the canted bulkhead and end bulkhead, for access to skid attachment fittings and general inspection in the bay. The panel construction in sandwich form will be the same as the other three main access panels in the tail boom and will be attached in a similar manner using screws and nutplates. A system of reinforcing mats will be introduced in the local skin surrounding the access hole similar to the other skin edge reinforcements previously described.

SCUFF AND EROSION PROTECTION

As shown in Figure 36, a one-ply nylon or other suitable material cover is bonded over the exterior tail boom and vertical fin composite areas to fulfill the following functions:

- Form a tough, durable exterior surface to absorb local scuffing and lacerations.
- Produce a smooth surface over the lightning strike mesh and protect the mesh from damage and corrosion.
- Protect the primary structural graphite and prevent erosion.

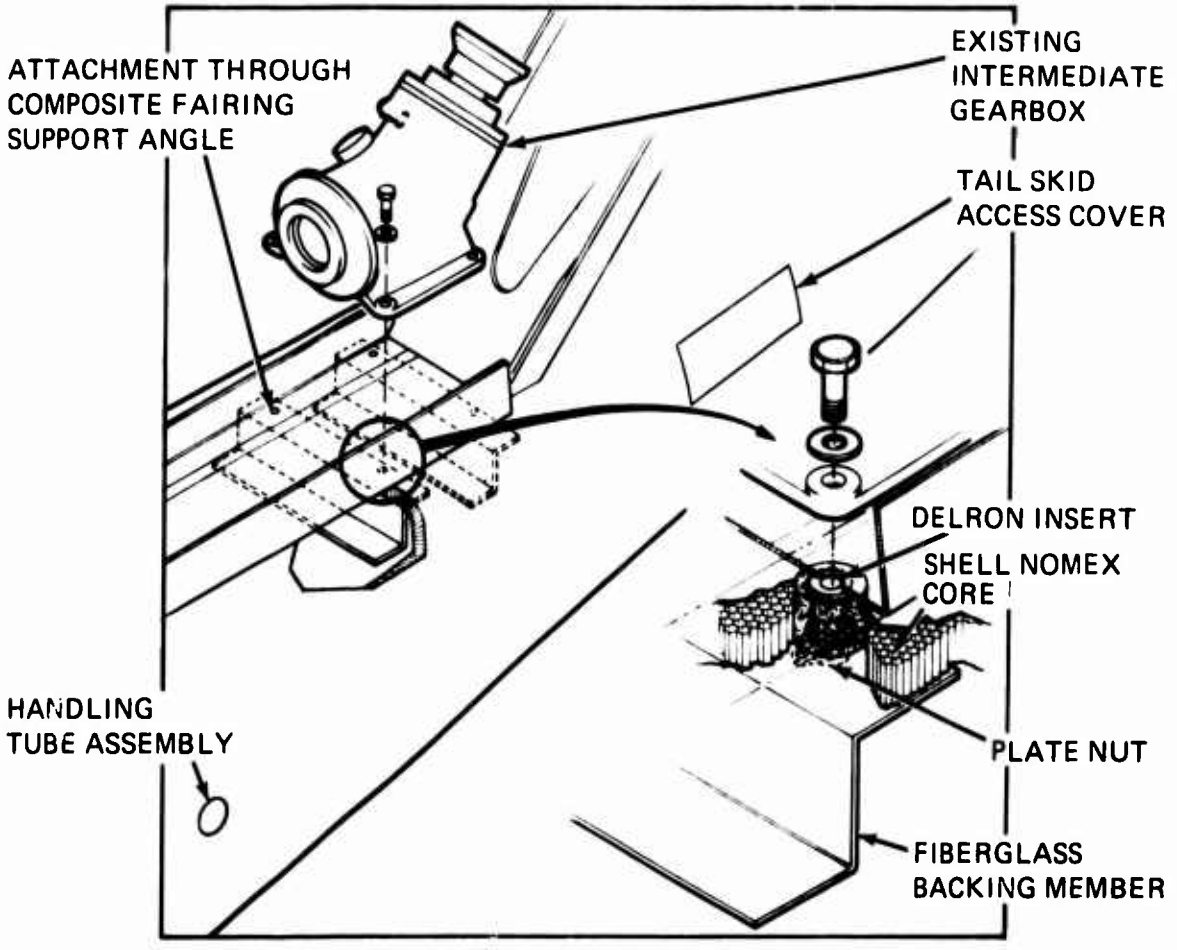

Figure 35. Intermediate Gearbox Mounting.

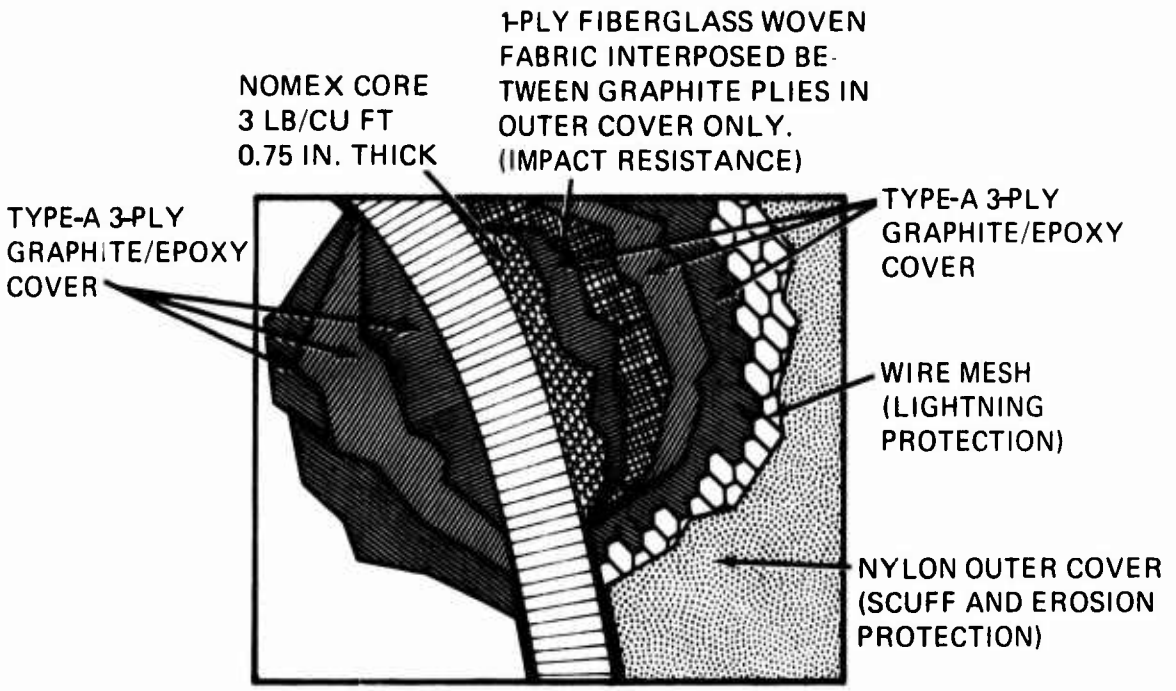

Figure 36. Basic Shell Construction.

TAIL-CONE FAIRING

Since this component is of compound curvature, it is designed as a single-skin graphite type-A molding stabilized by a system of ripple stiffeners. The fairing is bonded to the tail boom and fin structure and is load-carrying. Vertical and torsional loads are reacted from the fin and diffused into the tail boom at the rear bulkhead.

Access is provided at the lower forward edge of the fairing for removal of the tail bumper, and another panel centrally positioned allows access for inspection and minor repairs.

VERTICAL FIN

The fin arrangement is a straight-line element concept comprising a primary structural torque box and trailing-edge assembly. The fin attaches to the tail boom via a front spar splice channel and a rear spar fitting, also at its lower sides, left and right,by bonded shear angles.

The primary structure is a front and rear sandwich spar with interconnecting side panels,also of sandwich construction, which make up the primary fin torque box. The spar caps are graphite type-A molded 'L' section comprising primarily unidirectional laminations running spanwise down the length of the fin spar. Further graphite type-A molded angles are nested progressively in the locality of the front spar root end.

The sandwich arrangement of both spars and side skins consists of inner and outer graphite type-A skins over Nomex core. At the front spar the web flanges are facing back, and a doubler strap of graphite type-A extends over both the flanges of the spar cap and the web angle on each side, which augments the cap, and forms a rigid land for the side-panel connections to the rear of the spar; it also forms an extension skin forward of the spar on the left-hand side for the location of fastener receptacles for the nose fairing attachment and on the right-hand side for fastening the fairing hinge.

The skin in the rear spar locality is set back to allow the trailing-edge assembly to fit flush, comprising graphite type-A side skins bonded to a full-depth Nomex core which tapers down chordwise to nest into a trailing-edge graphite member. At tip and root ribs, graphite moldings seal off the Nomex core, top and bottom, and distribute the torque loads.

Superior structural efficiency is achieved with the integrated torque box arrangement which allows a greater portion of useful skins to work in compression, thus relieving the bending loads in both spars.

The front and rear spar cap sectional area is increased progressively down to the root of the spar by increasing the width of the cap legs. This serves the twofold purpose of meeting the maximum bending moment condition occurring at the fin root, and also facilitating diffusion of bending loads from the side panels of the torque box into the front and rear spars over the lower few inches, since the tail-boom shell at the interface with the fin has no backup structure capable of taking vertical loads between bulkheads.

Lateral bending loads from the fin front spar are carried across the tail-boom/fin joint by a splice channel with tapering-thickness walls which are at maximum thickness at the termination of the four fin cap members.

The bonded joint channel, in turn, distributes loads into the canted bulkhead webs, where it is sheared into the shell skins via the bonded bulkhead flanges. (See Figure 37.)

Access into the torque box on the left side is afforded by two spanwise load-carrying doors attached in a manner similar to that of the tail-boom panels.

VERTICAL FIN ATTACHMENT TO TAIL BOOM

An arrangement which allows an integral-type fin-to-tail-boom joint is designed with the advantage that the complete stabilizer structure may be fabricated as an independent assembly to ease manufacturing problems and to facilitate production before assembly onto the tail boom. The fin front spar is joined to the tail boom by means of a separate graphite joint channel which locates simultaneously on the forward face of the spar web and forward face of the tail-boom canted bulkhead, forming a simple splice joint. (See Figure 37.) At the rear spar a three-pronged fitting in metal or, alternatively, graphite forms the joining medium between the rear spar web and the aft bulkhead of the tail boom. The third leg of the fitting attaches to the fin root rib. (See Figure 38.)

Longitudinal drag loads from the fin are transferred into the tail-boom structure via a shear angle bonded around the fin lower contour, on each side, onto the skin. (See Figure 37.)

The described fin-to-tail-boom joints at the front and rear spars are primarily bonded with a fail-safe mechanical fastener system to carry up to the limit load in the event of subsequent bond failure.

A graphite type-A molded joint angle comprising unidirectional and cross-plied laminations is secondary bonded to the tail-boom shell and joint channel on assembly of spar. This member reinforces the skin around the cutout for the front spar joint angle and also effectively seals off the hole.

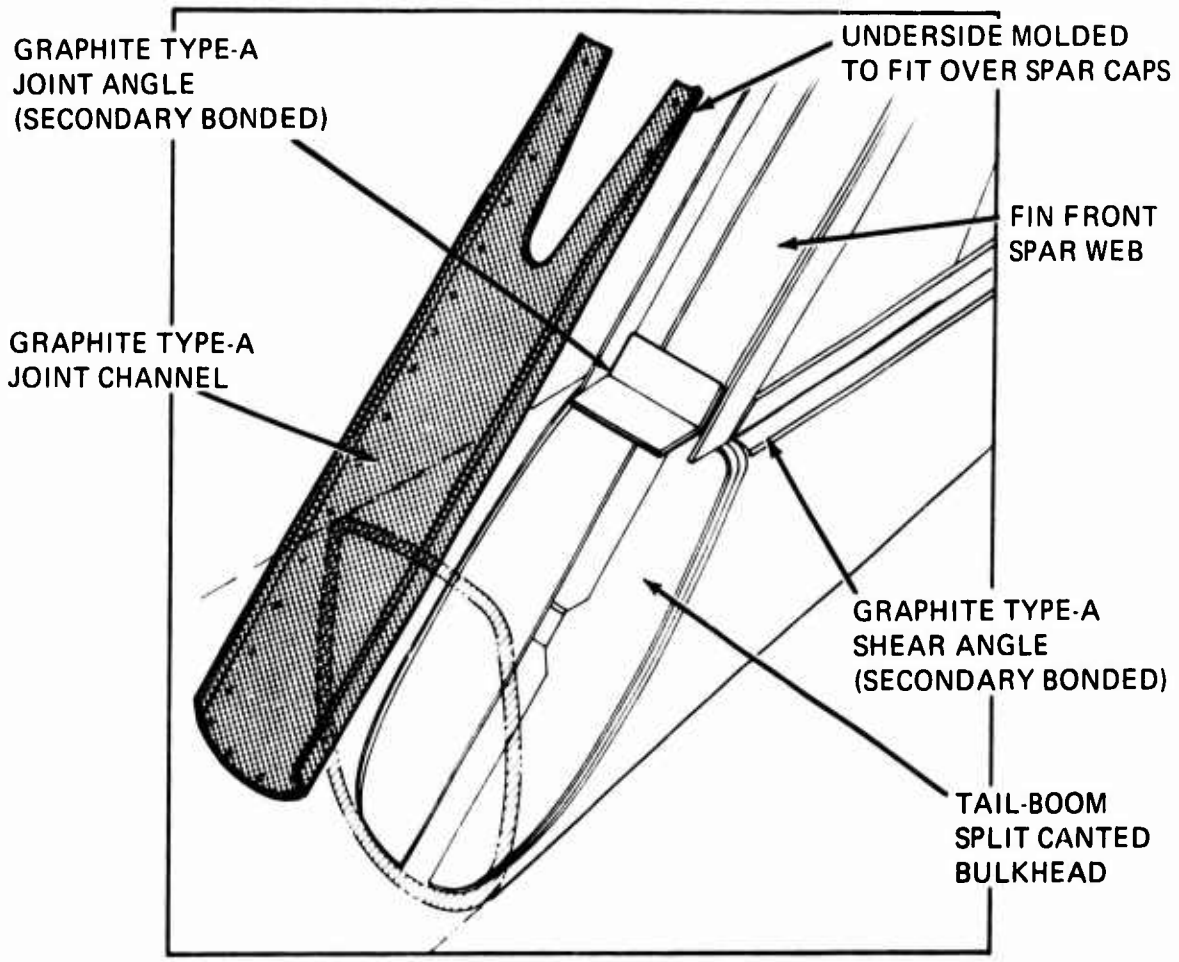

Figure 37. Front Spar-to-Tail-Boom Splice Joint.

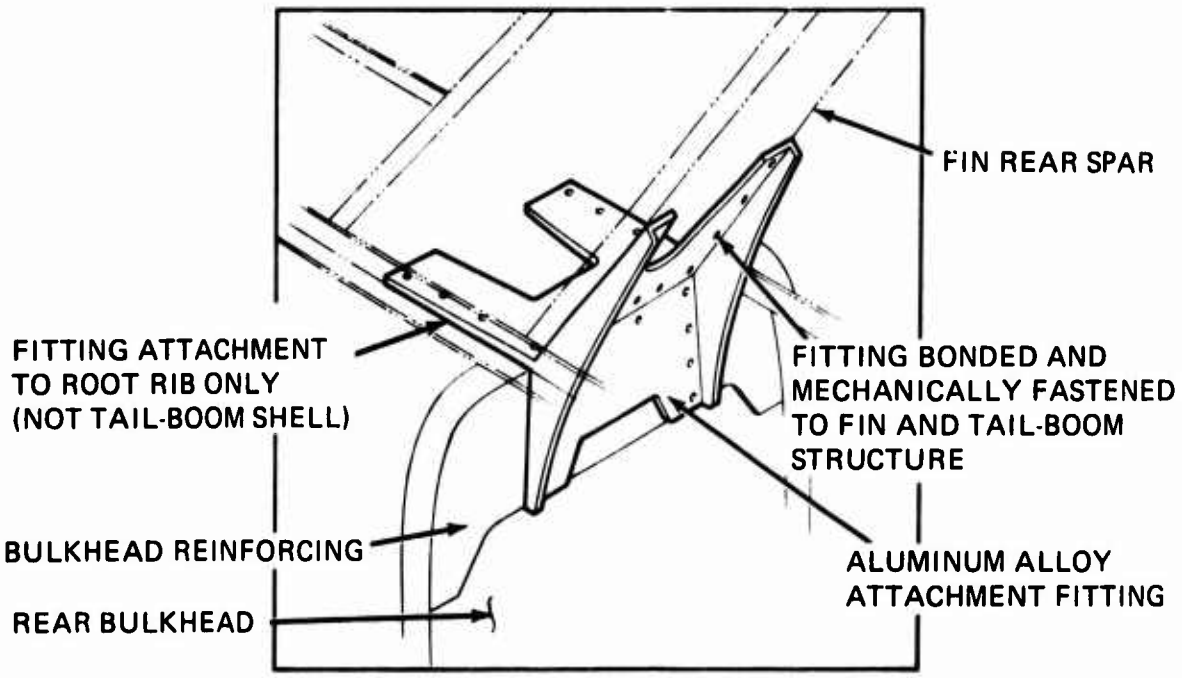

Figure 38. Rear Spar/Tail-Boom Bulkhead Attachment Fitting.

TAIL ROTOR SUPPORT

The tail rotor drive box is supported by the existing metal support fitting, which is cantilevered from the front spar and is mechanically attached to the composite structure in a manner similar to its metal counterpart.

A graphite torque box rib located in line with the top of the support fitting connects to the front spar via an aluminum alloy fitting and carries in-plane torque loads into the box. The main support fitting also redistributes the rotor torque and thrust loads into the fin structure through mechanical attachments at the front spar. (See Figure 39.)

An aluminum alloy fitting is used at the rib/spar intersection because of the magnitude of the combined loading felt by the fitting flange and the possibility of peeling problems if using a composite molded fitting.

Secondary Structure - Existing metal parts will be used for the upper fin leading-edge skin and fin tip fairings.

Control Attachment Points - Upper and lower pulley bracket assemblies for the tail rotor controls will be attached to the vertical fin front spar by bolting, similar to the existing arrangement, through the spar. SP250 SF 1 fiberglass angles are bonded on the rear face of the spar in line with these attachments, and the core is consolidated around the bolt holes by insertion of pot filler.

VULNERABILITY ASSESSMENT FOR TAIL SECTION

The proposed design is considered to be virtually invulnerable to nonexploding rounds up to and including 23mm. Vulnerability reduction is enhanced by the use of fiberglass in the matrix with the graphite. Such a mixture tends to isolate original ballistic damage to approximately the area removed. It also helps to prevent rapid propagation of damage due to high elongation to failure. Vulnerability to the large nonexplosive rounds may be expected only in small localized areas such as the fuselage attachment points, and even these can be improved by judicious detail design.

DAMAGE TOLERANCE

A recognized detraction to the use of relatively thin graphite skins for the basic tail boom and vertical fin covers is the poor resistance of the material to low-velocity impact. Whereas a projectile impacting at high velocity punches a clean hole through a graphite/epoxy skin supported by a

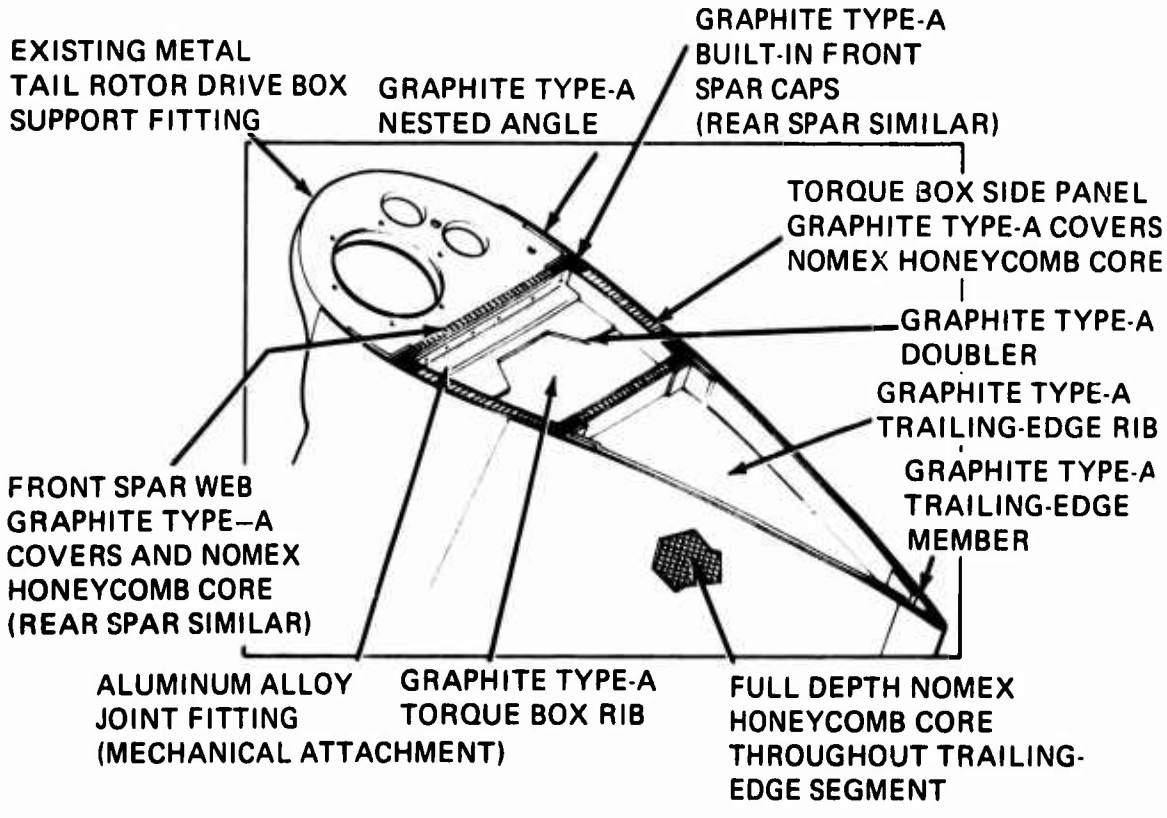

Figure 39. Upper Torque Box and Trailing-Edge Rib Installation.

honeycomb core, a tool dropping from a few feet, or a carelessly handled rifle butt, could inflict damage such as cracked or punctured skins and dented honeycomb core. This vulnerability to low-energy impact is unacceptable for Army combat airframes.

Boeing Vertol has conducted research and tests on various materials and hybrid combinations to develop suitable sandwich floor and fuselage shell panels; Boeing Vertol has also conducted a wider-ranging investigation where other variables such as improved adhesive systems and special ply orientation have also been considered.

The proposed approach to solving this problem on the composite tail boom and vertical fin is as follows:

- Selection of a type-A graphite which is more damage-resistant than the HT and HM grades.

- Placement of one ply of Style 181 S-glass woven fabric interposed within the existing graphite outer skin.

- Selection of an adhesive compatible with the existing graphite matrix epoxy which gives improved impact qualities.

An 18-x-16-inch test panel representative of the tail-boom sandwich structure was made with graphite type-A covers sandwiching a 7/16-inch-thick Nomex core, 3 pounds per cubic boot density, 3/16 inch cell size. There were three graphite plies per cover, oriented 0^{o}, -45^{o}, and $+45^{o}$ (0^{o} ply nearest to core).

The panel was supported around its periphery to simulate built-in conditions, and a 1-pound ball was dropped on the approximate center of the cover. When the ball was dropped from a height of 8 feet, visible damage was noted in the form of a crack about 1 inch long across the orientation of the outer crossply, with a pronounced denting of the core below the crack.

An identical panel was then tested except that one ply of Style 181 S-glass woven fabric was interposed between the 0^{o} and -45^{o} plies during lay-up on the outer cover of the panel only.

The same 1-pound ball was dropped on the outer cover of this panel from 30 feet with no visible sign of damage to either the skins or the core.

This preliminary panel test indicates that considerable improvements in low-velocity impact resistance of graphite skins are possible with the discrete addition of fiberglass laminates. Charpy impact energy tests performed by R.H. Toland* have demonstrated considerable improvement in the energy required to fail a hybrid mixture of HTS graphite and S-glass, threefold in the case of such a laminate with 25 percent S-glass, as shown in Figure 40.

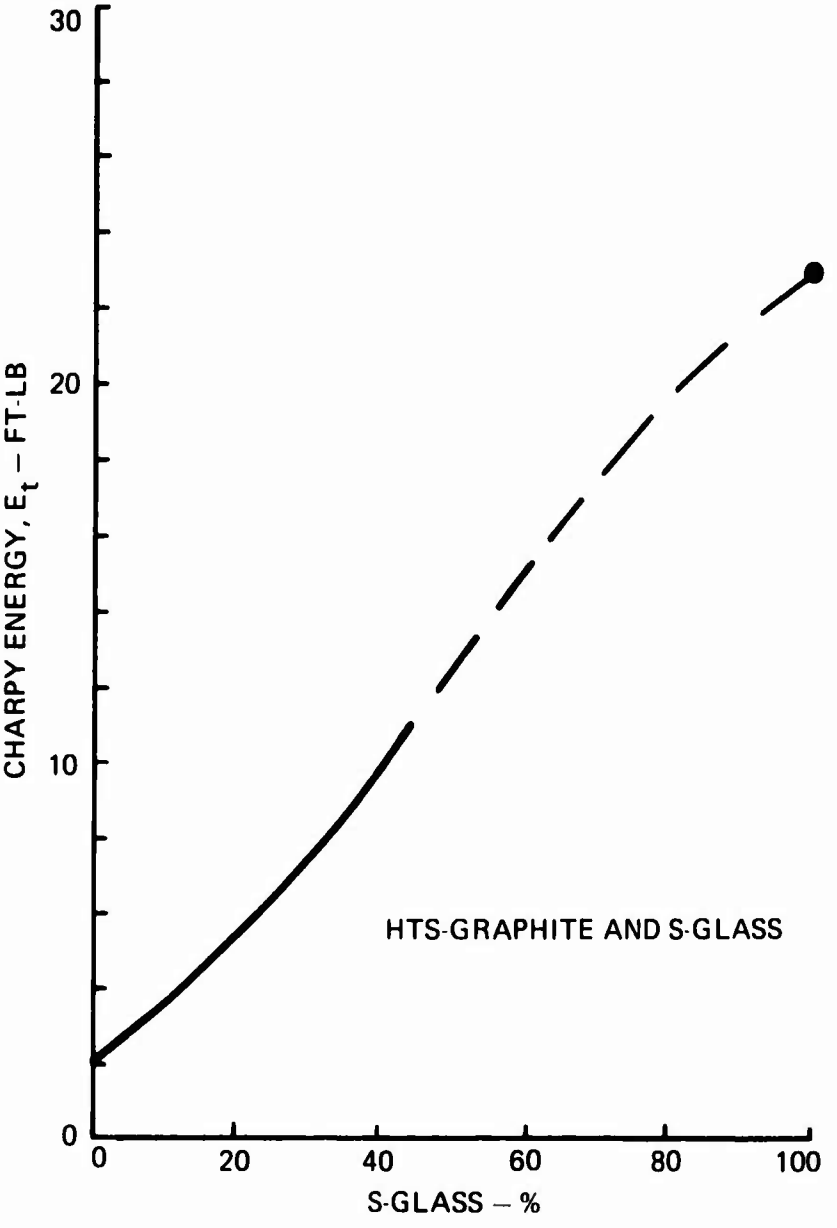

Figure 40. Charpy Impact Energy Relationship for a Hybrid Composite of Varied Proportions.

*Toland, R.H., FAILURE MODES IN IMPACT-LOADED COMPOSITE MATERIALS, AIME Symposium on Failure Modes in Composites, May 1972.

STRESS ANALYSIS - CONCEPT 1

METHOD OF ANALYSIS

The tail-boom shell is analyzed for bending and shear loading, with compressive bending combined with transverse and torsional shear being the most critical case. Preliminary analysis has shown the sides to be the most highly loaded. Due to the shallow curvature of the tail-boom sides, and to a lesser extent of the top and bottom, the compression and shear buckling allowable of the sides are determined considering the left and right sides to be flat panels simply supported at points Da and Ha, and Db and Hb, respectively (see Figure 41). Applied stresses and structural allowables are determined herein for a honeycomb shell with .018 in. GR/EP (Type A) facings; see Figure 42. The one-ply 181E-glass cloth added for damage tolerance decreases the laminate stress and increases the panel allowable and is, therefore, conservatively neglected in this analysis.

SIDE PANEL - COMPRESSION BUCKLING

The allowable compression buckling load per unit width of a sandwich panel as given in Reference (9), page 5-2, is

$$N_{cr} = K\pi^2 D/b^2 \tag{1}$$

The allowable compression buckling stress for an orthotropic panel with facings of equal thickness from equation (1) is

$$F_{cr} = \frac{N_{cr}}{2t} = \frac{K\pi^2 D}{2tb^2} \tag{2}$$

The bending stiffness is defined in Reference (9), page 1-5, and is given by the formula

$$D = \frac{E'th}{2\lambda} \tag{3}$$

where:

$$E' = \sqrt{E'_a \, E'_b} \tag{4}$$

$$\lambda = 1-\mu_{ab}\,\mu_{ba} \tag{5}$$

The additional parameters required to determine the buckling coefficient are stated in Reference (9), page 5-3.

$$U = G_c h \tag{6}$$

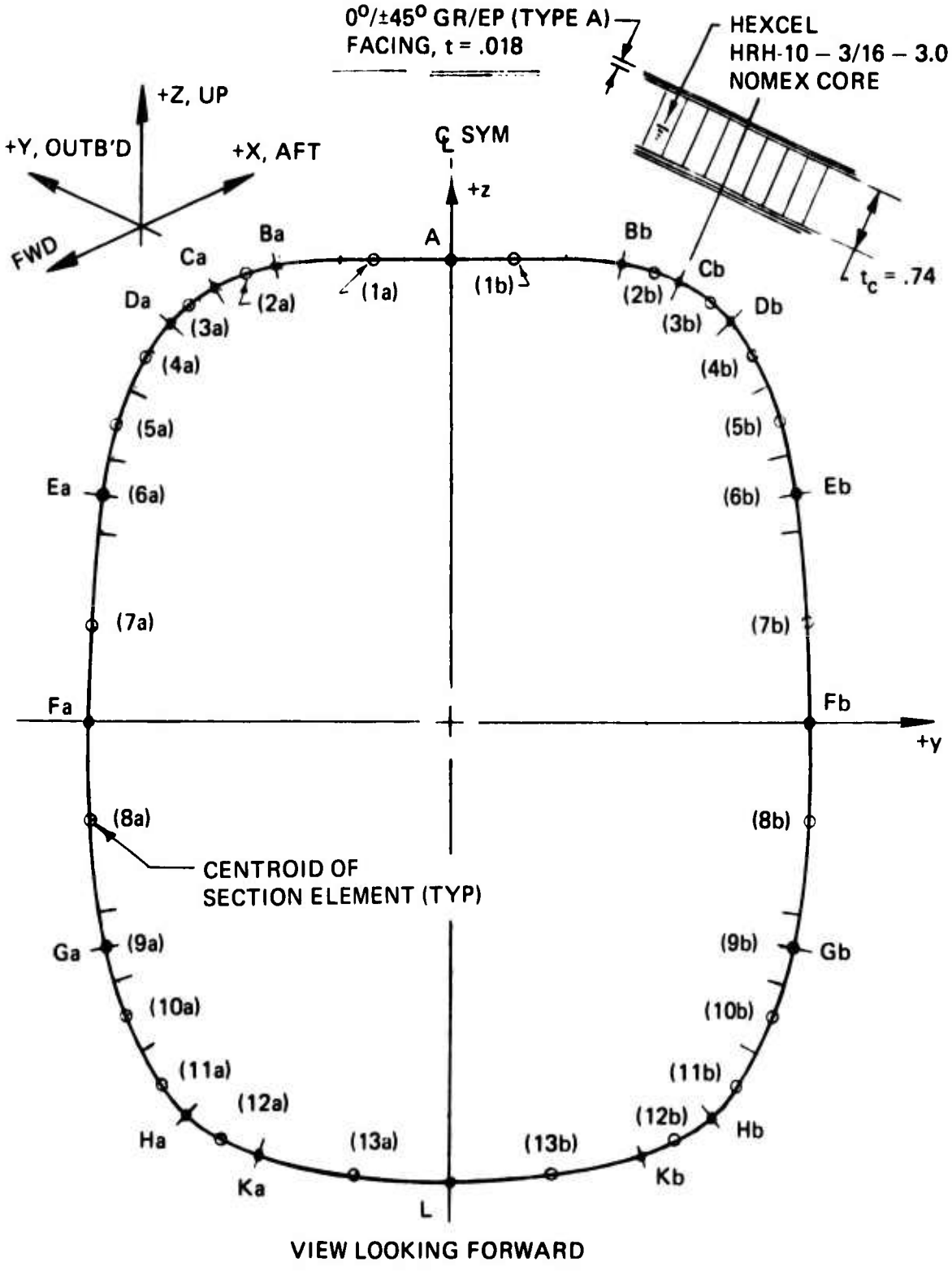

Figure 41. Concept 1 - Section Through Tail Boom.

$$V = \frac{\pi^2 D}{b^2 U} \tag{7}$$

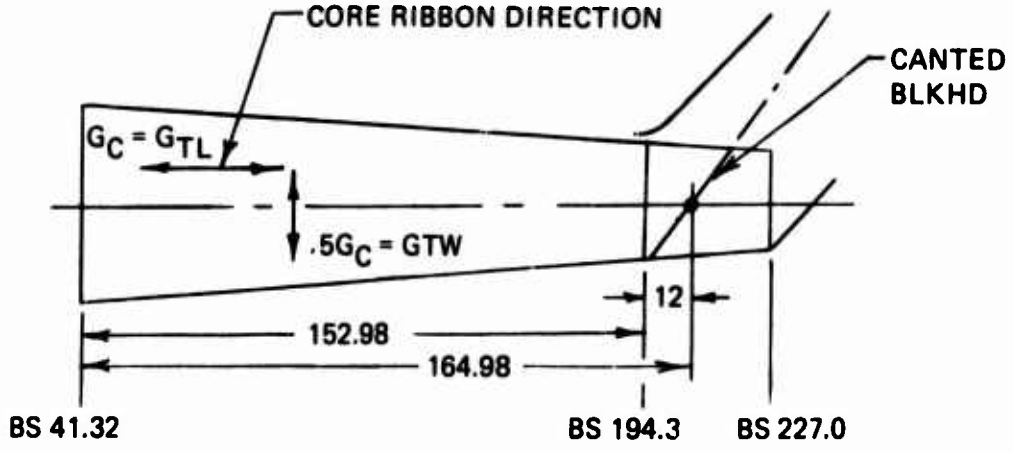

Figure 42. Side-Panel Geometry.

The facing material is $0^o/\pm45^o$ GR/EP (Type A), .018 in. thick, with a lay-up distribution of 0^o:33%, and $\pm45^o$:67% (see Figure 41). A section through the honeycomb shell is shown in Figure 43. The material properties are given in Table XIV.

$$E'_a = E_x = (7.4)(10)^6 \qquad \mu_{ab} = \mu_{xy} = .74$$
$$E'_b = E_y = (3.4)(10)^6 \qquad \mu_{ba} = \mu_{yx} = .31$$

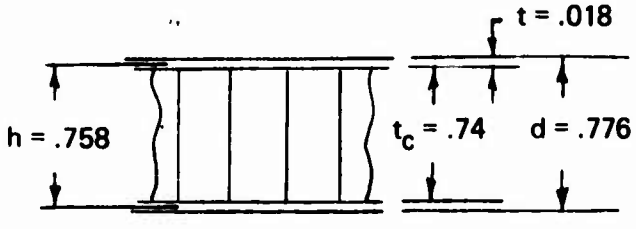

Figure 43. Honeycomb Panel Section.

The material properties for HRH-10-3/16-3.0 Nomex core are taken from Table XVII.

$$G_c = G_{TL} = 7{,}000 \text{ psi}$$

When substituting these material properties into equations (3), (4), (5), (6), and (7), the parameters are

$$E' = (4.98)(10)^6 \qquad \lambda = .786$$

$$D = 32790 \qquad U = 5310$$

The average width of the side panel as shown in Figure 42 is

$$b = 23.6 \text{ in.}$$

The side-panel aspect ratio is determined in Equation (8):

$$\frac{b}{a} = \frac{23.6}{164.98} = .143 \tag{8}$$

$$V = .1093$$

Referring to Reference (9), Figure 5-10, for orthotropic facings, the compression buckling coefficient is found to be

$$K_{Mc} = 2.50$$

When the values for D, K_{Mc}, b, and t are substituted into equation (2), the compression buckling allowable is

$$F_{cr} = 40{,}300 \text{ psi}$$

Preliminary analysis has shown local intra-cell buckling and wrinkling of facing not to be critical.

SIDE PANEL - SHEAR BUCKLING

The expression for the allowable shear buckling load per unit width of a sandwich panel is the same as that for a compression panel as stated in equation (1), with the exception of the shear buckling coefficient. The allowable shear buckling stress is

$$F_{scr} = \frac{K_{Ms} \pi^2 D}{2tb^2} \tag{9}$$

The basic parameters for the facing and core materials are the same as those determined for the compression panel. Referring to Reference (9), Figure 6-8, the shear buckling coefficient for orthotropic facing is found to be (Ref. Eq. (7))

$$V = .1093$$

$$K_{Ms} = 2.79$$

When the values for D, K_{Ms}, b, and t are substituted into equation (9), the shear buckling allowable is

$$F_{scr} = 44970 \text{ psi}$$

The ultimate shear strength of the GR/EP facing material as stated in Table XIV is $F_{su} = 36{,}000$ psi.

Therefore, ultimate shear strength is used for cutoff valve.

SIDE PANEL - APPLIED STRESSES

Bending and shear stresses are determined at BS 41.32, 90.49, 129.25, 143.28, and 194.30.

Maximum compression bending stresses due to combined vertical and lateral bending moments (see Figures 20 and 21) are applied on the right side panel in Condition VB Yaw, $+15^{o}$ Recover (Rec.). These bending stresses are circumferentially maximum at Fb and Gb, Figure 44, and vary only slightly between BS 90 and 194. The maximum bending stress is conservatively considered to be applied across the total panel width. A plot of side panel compression stress vs. boom station is shown in Figure 45.

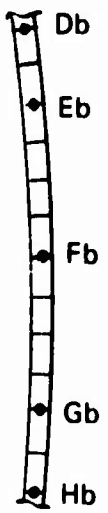

Figure 44. Side Panel.

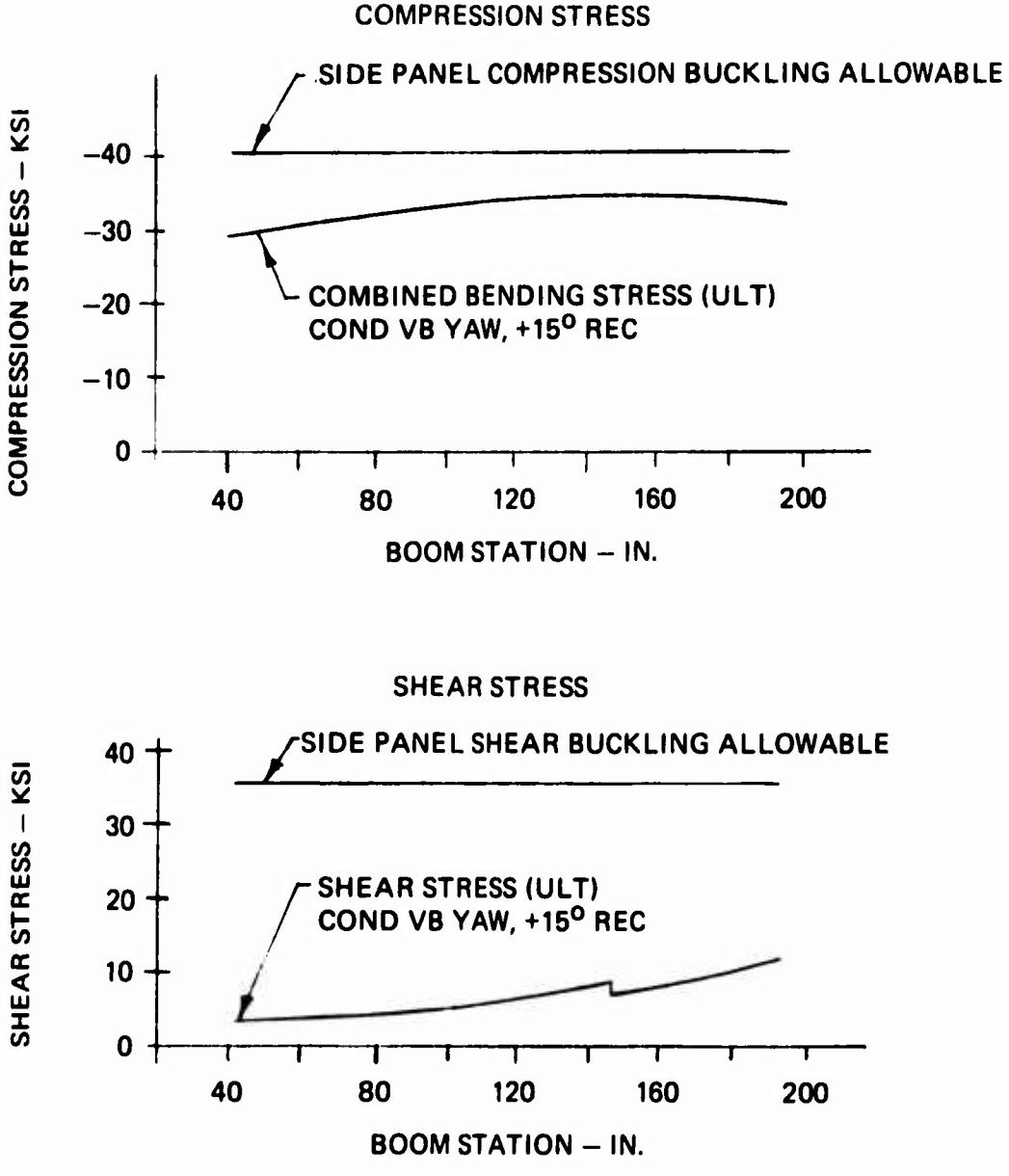

Honeycomb Panel: GR/EP (Type A) Facing, $0^{\circ}/\pm 45^{\circ}$, .018 in. Thick
Hexcel Nomex HRH-10-3/16-3.0 Core, .74 in. Thick

Figure 45. Panel Stresses.

$$fc_{MAX} = -34{,}130 \text{ psi}$$

$$R_c = \frac{fc_{MAX}}{F_{cr}} \qquad (10)$$

$$R_c = \frac{34130}{40300} = .845$$

Shear flows applied on the tail boom in this condition are lowest at BS 41.32 and increase going aft. This is due to the decrease of section depth and inclosed box area going aft. The maximum shear stress calculated at BS 194.30 is conservatively considered to be applied on the side panel. A plot of side panel shear stress versus boom station is shown in Figure 45.

$$fs_{MAX} = 12{,}720 \text{ psi}$$

$$R_s = \frac{fs_{MAX}}{F_{scr}} \qquad (11)$$

$$R_s = \frac{12720}{36000} = .354$$

The interaction formula for a panel loaded in compression and shear is given in Reference (9), equation 8:3:

$$R_c + R_s^2 = 1.0 \qquad (12)$$

Referring to Reference (10), page 1-24, the margin of safety is given by

$$MS = \frac{2}{R_c + \sqrt{R_c^2 + 4R_s^2}} - 1 \qquad (13)$$

Substituting values from equations (10) and (11) into equation (13), the margin of safety is calculated to be

$$MS = .020$$

VERTICAL FIN

The vertical fin is of a two-cell torque box structural design, using honeycomb panels for the skins and spar webs. The vertical fin geometry is shown in Figure 46. The fin structure is analyzed for spanwise and chordwise bending moments, and torsion. Compression bending combined with torsional shear is the most critical case.

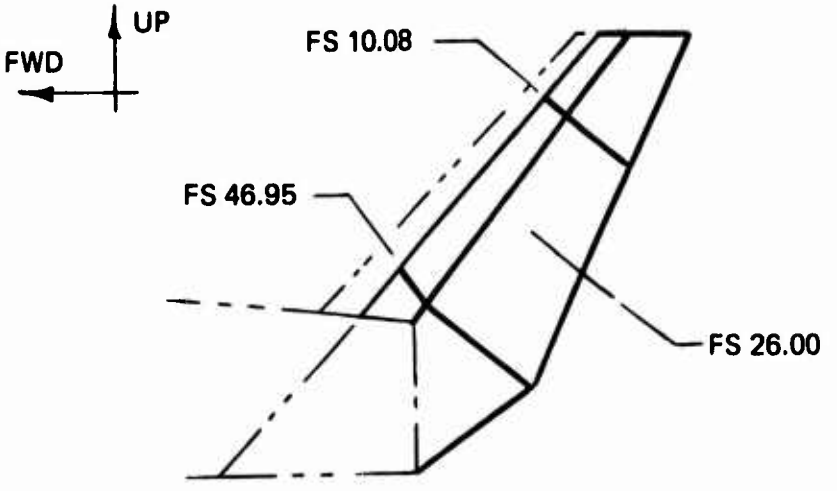

Figure 46. Vertical Fin Geometry.

Forward Panel

A section through the forward panel is shown in Figure 47.

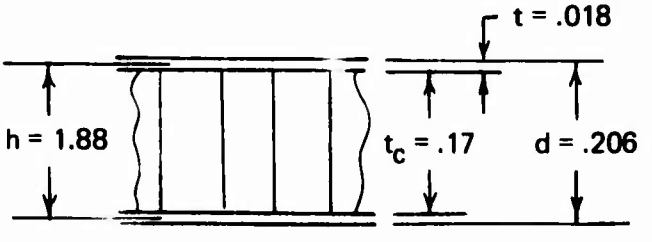

Figure 47. Forward Honeycomb Panel Section.

The allowable compression and shear buckling stresses are stated in equations (2) and (9). The facing material is the same as that used for the tail-boom shell, that is, GR/EP (Type A), .018 in. thick. The material properties are stated in the shell stress analysis.

$$E' = (4.98)(10)^6 \qquad \lambda = .786$$

The core is Nomex HRH-10-3/16-2.0, and the material properties are taken from Table XVII.

$$G_c = G_{TL} = 4{,}200 \text{ psi}$$

From equation (3), the parameter D is

$$D = 2013$$

The average panel width b = 7.0 in. (Figure 48).

$$\frac{b}{a} = .190$$

Substituting the material properties and parameters into equations (6) and (7)

$$U = 790$$

$$V = .512$$

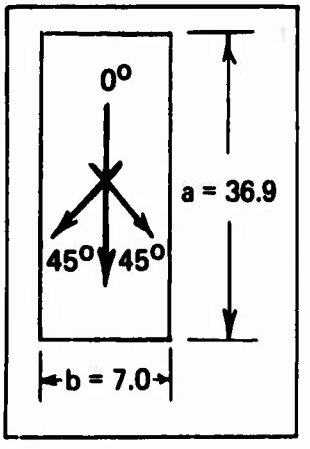

Figure 48. Forward Panel.

The compression and shear buckling coefficients are taken from Reference (9), Figures 5-10 and 6-8, for orthotropic panels:

$$K_{Mc} = 1.46 \qquad K_{Ms} = .95$$

Substituting into equations (2) and (9),

$$F_{cr} = 16{,}450 \text{ psi}$$

$$F_{scr} = 10{,}700 \text{ psi}$$

Aft Panel

The aft panel facing and core material is the same as that used for the forward panel, with the exception of the core depth.

$$t_c = .30 \text{ in.} \qquad b = .318 \text{ in.}$$

The average panel width b = 17.5 in.; length is 39.5 in. Panel curvature is conservatively neglected.

$$\frac{b}{a} = .443$$

The panel parameters are calculated using the same method of analysis as that shown in the forward panel.

$$D = 5{,}766 \qquad U = 1{,}336 \qquad V = .139$$

From Reference (9), Figures 5-10 and 6-8, for orthotropic panels,

$$K_{Mc} = 2.3 \qquad K_{Ms} = 2.6$$

Substituting into equations (2) and (9),

$$F_{cr} = 11{,}800 \text{ psi}$$

$$F_{scr} = 13{,}380 \text{ psi}$$

Applied Stresses

Bending and shear stresses are determined at Fin Station (FS) 26.0, and are considered to be the average stresses applied on the fin skin panels. Maximum compression bending stresses due to combined spanwise and chordwise bending moments are applied on right side panels in Condition VB Yaw, +15° Rec. The applied loads on the fin section are shown in Figure 49.

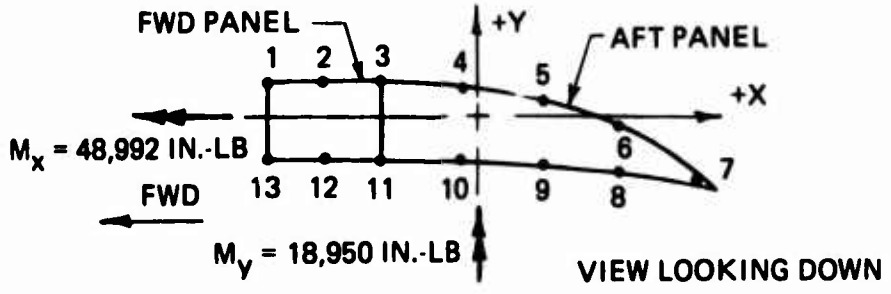

Figure 49. Applied Limit Fin Section Loads, FS 26.0.

The applied compression and shear stresses on the forward panel are

$$f_c = 15{,}100 \text{ psi} \qquad f_s = 1{,}720 \text{ psi}$$

Substituting into equations (10) and (11), and solving,

$$R_c = .918 \qquad R_s = .161$$

The interaction formula is stated in equation (12), and the margin of safety is given in equation (13). Substituting into equation (13), the margin of safety is calculated to be

$$M_s = .05$$

The aft panel stress distribution is shown in Figure 50.

The average compression stress shown in Figure 50 is considered to be applied on the panel. The maximum shear stress is

$$f_s = 3{,}920 \text{ psi}$$

Substituting into equations (10), (11), and (13), and solving,

$$M_s = .02$$

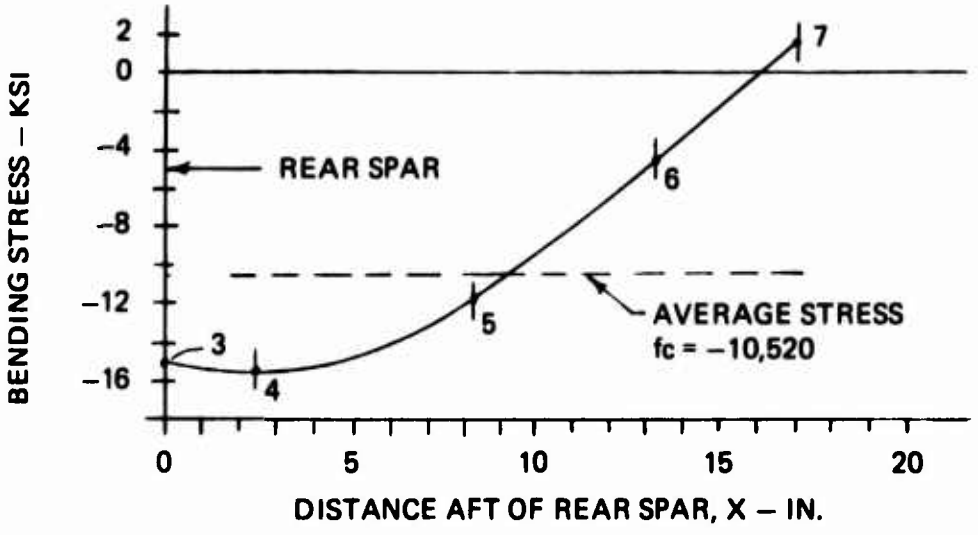

Figure 50. Aft Fin Panel Stress Distribution, Right Side.

BENDING AND TORSIONAL STIFFNESSES

Vertical and lateral bending and torsional stiffnesses for the honeycomb shell are determined at BS 41.32, 90.49, 129.25, 143.28, 194.30. The tail-boom lateral bending stiffness as calculated for the shell using the $0^{o}/\pm45^{o}$ GR/EP (Type A) facings, .036 inch total thickness, indicated good correlation, but was slightly less than that given in the design requirement curve, Figure 22. Therefore, doublers of unidirectional GR/EP (high-modulus (HM)) material and varying plies are added at selective locations, as shown in Figure 51. The resulting bending stiffness calculations show that the lateral bending stiffness closely matches the design requirement, and the vertical bending stiffness now slightly exceeds that requirement. Adjustment can be made by moving the doublers from the corners to a point closer to the mid-point of the sides and by adding or subtracting plies as desired to finally match the basic curve. The elastic moduli used in these calculations are given in Table XIV.

$0^{o}/\pm45^{o}$ GR/EP (Type A): $E_x = (7.3)(10)^6$

0^{o} GR/EP (HM): $E_x = (25.0)(10)^6$

The lateral and vertical bending stiffnesses for Concept 1 are shown in Figures 52. The design requirement curves given in Figure 22 are also shown therein for comparison.

In addition, the bending stiffnesses for the shell including one ply of 181E glass cloth is also shown. The modulus of elasticity for the 181E glass cloth is given in Table XIX.

$E_x = (3.12)(10)^6$

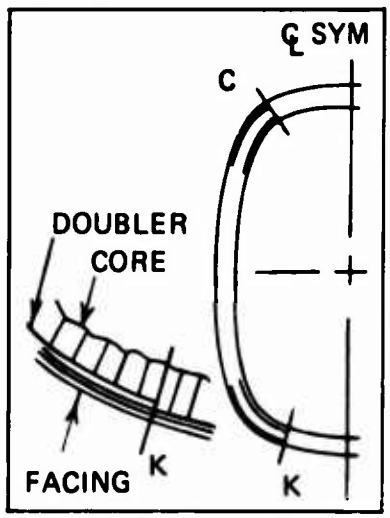

Figure 51. Doublers.

The torsional stiffness GJ is calculated by using the equation

$$J = \frac{4A_e^2}{\Sigma s/t} \qquad (14)$$

The modulus of rigidity is given in Table XIV.

$G = (3.23)(10)^6$

The torsional stiffness is plotted in Figure 52, and the design requirement curve given in Figure 22 is included therein for comparison.

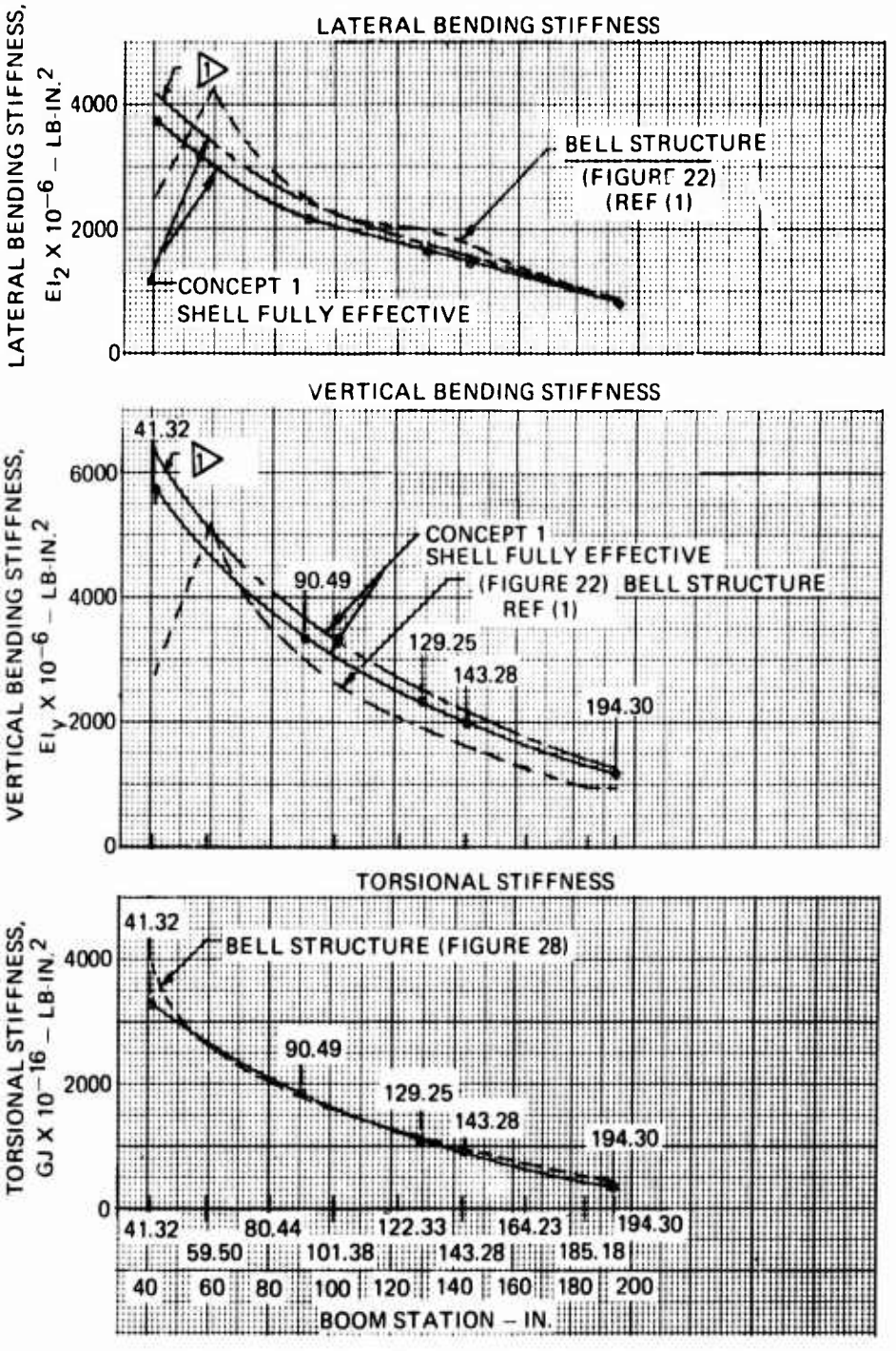

FACING: GR/EP (TYPE A), ($0^0/\pm45^0$), .018 IN. THICK, WITH UNI (0^0) GR/EP (HM) DOUBLERS

CORE: HEXCEL NOMEX HRH-10-3/16-3.0, .74 IN. THICK

▷ STIFFNESS CURVES WITH ADDITION OF ONE PLY OF IBIE GLASS CLOTH, .010 IN. THICK

Figure 52. Concept 1 Stiffnesses.

STRUCTURAL CONFIGURATION OF CONCEPT 2
THIN SANDWICH SHELL WITH FRAMES AND LONGERONS

TAIL SECTION

The tail section comprising the tail-boom shell with integrated vertical fin and tail-cone fairing is the same envelope as the existing AH-1G Cobra. (See Figure 11.)

This structure concept differs from Concept 1 in that the tail boom, in addition to having a sandwich shell construction (albeit a little thinner), also has a longeron/frame system which takes 85 percent of the bending loads. This arrangement confers improved fail safety and ballistic tolerance, in that skin panels are segmented by longeron and frames to reduce crack propagation and afford alternate load paths.

The design logic applicable to this concept is based on the following:

- Placed second in the parametric trade-off study out of a possible eight configurations.

- PRD 49-3/sandwich covers with Nomex core tail-boom shell covering appears to be as good from the ballistic tolerance aspect and superior with regard to low-velocity impact as the graphite used on Concept 1.

- PRD 49-3 material used is easy to handle and fabricate and exhibits exceptional adhesive qualities with Nomex core.

- Improved fail-safe construction over Concept 1.

  1. With utilization of frames and longerons, the skins are divided into bays which would contain any serious crack propagation in the covers.

  2. Some bending load in addition to torsional shear is taken by the skin, thus affording dual load paths for primary vertical and lateral bending modes.

- PRD 49-3 material price steadily dropping. Price expected to be reduced to $15 per pound shortly, compared with the present $35 per pound.

TAIL BOOM

The primary structure comprises a thin sandwich shell with inner and outer PRD 49-3 covers over a Nomex core. There are three bulkheads: one forward, one aft, and one canted to match the front spar web as in Concept 1. The forward and aft bulkheads are of honeycomb construction with graphite type-A covers sandwiching Nomex core. The canted bulkhead is a conventional flanged web configuration for the same reasons as outlined in Concept 1. Seven ring frames of flanged web arrangement in graphite type-A material are located between bulkheads and are notched to clear longerons. Four pultruded graphite type-A longerons extend from the forward to rear bulkhead and are located on straight-line elements in positions similar to the existing AH-1G.

The shell is designed to be made ir two halves with an upper and lower longitudinal, all-bonded splice joint to facilitate easy assembly of all secondary structure items to each shell half prior to main assembly.

At the forward end of the tail boom, substantial PRD 49-3 fingerplate reinforcings located inside the shell extend circumferentially to afford skin-to-fitting shear diffusion capability and to consolidate the four main attachment fittings located on the shell at the finger reinforcing positions.

There are alternative designs shown for these fittings. One arrangement (Figure 11, sheet 1, view X) indicates a long flanged Al Aly 7075 fitting bolt attached to the graphite longeron. At each bolt position, a thick graphite pad bonded to the longeron relieves stress concentrations at attachment hole edges. (See Figure 11, Sheet 1, Sect. D-D.) The longeron is mechanically fastened to the shell in the way of the fitting as well as bonded to prevent any possibility of peeling and for fail safety. The honeycomb core in areas of fasteners has potted inserts, and at the fitting shear connection into the sandwich bulkhead, there are also potted inserts.

The alternative attachment fitting (Figure 11, Sheet 1, view H) is again an Al Aly 7075 fitting but more symmetrically disposed by terminating the longeron some inches from the bulkhead and interposing the attachment fitting. A splice joint is made on each side between longeron and fitting by the introduction of molded S-glass angle members which pick up base and web attachments in fitting and longeron. Fiberglass was selected for this application so as to obtain a compliant joint without incurring the loss of any appreciable strength or stiffness in the overall joint. In this attachment arrangement, a solid pad insert of E-glass or PRD is inserted between covers, replacing the Nomex core over the extent of the joint.

TAIL-CONE FAIRING

This compound curvature member has to transfer loads of a relatively low order from fin into tail boom and is made of PRD 49-3 in a molded lay-up.

Tail-Boom Access Panels

There are three large load-carrying access panels in the tail boom of the same size and located in the same position as in the existing AH-1G Cobra. The panels are fastened with screws and nut plates and are constructed in sandwich form similar to the basic shell.

At access panel positions, the surrounding structure is reinforced with doily configuration mats as on Concept 1 but made in PRD 49-3. The inner surround molding and also the panel surround molding are molded in a one-piece "picture frame" configuration in PRD 49-3 material.

Avionics Support Structure

The avionics shelf support beams and rails, which are considered as secondary structure, are made in PRD 49-3. Other more highly loaded support structures, such as elevator mounting members and drive shaft gearbox mounting structures are designed in graphite type-A, due mainly to poor compressive load capability of PRD 49.

Vertical Fin

The vertical fin is designed exactly as Concept 1 using graphite type-A. Fin covers were initially considered in PRD 49-3; but again, due to the low compressive and marginal shear strength which drove up the required cover thicknesses, it was opted to change material to graphite type-A as there was concern that the increased weight so far back might move aircraft c.g. aft, which was not acceptable.

DYNAMIC RESPONSE

Fine tuning of the tail boom is afforded by the bonded placement of graphite type-A straps in calculated positions to control critical bending stiffness modes.

STRESS ANALYSIS - CONCEPT 2

METHOD OF ANALYSIS

The structural configuration of Concept 2 is shown in Figure 53. A typical cross-section through the boom, Section A-A, is shown in Figure 54. Concept 2 is of a hybrid design, using GR/EP (Type-A) longerons and PRD-49-III honeycomb skin panels. The four longerons react the applied vertical and lateral bending moments. The primary purpose of the honeycomb skin panels is to react the applied vertical, lateral, and torsional shears. However, the skin panels also partially react the bending moments, and the bending stresses are applied on the panels in proportion to the elastic moduli of the two materials.

Preliminary analysis has shown the longerons to be most highly loaded in compression, and are analyzed as columns supported at the frames shown in Figure 53. The side panels are critical in combined compressive bending and shear, and are considered to be flat panels simply supported at the longerons. The method of analysis used to determine the panel compression and shear buckling allowables is the same as that described in Concept 1.

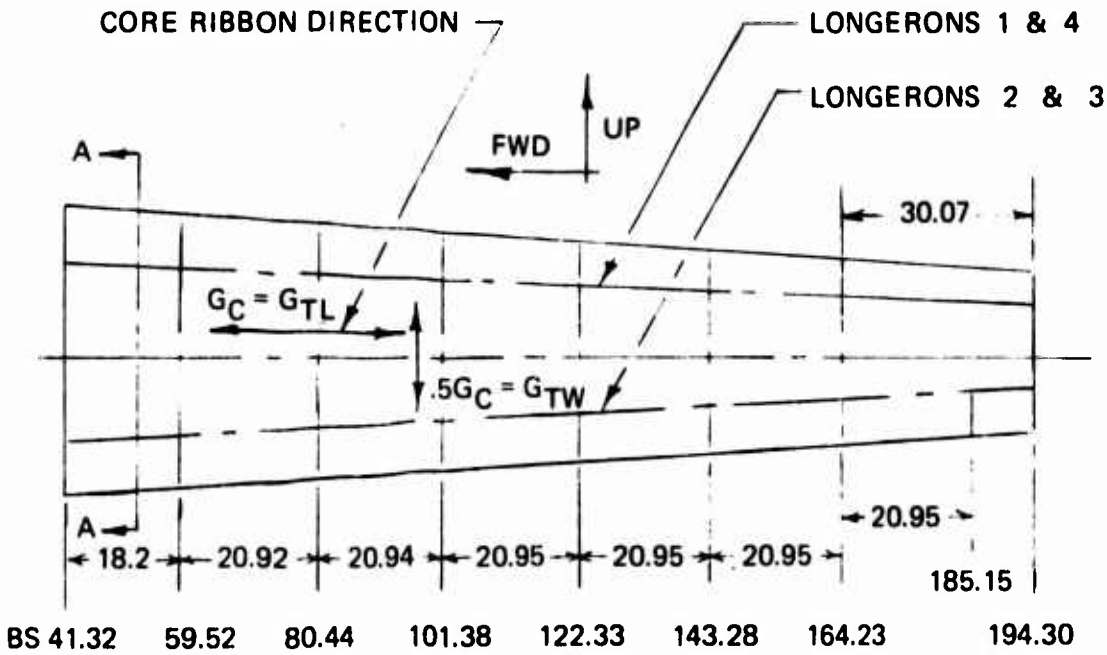

Figure 53. Longerons and Frame Spacing Geometry BS 41.32 - 194.30.

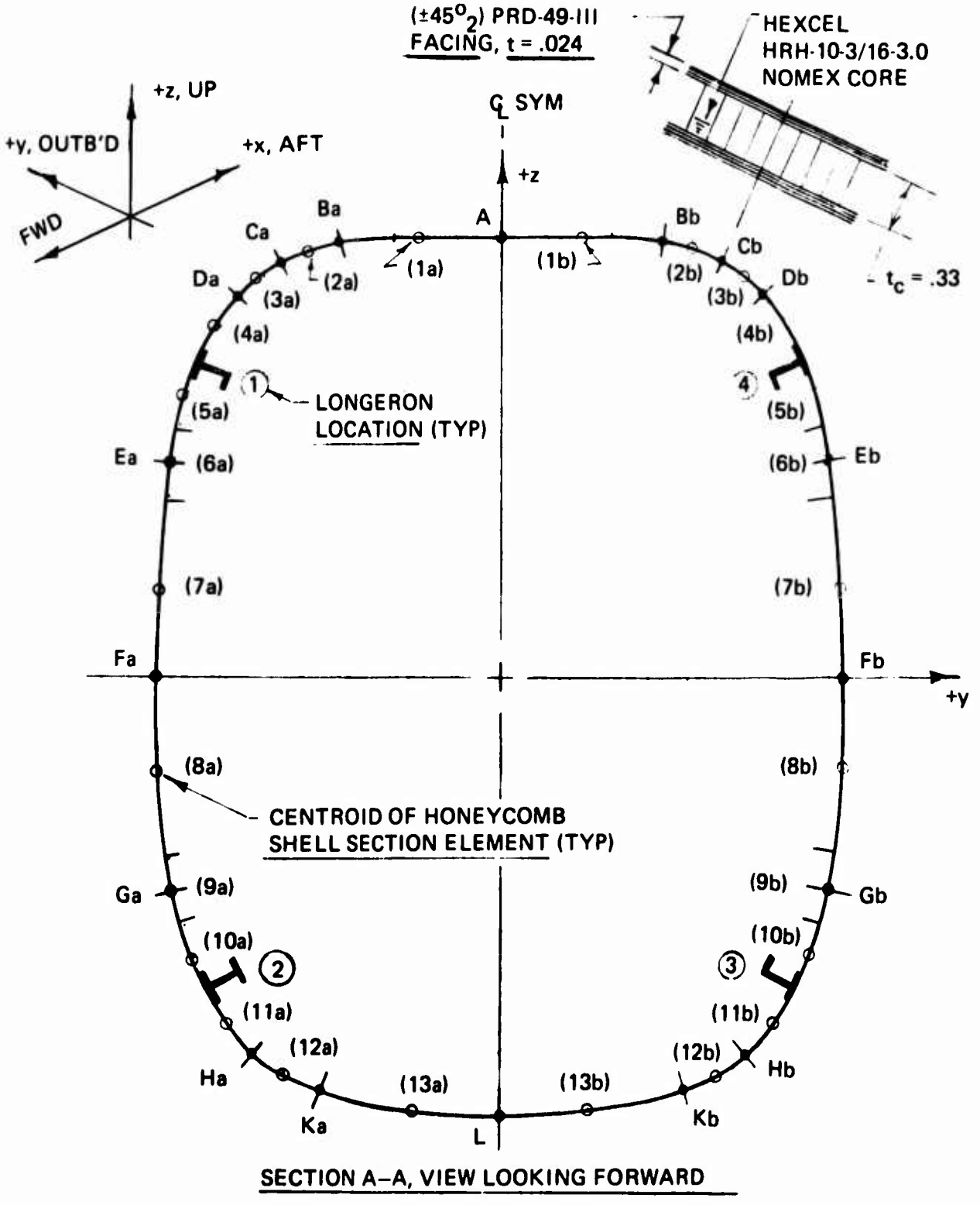

Figure 54. Concept 2 - Section Through Tail Boom.

LONGERON - COLUMN BUCKLING ALLOWABLE

The longeron section is shown in Figure 55. The section properties calculated for the longeron are:

$$A = .322 \text{ in.}^2$$

$$I_{x-x} = .121 \text{ in.}^4$$

$$P_{x-x} = .612 \text{ in.}$$

The longeron material is $(0^o_3, \pm 45^o, 0^o_3)$ GR/EP (Type A), .096 in. thick, with a lay-up distribution of 0^o:75%, and $\pm 45^o$:25%; see Figure 55. The material properties are given in Table XIV.

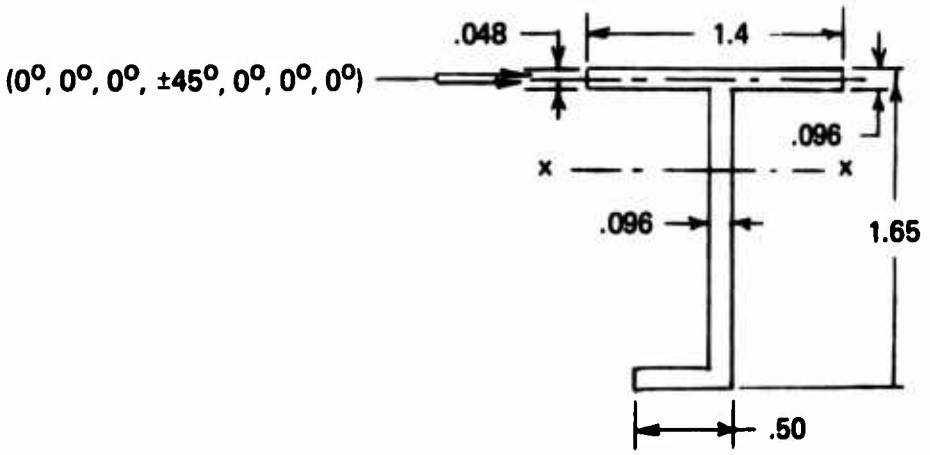

Figure 55. Longeron Section.

The longerons supported at the frame locations shown in Figure 53 are short columns. The allowable buckling stress is calculated from the equation

$$F_c = F_{cu} \left(1 - \frac{F_{cu} (L'/\rho)^2}{4\pi^2 E}\right) \qquad (15)$$

The material properties are taken from Table XIV.

$$E = (13.2)(10)^6$$

$$F_{cu} = F_{cux} = 128{,}000 \text{ psi}$$

Assume the column end fixity coefficient c = 1.5. For the longeron between BS 41.32-59.52, the length L = 18.2 in., and ρ = .612 in.

$$\frac{L'}{\rho} = \frac{L}{\rho\sqrt{c}} \qquad (16)$$

$$\frac{L'}{\rho} = 24.3$$

The column buckling allowable is calculated from Equation (15).

$$F_c = 109{,}400 \text{ psi}$$

SIDE PANELS - COMPRESSION AND SHEAR BUCKLING

The allowable compression and shear buckling stresses are stated in equations (2) and (9).

The facing material is $(\pm 45_2)$ PRD-49-III, .024 in. thick; see Figure 54. A section through the honeycomb side panel is shown in Figure 56. The material properties are given in Table XV,

$$E'_a = E'_b = (1.0)(10)^6 \qquad \mu_{ab} = \mu_{ba} = .80$$

From equations (3), (4), and (5), the parameter D is

$$D = 4{,}170$$

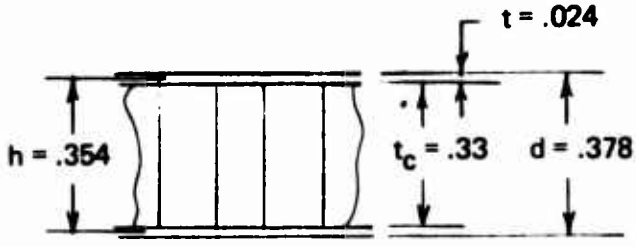

Figure 56. Honeycomb Panel Section.

Due to the core ribbon direction and panel size, the geometry designation for the compression and shear panels as specified in Reference (9) is shown in Figure 57.

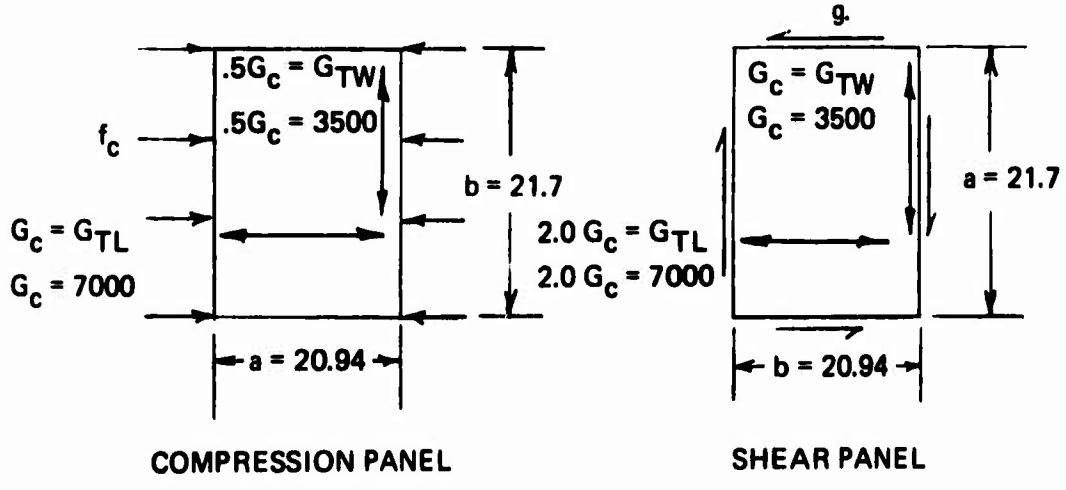

Figure 57. Side-Panel Geometry BS 80.44-101.38.

Compression Panel

The material properties for HRH-10-3/16-3.0 Core are taken from Table XVII.

$$G_c = G_{TL} = 7{,}000 \text{ psi}$$

The parameters U and V are calculated using equations (6) and (7).

$$\frac{a}{b} = .965$$

$$U = 2480$$

$$V = .0755$$

Referring to Reference (9), Figure 5-10, for orthotropic facings, the compression buckling coefficient is found to be

$$K_{Mc} = 2.95$$

Substituting into equation (2),

$$F_{cr} = 5,320 \text{ psi}$$

Shear Panel

From the data shown in Figure 57 and Table XVII for the core material,

$$G_c = G_{TW} = 3,500 \text{ psi}$$

$$\frac{b}{a} = .965$$

$$U = 1240$$

$$V = .0755$$

Referring to Reference (9), Figure 6-9, for orthotropic facings, the shear buckling coefficient is found to be

$$K_{Ms} = 5.95$$

Substituting into equation (9),

$$F_{scr} = 11,600 \text{ psi}$$

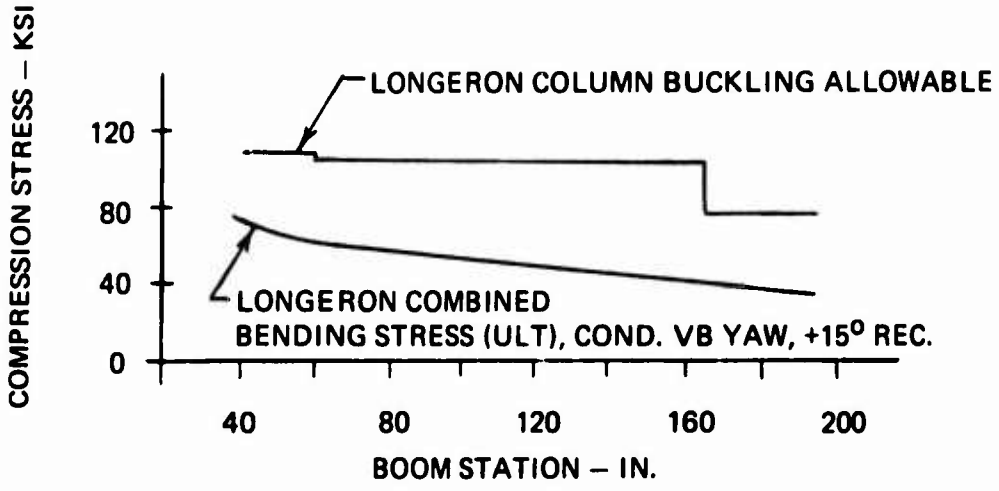

Figure 58. Compression Stress - Longeron ③.

APPLIED STRESSES

As stated in the Method of Analysis, both the GR/EP (Type A) longerons and the PRD-49-III honeycomb skin panels react the applied bending moments. The bending stresses at any boom station are calculated using an effective bending section, where the PRD skin panel material is included in terms of effective GR/EP for the determination of section moment of inertia. Maximum longeron and skin panel stresses are applied in Condition VB Yaw, +15° Rec.

Bending and shear stresses are determined at BS 41.32, 90.49, 129.25, 143.28, and 194.30.

Longeron

Maximum compression bending stresses due to combined vertical and lateral bending moments (see Figure 18) are applied on Longeron (3) in Bay BS 41.32-59.52. Tension is not critical.

$$f_c = -73{,}100 \text{ psi}$$

The margin of safety for the longeron is calculated to be

$$M_s = \frac{F_c}{f_c} - 1 \qquad (17)$$

$$M_s = \frac{109400}{73100} - 1 = .49$$

A plot of compression stress vs. boom station for Longeron (3) is shown in Figure 58.

Side Panel

The right side panel in Bay 80.44-101.38 is the most highly loaded in combined compression and shear. The effective side panel is shown in Figure 59. The compression bending stresses in this panel increase from Longeron (4) to a maximum at points Fb and Gb and decrease going toward Longeron (3). The maximum bending stress is conservatively considered to be applied across the total panel width.

$$fc_{MAX} = -4{,}170 \text{ psi}$$

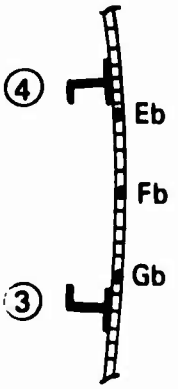

Figure 59. Side Panel.

Substituting into equation (10) and solving,

$$R_c = \frac{4170}{5320} = .784$$

A plot of right side panel compression stress vs. boom station is shown in Figure 60.

The applied vertical shear is reacted by the side skin panels between the upper and lower Longerons, ① -②, ③-④, and the lateral by the upper and lower skin panels between Longerons ①-④ and ②-③ respectively, Figure 54. The torsional moment is reacted by all four skin panels, circumferentially.

$$f_s = 3{,}960 \text{ psi}$$

Substituting into equation (11) and solving,

$$R_s = \frac{3960}{11600} = .341$$

A plot of right side panel shear stress vs. boom station is shown in Figure 60.

The interaction formula is stated in equation (12), and the margin of safety is given in equation (13). Substituting the values calculated for R_c and R_s into equation (13), the margin of safety is calculated to be

$$M_s = .10$$

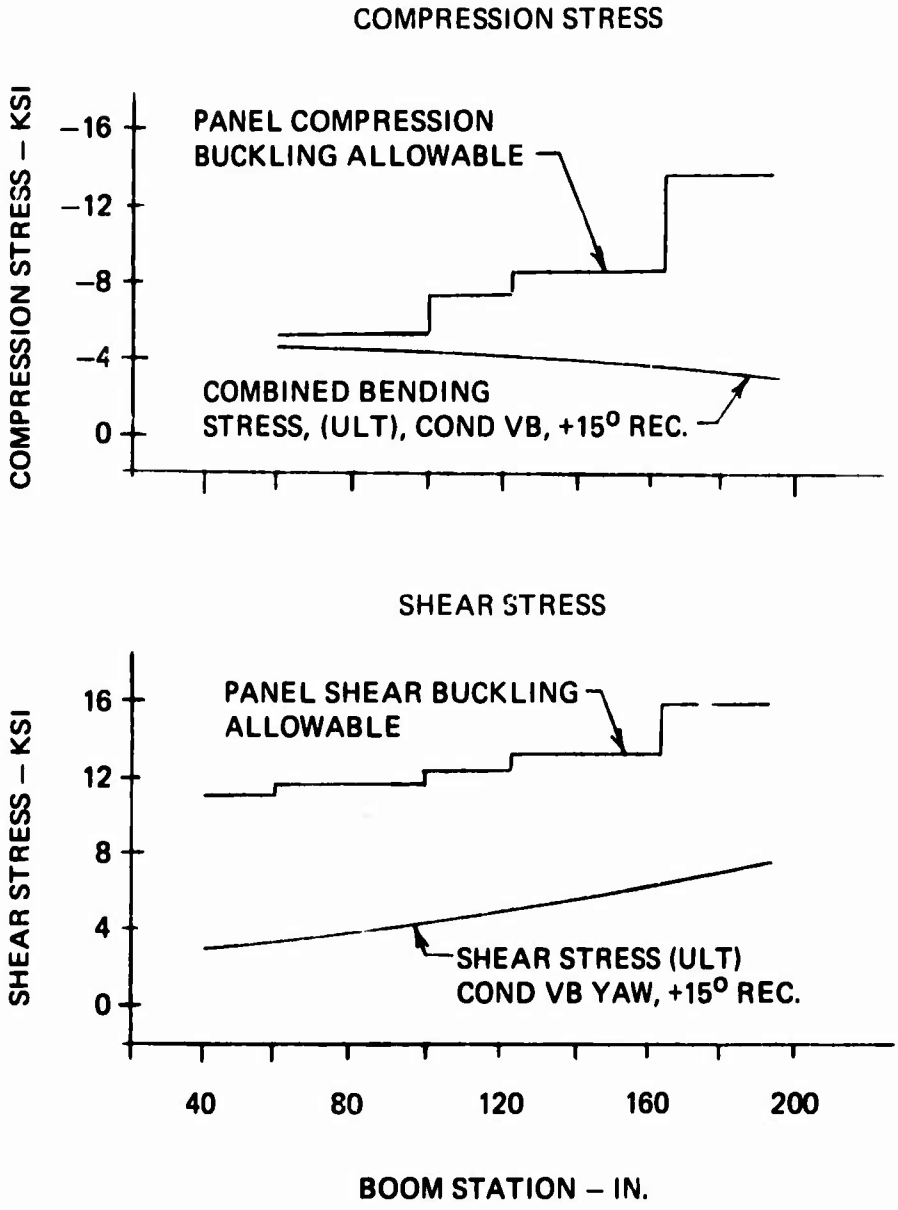

Honeycomb Panel: PRD-49-III Facing, $(\pm 45^{\circ}_2)$
.024 in. Thick
Hexcel Nomex HRH-10-3/16-3.0 Core
.33 in. Thick

Figure 60. Right Side-Panel Stresses.

BENDING AND TORSIONAL STIFFNESSES

Vertical and lateral bending and torsional stiffnesses for Concept 2 are determined at BS 41.32, 90.49, 129.25, 143.28, and 194.30. The moments of inertia about the two axes at any boom station are calculated for the GR/EP longeron areas concentrated at their centroids, and for the PRD honeycomb skin circumferentially divided into area elements concentrated at their centroids as shown in Figure 54. The bending stiffnesses are determined by multiplying these cross-section moments of inertia for each material by the applicable modulus of elasticity as stated in equation (18).

$$EI\ (SECTION) = E(GR/EP)I(LONG.) + E(PRD)I(SKIN) \qquad (18)$$

The moduli for GR/EP (Type A) and PRD-49-III are taken from Tables XIV and XV respectively.

GR/EP (Type A) Longeron, 0^{o}:75%, $\pm 45^{o}$: 25%: $E_x = (13.2)(10)^6$

PRD-49-III Honeycomb Skin, $(\pm 45^{o}_2)$: $E_x = (1.0)(10)^6$

The resulting calculations show that both the vertical and lateral bending stiffness curves very nearly match the design requirement. The lateral and vertical bending stiffnesses are shown in Figure 61. The design requirement curves given in Figure 22 are also shown therein for comparison.

The torsional stiffness GJ of the PRD honeycomb skin is calculated from equation (14). The modulus of rigidity is given in Table XV.

$$G = (2.8)(10)^6$$

The torsional stiffness is plotted in Figure 61, and the design requirement curve given in Figure 22 is included for comparison.

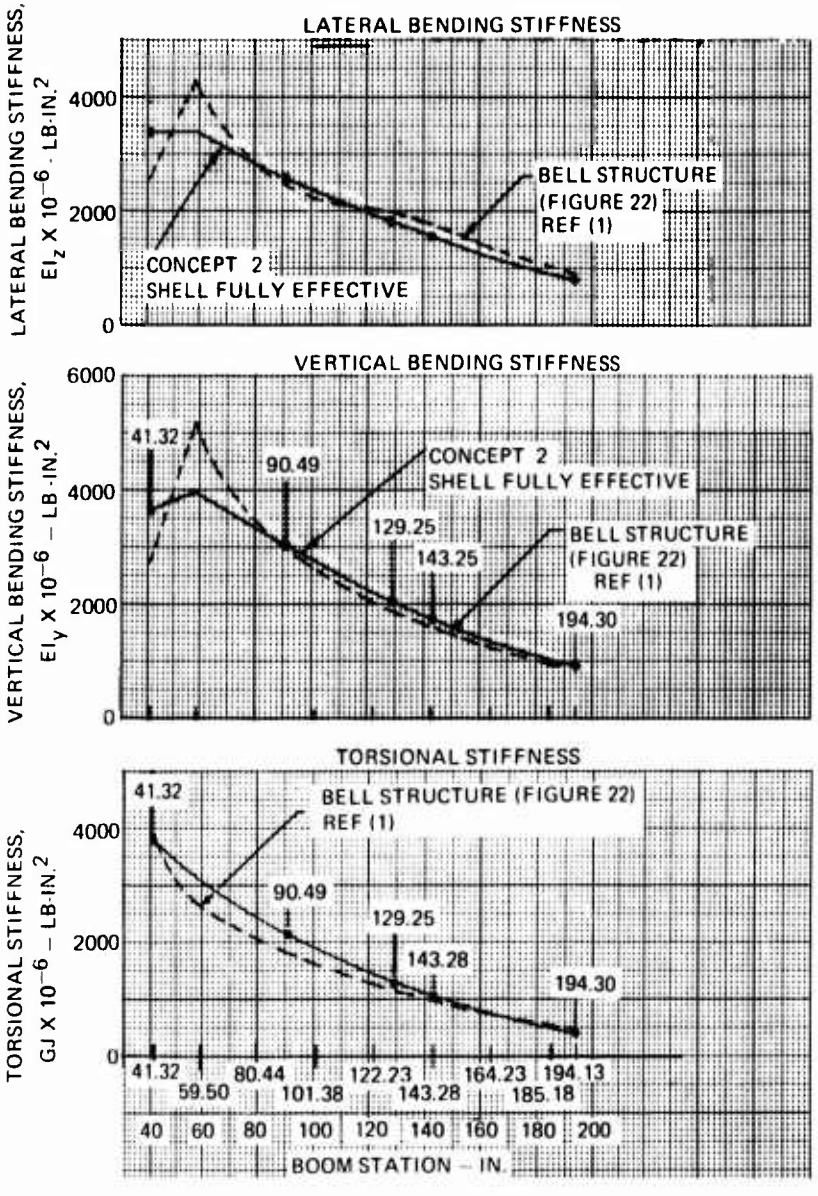

LONGERON: GR/EP (TYPE A); UNI (0^o) 75%, (± 45): 25%
FACING: PRD-49-III, ($\pm 45_2$), .024 IN. THICK
CORE: HEXCEL NOMEX HRH 10-3/16 – 3.0, .33 IN. THICK

Figure 61. Concept 2 Stiffnesses.

STRUCTURAL CONFIGURATION OF CONCEPT 3 INTEGRALLY MOLDED SKIN/STRINGER CLAMSHELL

TAIL SECTION

The tail section comprising the tail-boom shell with integrated vertical fin and tail-cone fairing is the same envelope as the existing AH-1G Cobra. (See Figure 12.)

This structural arrangement differs considerably from the semimonocoque sandwich construction of Concept 1 and the sandwich shell with frame longeron system of Concept 2 and is essentially the application of composite materials to a conventional skin/stringer/frame design.

The design logic applicable to Concept 3 is based on the following:

- Placed third in parametric trade-off study out of a possible eight configurations.

- S-glass thick skin cover - no honeycomb core. Appears to be slightly better from the ballistic tolerance aspect and superior with regard to low-velocity impact compared to Concepts 1 and 2.

- S-glass material is easy to handle and fabricate, and more experience has been accrued with fiberglass than any other composite. Its main detraction, however, is high density and low modulus compared to graphite and PRD 49.

- Improved fail-safe construction over Concepts 1 and 2.

  1. Stringers and frames divide skins into relatively small bays which would contain any serious crack propagation in the covers.

  2. Multiple stringer arrangement affords alternative load paths for the primary bending structure.

- Price of S-glass laminates is low - $12 per pound.

TAIL BOOM

The primary structure shell comprises a system of graphite stringers, frames, and bulkheads supporting an 8-ply S-glass skin. The hat section molded graphite type-A stringers extend from the forward to the rear bulkhead.

There are three bulkheads of flanged web construction positioned forward, aft, and canted in line with front spar web similar to Concept 1. Seven flanged web type ring frames are spaced between bulkheads. Frames and bulkheads are of graphite Type-A. The canted bulkhead and frames are notched to allow stringers to pass through. The shell is fabricated in two halves with vertical longitudinal splice joints as on Concepts 1 and 2. Each side shell has six hat stringers running in straight-line elements.

There are three large load-carrying access panels in the tail boom of same size and located in same position as in the existing AH-1G Cobra. The panels are fastened with screws and nut plates and are constructed in sandwich form similar to Concept 1 panels.

The access panel surround structure is reinforced by an S-glass flanged surround doubler which extends under adjacent stringers. The left-hand side panel surround doubler extends forward and rearward also to pick up ends of stringer which are discontinuous across the hole.

At the forward end of the tail boom, segmented S-glass finger plate reinforcings bonded to the inside of the skin extend circumferentially to afford skin to fitting shear diffusion capability and consolidate the four main attachment fittings mounted on the doubler fingers.

There are two types of attachment fittings shown, one being an alternative arrangement. The preferred fitting is shown at view on arrow L on Figure 12, Sheet 1. This fitting is Al Aly 7075T73, which is grown out at the forward end to accommodate a barrel nut and is then reduced to a long solid finger so as to lay inside the stringer end, which has been reinforced to increase side walls substantially. The cap of the hat section is cut away locally in order for the fitting to be detachable by removing bolt attachments passing through stringer side walls and fitting.

TAIL-CONE FAIRING

This compound curvature member is designed as a one-piece molding in S-glass and is stiffened in order to transfer loads from the fin trailing-edge section into the tail boom by an internal system of simple ripple S-glass stiffeners.

DYNAMIC RESPONSE

Fine tuning of the tail boom is afforded by the combined addition of nested doublers in selected stringers at the

forward end and bonded doubler strips in selected hat section flanges in other positions shown.

VERTICAL FIN

The vertical fin is fabricated in graphite type-A material for the same reasons as outlined in Concept 2. However, the basic construction is different from that described for Concepts 1 and 2. It should be noted that this method is suitable for all three concepts and is the preferred design.

The fin arrangement is a straight-line-element concept comprising a primary structural torque box and trailing-edge assembly. The fin attaches to the tail boom via a front spar splice channel and a rear spar fitting and at its lower sides, left and right, by bonded shear angles.

Primary Structure - Front and rear sandwich spars with interconnecting side panels, also of sandwich form, make up the torque box, with the spar material, primarily unidirectional, being configured into angle sections and built in at each corner to form simple, efficient lapjoint lands for the skins. The sandwich arrangement in both spars and side skins consists of graphite type-A skins, inner and outer, enclosing Nomex core.

An extension of the side skins forward of the front spar combines with nested angles on each side to form a rigid land for the attachment of the nose fairing hinge on the right side and for affixing of quick-release fasteners on the left side.

The skin in the rear spar locality is set back to allow the trailing-edge assembly to fit flush, comprising graphite type-A side skins bonded to a full-depth Nomex core which tapers down chordwise to nest into a trailing-edge graphite member. At tip and root ribs, graphite moldings seal off the Nomex core top and bottom and distribute the torque loads.

Superior structural efficiency is achieved with the integrated torque box arrangement, which allows a greater portion of useful skins to work in compression, thus relieving the bending loads in both spars.

The front and rear spar cap sectional area is increased progressively down to the root of the spar by increasing the width of the cap legs. This serves the twofold purpose of meeting the maximum bending moment condition occurring at the fin root, and also facilitating diffusion of bending loads from the side panels of the torque box into the front and rear

spars over the lower few inches, since the tail-boom shell at the interface with the fin has no backup structure capable of taking vertical loads between bulkheads.

Lateral bending loads from the fin front spar are carried across the tail-boom/fin joint by a splice channel with tapering-thickness walls, which are at maximum thickness at the termination of the four fin cap members.

The bonded-joint channel in turn distributes loads into the canted bulkhead webs, where it is sheared into the shell skins via the bonded bulkhead flanges.

Access into the torque box on the left side is afforded by two spanwise load-carrying doors attached in a manner similar to that of the tail-boom panels.

Secondary Structure - Existing metal parts will be used for the upper fin leading-edge skin and fin tip fairings.

CONTROL ATTACHMENT POINTS

Upper and lower pulley bracket assemblies for the tail rotor controls will be attached to the vertical fin front spar by bolting, similar to the existing arrangement, through the spar. SP250 SF 1 fiberglass angles are bonded to the rear face of the spar in way of these attachments, and the core is consolidated around the bolt holes by insertion of pot filler.

STRESS ANALYSIS - CONCEPT 3

METHOD OF ANALYSIS

The structural configuration of Concept 3 is of a skin-stringer design using a total of twelve stringers, six per side, and thin skin shear webs. The frame locations for this concept are the same as those shown in Figure 53 for Concept 2. A typical cross section through the boom is shown in Figure 62. The stringers react the vertical and lateral bending moments, and the skin reacts the vertical, lateral, and torsional shears.

The basic stringer is of a hat section design using GR/EP (Type A) material with a $(0_3, \pm 45, 0_3)$ lay-up, a distribution of 0^o:75%, $\pm 45^o$:25% laminates. This results in an optimum combination of stringer area, compression strength, and elastic modulus. The skin material is XP251S glass with a $(\pm 45^o_4)$ lay-up, .060 in. thick. This is the minimum thickness required to meet the torsional stiffness criteria.

Stringer bending stresses and skin shear flows are calculated at the desired boom station locations using the Boeing Vertol Company S-25 Computer Program, Reference (12).

The analysis has shown the stringers to be most highly loaded in compression, and they are analyzed as columns simply supported at the frames, shown in Figure 53. In the region where high compression loads are applied, laminated doublers are added to the basic hat section stringer at the flanges, adjacent to the skin, to increase both the stringer section area and crippling allowable. In the area of the tail-boom cutouts, the terminated stringers are considered to be ineffective in the bays immediately adjacent to the cutouts. In the forward bay at the fuselage interface, BS 41.32-59.52, only the four attachment stringers are considered to be effective.

All skin panels are considered to be flat panels, simply supported at the frames and stringers. The minimum thickness of the skin panels is .060 in. as previously stated, and they are designed to be shear resistant, nonbuckling at limit load. In regions of high local shear stresses, $\pm 45^o$ laminate doublers are added to meet the nonbuckling requirement.

STRINGERS

Section Properties

The basic stringer section is shown in Figure 63. The doublers added to the flanges, as stated in the Method of Analysis, are

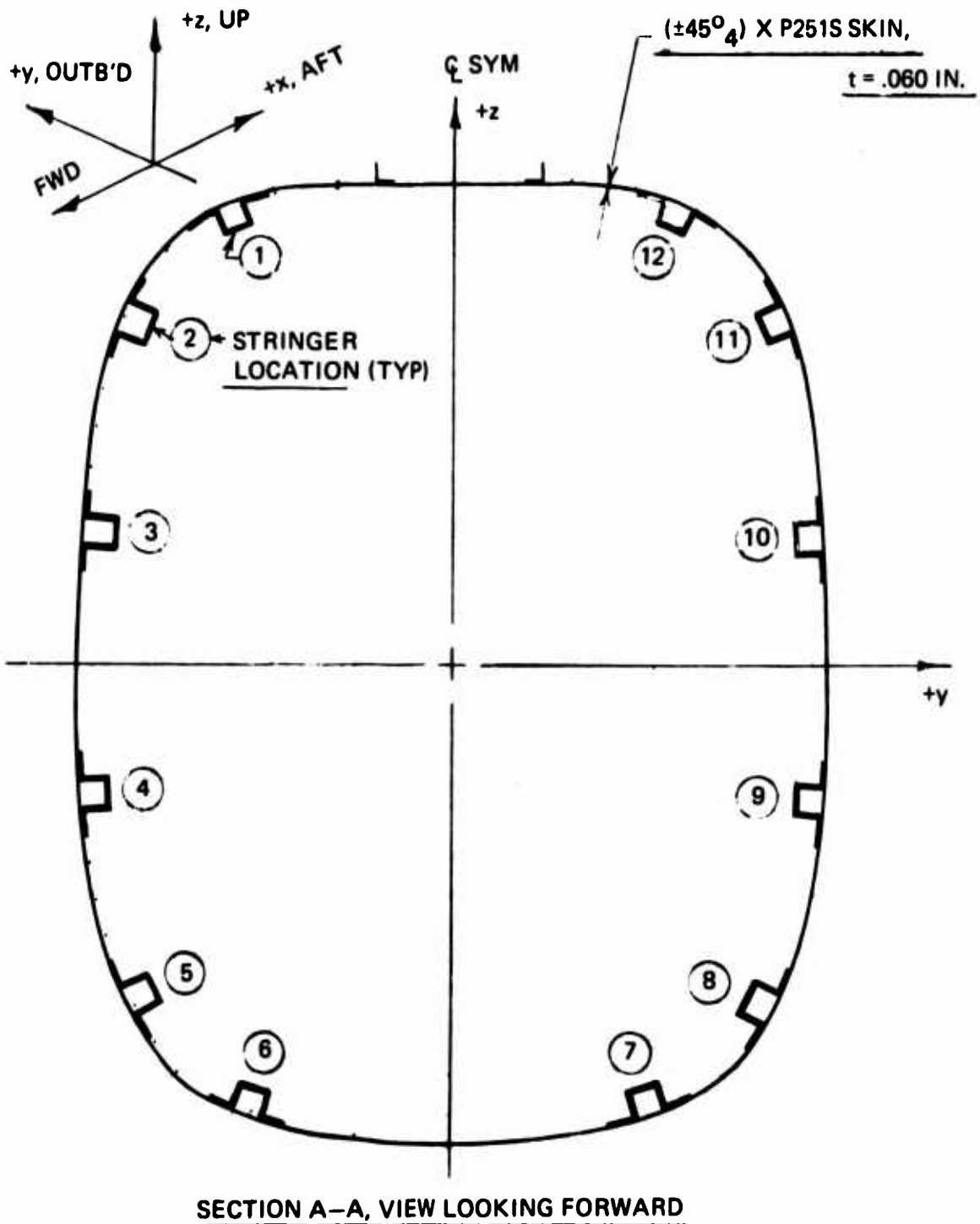

Figure 62. Concept 3 - Section Through Tail Boom.

also shown therein. These doublers are five ply and ten ply, .030 in. and .060 in. thick, respectively.

The stringer configuration in the interface bay, BS 41.32-59.52, includes a nested doubler with the same section area as the basic stringer section.

The section properties of the tail-boom stringer sections used in the Concept 3 design are tabulated in Table XXI.

TABLE XXI. STRINGER SECTION PROPERTIES

Designation	A	I	ρ
Basic Section	.197	.0254	.359
Mod. A	.242	.0295	.349
Mod. B	.288	.0316	.331
Nested Doubler	.394	.0507	.359

Crippling Allowables

To calculate the stringer crippling allowable, which is based on the theory of buckling of flat plates, assume the effective modulus to be defined as stated in equation (4). The stringer modulus orientation is shown in Figure 64. For the basic stringer section, with the lay-up shown in Figure 63, 0^{o}:75%, $\pm 45^{o}$:25%, the material properties are given in Table XIV. Substituting into equation (4),

$$E' = (5.63)(10)^{6}$$

The crippling allowables for the stringer elements are determined from Reference (13), Figure 11.2.1-1.

TABLE XXII. CRIPPLING ALLOWABLE OF BASIC STRINGER SECTION

Item	b	t	b/t	$\frac{F_{cc}}{\sqrt{F_{cu}E^{*}}}$	F_{cc}	A	$F_{cc}A$
1	.76	.048	15.8	.036	30500	.0365	1133
2	.76	.048	15.8	.036	30500	.0365	1133
3	.84	.048	17.5**	.066	55900	.0403	2255
4	.84	.048	17.5**	.066	55900	.0403	2255
5	.90	.048	18.8**	.062	52500	.0432	2270
					$\Sigma \longrightarrow$	.1968	9046

* $\sqrt{F_{cu}E} = (8.48)(10)^{5}$

**No edge free

$$F_{cc} = \frac{9046}{.1968} = 46{,}000 \text{ psi}$$

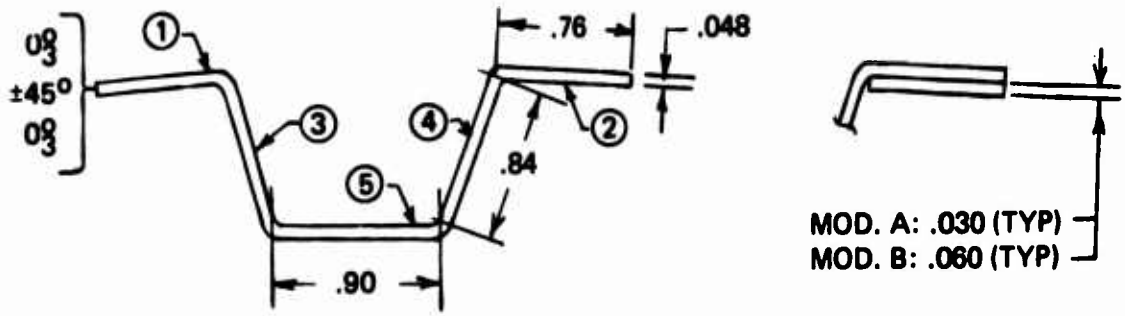

Figure 63. Basic Stringer Section and Flange Doublers, .006-Inch Ply Thickness.

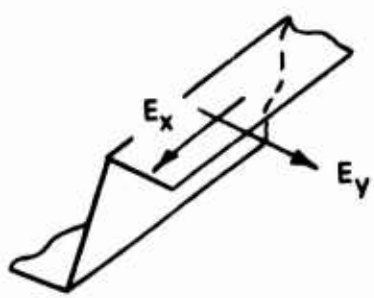

Figure 64. Modulus Orientation.

Similarly, for the additional stringer configurations itemized in Table XXI, the crippling allowables are calculated to be:

Basic Stringer, Mod. A: F_{cc} = 50,800 psi

Basic Stringer, Mod. B: F_{cc} = 57,300 psi

Basic Stringer, Nested: F_{cc} = 81,800 psi

Column Allowable

The stringers supported at the frame locations shown in Figure 53 are short columns. The allowable column buckling stress for a section with a maximum compression allowable of F_{cc} is calculated from the equation

$$F_c = F_{cc} \left[1 - \frac{F_{cc}(L'/\rho)^2}{4\pi^2 E} \right] \qquad (19)$$

The modulus of elasticity is taken from Table XIV.

$$E = (13.2)(10)^6$$

Assume the column end fixity coefficient, c = 1.5. For the basic stringer section from Tables XXI and XXII,

ρ = .359 in. $\qquad F_{cc}$ = 46,000 psi

For the stringer between BS 80.44-101.38, the length L = 20.94 in. Substituting into equations (16) and (19), the column buckling allowable for the basic stringer is calculated to be

$$\frac{L'}{\rho} = 47.6$$

$$F_c = 36{,}800 \text{ psi}$$

SKIN PANELS - SHEAR BUCKLING

The allowable shear buckling load for a simply supported composite panel of width b and thickness t is given in Reference (14), Table 4.3.2.1.

$$N_{xy,\,cr} = \left(\frac{2}{b}\right)^2 \sqrt{D_{22}\,(D_{12} + 2D_{66})} \left\{ 11.7 + .5320 + .9380^2 \right\}, \quad \frac{a}{b} = \infty \qquad (20)$$

where

$$\theta = \frac{\sqrt{D_{11}\, D_{22}}}{D_{12} + 2D_{66}} < 1 \tag{21}$$

The allowable shear buckling stress is calculated from equation (20):

$$F_{scr} = \frac{N_{xy,cr}}{t} \text{ psi} \tag{22}$$

The stiffness parameters are defined in Reference (14), page 4.3.4.

$$D^1_{11} = \frac{E_{xt}^3}{12(1-\mu_{xy}\mu_{yx})} \tag{23}$$

$$D^1_{22} = \frac{E_{yt}^3}{12(1-\mu_{xy}\mu_{yx})} \tag{24}$$

$$D^1_{12} = \frac{E_{x}\mu_{yx}t^3}{12(1-\mu_{xy}\mu_{yx})} \tag{25}$$

$$D^1_{66} = \frac{G_{xyt}^3}{12} \tag{26}$$

The skin material is $(\pm 45^{\circ}_4)$ XP251S-glass, t = .060 in., .0075 in. thick per ply; see Figure 62. The material properties are given in Table XVI.

$$E_x = E_y = (2.4)(10)^6 \qquad \mu_{xy} = \mu_{yx} = .63$$

$$G_{xy} = G = (2.21)(10)^6$$

When substituting these material properties and the thickness into equations (21), (23) to (26), the parameters are

$$D^1_{11} = D^1_{22} = 71.6 \qquad D^1_{12} = 45.1$$

$$D^1_{66} = 39.8 \qquad \theta = .574$$

When the values for the D parameters and θ are substituted into equations (20) and (22), the shear buckling allowable is

$$N_{xy,cr} = \frac{4650}{b^2} \text{ lb/in.} \qquad (27)$$

$$F_{scr} = \frac{77500}{b^2} \text{ psi} \qquad (28)$$

For the skin panel between Stringers (10) - (11) and BS 80.44-101.38, the average panel width b = 4.96 in. Substituting into equations (27) and (28), the shear buckling allowable is calculated to be

$$N_{xy,cr} = 189 \text{ lb/in.}$$

$$F_{scr} = 3150 \text{ psi}$$

APPLIED STRESSES

As stated in the Method of Analysis, the stringers react the applied bending moments, and the skin panels react the applied shears and torsional moment. Maximum stringer stresses and skin shear flows are applied in Condition VB Yaw, +15° Rec.

Bending stresses and skin shear flows for this condition are determined at BS 41.32, 90.49, 129.25, 143.28, 194.30, using the Boeing Vertol S-25 computer program, Reference (12).

Stringer

Maximum compression bending stresses due to combined vertical and lateral bending moments (see Figure 18) are applied on Stringer (8) in Bay BS 80.44-101.38. Tension is not critical.

$$fc = -36700 \text{ psi}$$

The stringer is of the basic section configuration; see Table XXI. The formula for margin of safety is given in equation (17).

$$MS = \frac{36800}{36700} - 1 = .01$$

A plot of stringer compression stress vs. boom station for Stringers (8) and (9) is shown in Figure 65.

Skin Panel

The skin panel between Stringers (10) - (11) in Bay 80.44-101.38 is the most highly loaded in shear. The skin panel is analyzed for no buckling at limit loads. The limit shear stress is

$$f_s = 2520 \text{ psi.}$$

The margin of safety based on buckling at limit load is calculated to be

$$MS = \frac{F_{scr}}{fs} - 1 \qquad (29)$$

$$MS = \frac{3150}{2520} - 1 = .25$$

A plot of the panel shear stress vs. boom station is shown in Figure 66.

BENDING AND TORSIONAL STIFFNESSES

Vertical and lateral bending and torsional stiffnesses for Concept 3 are determined at BS 41.32, 90.49, 129.25, 143.28, and 194.30. The moments of inertia about the two axes at any boom station are calculated for the GR/EP stringer areas concentrated at their centroids shown in Figure 62. The glass skin is considered to be ineffective in bending. The elastic modulus for the stringer material is given in Table XIV.

GR/EP (Type A) Stringer, 0^o:75%, $\pm 45^o$:25%: $E_x = (13.2)(10)^6$

The resulting calculations show that both the vertical and lateral bending stiffness curves closely match the design requirement. The lateral and vertical bending stiffnesses are shown in Figure 67. The design requirement curves given in Figure 22 are also shown therein for comparison.

The torsional stiffness GJ of the XP251S glass skin is calculated from equation (14). The modulus of rigidity is taken from Table XVI.

XP251S Skin, $(\pm 45^o_4)$: $G = (2.21)(10)^6$

Calculation of the torsional stiffness shows good correlation with the design requirement. The torsional stiffness is plotted in Figure 67, and the design requirement curve given in Figure 20 is included therein for comparison.

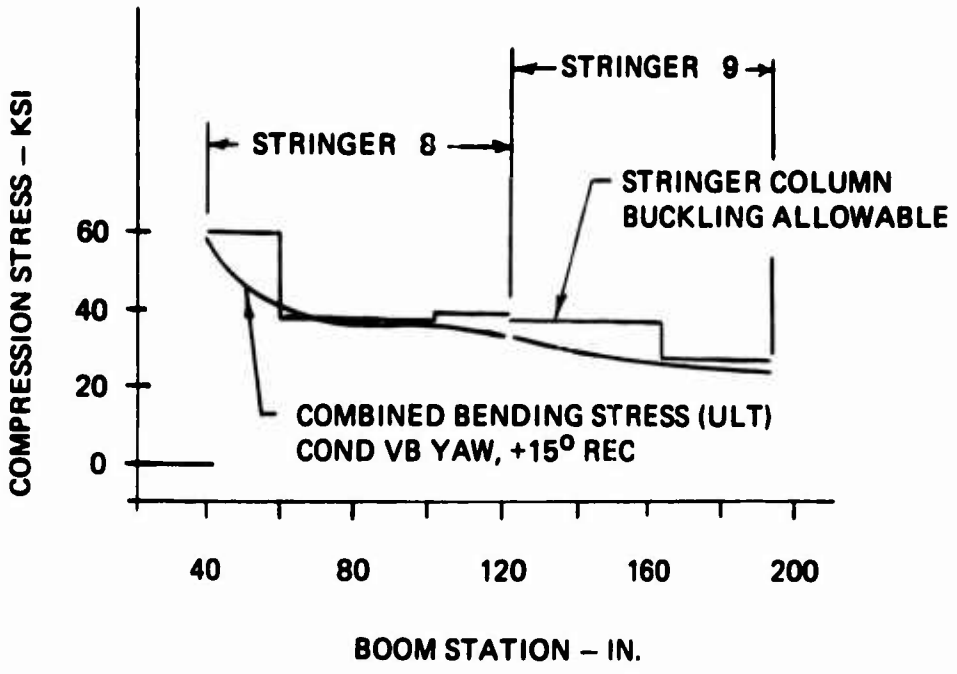

Figure 65. Compression Stress - Stringers ⑧ and ⑨ .

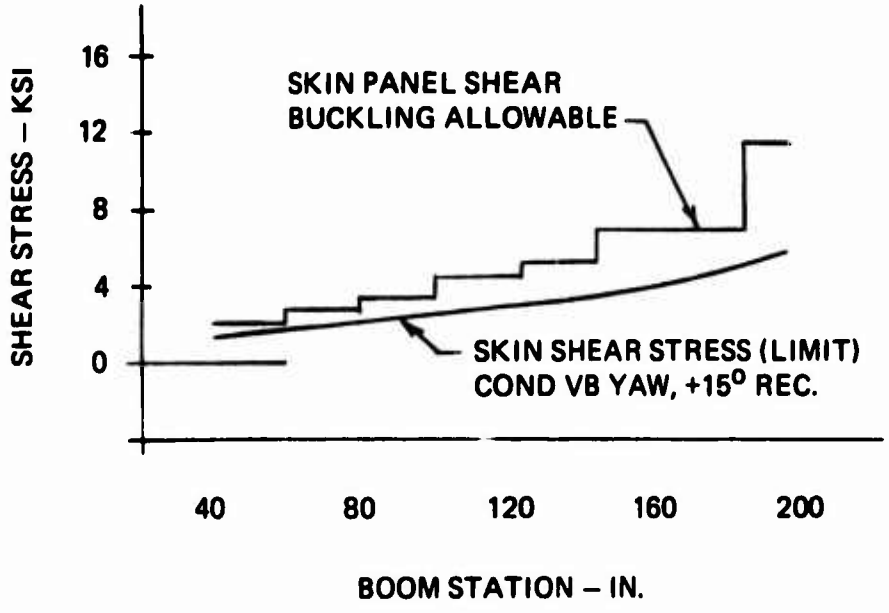

Figure 66. Shear Stress - Panel, Stringers ⑩ and ⑪ .

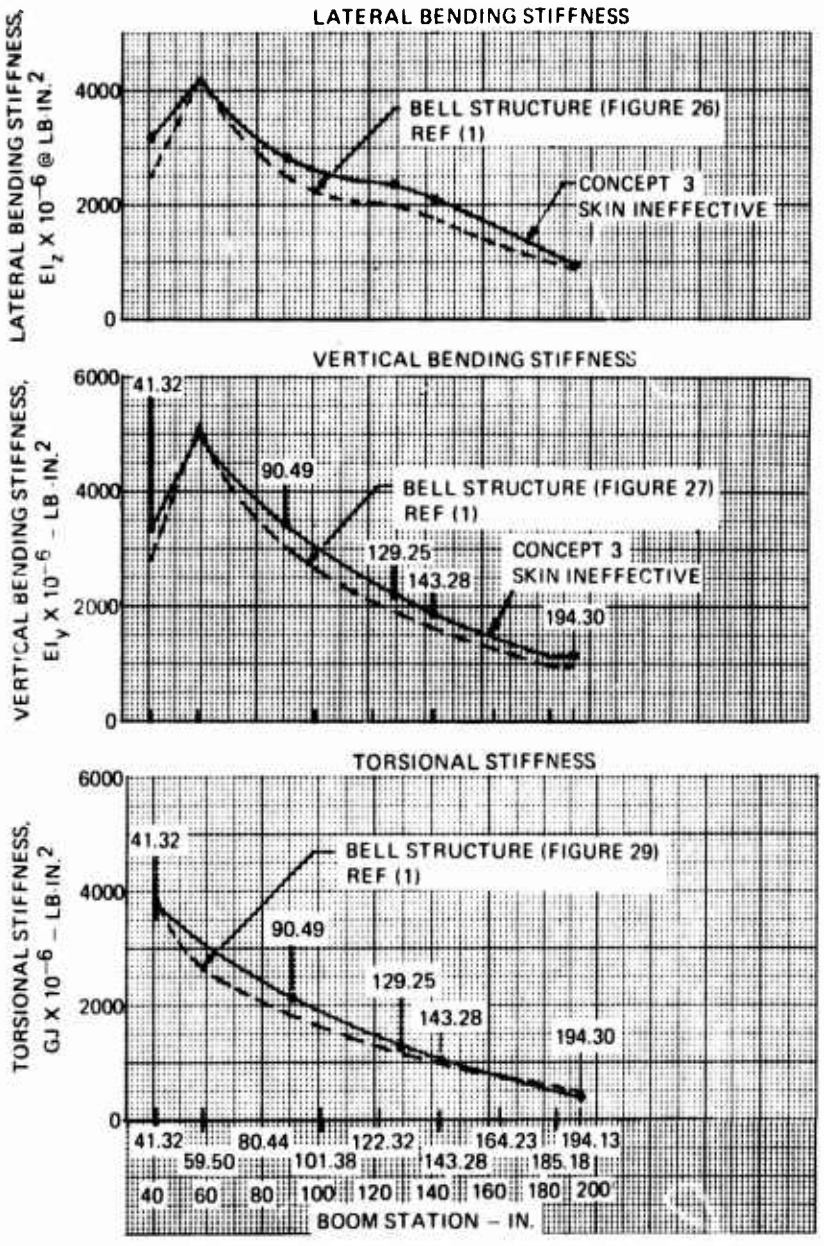

STRINGERS: GR/EP (TYPE A); UNI (0^0): 75%, (± 45): 25%
SKIN: XP251S FIBERGLASS, $(\pm 45_4)$, .060 IN. THICK

Figure 67. Concept 3 Stiffnesses.

MATH MODEL

PURPOSE

The purpose of the math model was to rank the candidate tail-section concepts from the viewpoint of life-cycle cost effectiveness.

METHOD

The model determined the discounted life-cycle cost of the component plus the effect of the component on the full aircraft system, measured in dollars.

Life-cycle costs are:

Research and Development and Initial Investment Non-recurring Costs

- Engineering design
- Tooling
- Prototypes
- Fatigue test article
- Static test article
- Systems management

Initial Investment Recurring Costs

- Flyaway aircraft
- Initial spares
- Initial training
- Initial fuel stocks
- Aircraft ground support equipment
- Nonaircraft supplies

Operating and Maintenance Costs

- Crew pay and allowances
- Crew training
- Maintenance personnel pay and allowances
- Maintenance personnel training
- Support personnel pay and allowances
- Support personnel training
- Medical and Army-wide expenses
- Petroleum, oil and lubricants
- Consumed spare parts

The effects of the component on the aircraft which were evaluated were:

Availability

Maintenance float quantity was adjusted to retain constant availability of the operational fleet for all concepts. (This capability was included in the math model but was not required because no differences in maintenance time between the concepts were identified.)

Useful Load

The operational fleet size was adjusted to retain constant simultaneous lift capability for all concepts. Useful load at constant takeoff gross weight is affected by component weight.

Vulnerability

The attrition aircraft buy was adjusted to retain a constant operational fleet size throughout the operational life of each concept. Attrition rates resulting from HEI hostile action were assessed to vary with design concept of the tail section. No changes in operational (nonhostile) attrition rates were attributed to design concept.

A detailed description of the math model logic and the input values for the various design concepts and production quantities are found in the appendix.

ASSUMPTIONS

General

Costs are in CY 1972 dollars.
A new design program, as opposed to a retrofit program, is assumed.

Protype aircraft quantity	5
Program production quantity	
(primary)	1000
(alternate)	500
Avionics cost per production aircraft	$20000
Weapons cost per production aircraft	$80000
Program operational life	10 yrs
Wartime during operational life	3 yrs

Operational

Basic maintenance float ratio	0.1
Peacetime flying rate	40 hr/mo
Wartime flying rate	100 hr/mo
Base case attrition rate	10%/yr

Discount

Discount rate	0.10
R&D years	1 thru 4
Production years	5 thru 9
Operation years	10 yrs including year acft was produced.

RESULTS

The results of the math model analysis are presented in Figures XXIII and XXIV for production quantities of 1000 and 500. The discounted costs are for the life cycle of the tail section, including the effect of the tail section on the complete aircraft system. Concept 1 has the lowest discounted cost and therefore ranks first. Concepts 2 and 3 rank second and third, in that order.

The ratios to Concept 1 are presented for convenience only. They do not represent the ratios by which Concept 1 is "better" than the other two, since the method of analysis eliminated the large constant costs for the aircraft system (other than tail section). Inclusion of these large constant costs would greatly reduce the ratios.

The last seven lines of data in each table give the significant input or calculated values for each concept.

Results of several sensitivity runs are shown in Table XXV. No change in rankings resulted from the assumed changes.

TABLE XXIII. LIFE-CYCLE COST EFFECTIVENESS

QUANTITY 1000
($ MILLIONS)

	BV CONCEPT 1	BV CONCEPT 2	BV CONCEPT 3
DESIGN	0.157892	0.248913	0.208867
TOOLING	0.544251	0.896040	0.859892
PROTOTYPES	0.360106	0.532685	0.538443
FATIGUE ARTICLE	0.095947	0.139559	0.140797
STATIC ARTICLE	0.095947	0.139559	0.140797
SYSTEMS MANAGEMENT	0.100331	0.156540	0.151104
TOTAL NONRECURRING	1.354473	2.113296	2.039899
FLYAWAY COSTS	22.900980	33.417170	36.550760
INITIAL SPARES	0.370448	0.786899	1.389375
INITIAL TRAINING	0.000000	0.210632	0.588023
INITIAL FUEL STOCKS	0.000000	0.002944	0.008219
GROUND SUPT. EQPT.	0.688374	0.799601	0.999148
NON ACFT SUPPLIES	0.000000	0.184463	0.514967
TOTAL INIT. INVEST.	23.959770	35.401680	40.050440
CREW PAY	0.000000	0.699411	1.952547
CREW TRAINING	0.000000	0.226721	0.632937
MAINT. PAY	0.000000	1.602640	4.474099
MAINT. TRAINING	0.000000	0.174573	0.487355
SUPPORT PAY	0.000000	4.752948	13.268810
SUPPORT TRAINING	0.000000	0.630487	1.760131
MEDICAL & ARMY WIDE	0.000000	2.913041	8.132351
P.O.L.	0.000000	0.131772	0.367868
CONSUMED SPARES	19.622800	21.569440	24.685340
TOTAL O&M	19.622800	32.701030	55.761420
TOTAL COST	44.937050	70.216010	97.851760
DISCOUNTED COST	21.365990	33.024960	43.966350
RATIO TO CONCEPT 1	1.000000	1.545678	2.057772
USEFUL LOAD - LB	3279.0000000	3270.0000000	3254.0000000
AVAILABILITY - %	0.7934505	0.7934505	0.7934505
HOSTILE ATTRIT. RATE	0.0000116	0.0000115	0.0000109
AIRCRAFT QUANTITIES			
PRODUCTION	1000.0000000	1002.5320000	1006.1350000
OPERATIONAL	609.4624000	611.1396000	614.1447000
MAINT. FLOAT	60.9462400	61.1136700	61.4141800
ATTRITION	329.5913000	330.2790000	330.5766000

TABLE XXIV. LIFE-CYCLE COST EFFECTIVENESS

QUANTITY 500
($ MILLIONS)

	BV CONCEPT 1	BV CONCEPT 2	BV CONCEPT 3
DESIGN	0.157892	0.248913	0.208867
TOOLING	0.544251	0.896040	0.859892
PROTOTYPES	0.360106	0.532685	0.538443
FATIGUE ARTICLE	0.095947	0.139559	0.140797
STATIC ARTICLE	0.095947	0.139559	0.140797
SYSTEMS MANAGEMENT	0.100331	0.156540	0.151104
TOTAL NONRECURRING	1.354473	2.113296	2.039899
FLYAWAY COSTS	12.850490	19.137020	20.895210
INITIAL SPARES	0.198556	0.444914	0.799161
INITIAL TRAINING	0.000000	0.105316	0.293996
INITIAL FUEL STOCKS	0.000000	0.001472	0.004109
GROUND SUPT. EQPT.	0.688502	0.752474	0.867096
NON ACFT SUPPLIES	0.000000	0.092232	0.257470
TOTAL INIT. INVEST.	13.737550	20.533400	23.117000
CREW PAY	0.000000	0.349706	0.976223
CREW TRAINING	0.000000	0.113360	0.316452
MAINT. PAY	0.000000	0.801321	2.236933
MAINT. TRAINING	0.000000	0.087286	0.243665
SUPPORT PAY	0.000000	2.376472	6.634064
SUPPORT TRAINING	0.000000	0.315243	0.880020
MEDICAL & ARMY WIDE	0.000000	1.456520	4.065963
P.O.L.	0.000000	0.065886	0.183924
CONSUMED SPARES	9.868677	10.899570	12.457960
TOTAL O&M	9.868677	16.465360	27.996190
TOTAL COST	24.960690	39.112060	53.152080
DISCOUNTED COST	12.223280	18.973990	24.554970
RATIO TO CONCEPT 1	1.000000	1.552283	2.008869
USEFUL LOAD - LB	3279.0010000	3270.0010000	3254.0010000
AVAILABILITY - %	0.7934505	0.7934505	0.7934505
HOSTILE ATTRIT. RATE	0.0000116	0.0000115	0.0000109
AIRCRAFT QUANTITIES			
PRODUCTION	500.0000000	501.2658000	503.0673000
OPERATIONAL	304.7312000	305.5698000	307.0722000
MAINT. FLOAT	30.4731100	30.5567000	30.7069500
ATTRITION	164.7956000	165.1396000	165.2883000

TABLE XXV. SENSITIVITY STUDY RANKINGS

	Concept		
	1	2	3
Base case			
1000 Production Aircraft	1	2	3
500 Production Aircraft	1	2	3
Discount rate = 0.06	1	2	3
Discount rate = 0.00	1	2	3
Component maintenance man-hours per flight hour and inactive maintenance time halved	1	2	3
All operations in peacetime	1	2	3
Hostile action attrition rate increased 6 times	1	2	3
Takeoff gross weight = 8500 lb	1	2	3

DESIGN AND MATH MODEL RESULTS

CONCEPTS IN WINNING ORDER FROM MATH MODEL EVALUATION

FIRST - CONCEPT NO. 1	1.00 RATIO
(Monocoque Sandwich Clamshell)	
SECOND - CONCEPT NO. 2	1.55 RATIO
(Thin Sandwich Shell with Longerons)	
THIRD - CONCEPT NO. 3	2.06 RATIO
(Integrally Molded Skin/Stringer Clamshell)	

It is stressed that the above results evolve strictly from math model runs. No other factors influenced the selection.

CONCEPTS IN WINNING ORDER FROM PRELIMINARY DESIGN SELECTION (PARAMETER RATINGS)

	TOTAL POINTS
FIRST - CONCEPT NO. 1	91-1/2
(Monocoque Sandwich Clamshell)	
SECOND - CONCEPT NO. 2	73-1/2
(Thin Sandwich Shell with Longerons)	
THIRD - CONCEPT NO. 3	72
(Integrally Molded Skin/Stringer Clamshell)	

CONCLUSIONS

Results of both the parameter rating studies and math model analysis indicate that a semimonocoque clamshell is the superior arrangement for constructing the AH-1G Cobra tail section in advanced composite materials. Graphite type-A is the recommended primary structure composite material mainly due to its high strength/weight ratio, relatively economical price, and good stiffness characteristics.

Technical risk is minimized by the selection of epoxy matrix and adhesive systems which have been extensively used in numerous structural applications under varying environmental conditions.

The utilization of well tried and tested sandwich construction methods for the tail-boom and fin covers and main bulkheads and spars eliminates many parts, thereby reducing numerous joints and attachments with their potential fatigue damage problems, thus minimizing airframe cost.

The susceptibility of thin graphite skins to low-velocity impact damage is considerably lessened by the unique method of discrete fiberglass insertion proposed by Boeing Vertol, which simultaneously increases ballistic tolerance of the skin.

Design and fabrication of the tail boom in split clamshell arrangement affords many manufacturing advantages which facilitate rapid production, allow low-risk lay-up and cure systems to be utilized, and permit comprehensive inspection in the critical subassembly stages.

RECOMMENDATIONS

1. A program should be initiated which will result in the design, fabrication, static and dynamic test, and finally a flight test of a composite tail section by replacement of an existing metal, AH-1G tail section with a composite version. This should be a semi-monocoque clamshell design using construction and materials as outlined in Concept 1 (Figure 10).

2. Programs should be conducted to develop concentrated load fittings in various composite materials with consideration given to hybrid or mixed systems. There are numerous types of simple tension, compression, shear, and torsional joints which have been fabricated, tested and the results analyzed. However, there are few complete fitting designs which have been developed, especially with regard to the larger, more complex fitting which may be required to carry moderate to high out-of-plane loads or to react combinations of loads from several directions.

3. More investigation should be conducted into the factors governing the design of composite fittings which will possess fatigue resistant characteristics to meet the increasing demands of safe-life philosophy.

4. Realistic cost effective fabrication concepts and techniques must be developed, as the few concepts explored in the past have used metals in the primary load path, with attendant cost of machining, processing, and adhesively bonding them into the structure. Combinations of compression molded materials combined with continuous fibers and hybrid fiber systems is believed to be a potentially feasible approach. In addition, metal matrix systems using compatible fibers such as boron, silicon carbide, or aluminum oxide, with their high interlaminar shear characteristics, high matrix modulus, and potential ductility are another avenue worthy of investigation.

5. Vacuum infiltration of complex dry fiber configurations should be evaluated.

6. Further investigation should be made into the ballistic tolerance of composite airframe structures. Survivability evaluation of sandwich construction versus skin/stringer and other structural configurations, when subject to varying gunfire levels up to 32mm HEI delayed action rounds, can only be realistically appraised by the fabrication of reasonably complete sections of structure in various composite materials which should be gunfire tested under simulated load conditions.

LITERATURE CITED

1. Ambrose, E., Clarke, D., TAILBOOM, VERTICAL FIN AND HORIZONTAL STABILIZER STRUCTURAL ANALYSIS, MODEL 209 (AH-1G), Bell Helicopter Company, Technical Report 209-099-056, January 23, 1967.

2. ADVANCED COMPOSITES DESIGN GUIDE, VOLUME I, DESIGN, Advanced Composites Division, Air Force Materials Laboratory, Air Force Systems Command, Wright-Patterson Air Force Base, Ohio, November 1971.

3. Durchlaub, E., DESIGN ALLOWABLE PROPERTIES FOR PRD 49/EPOXY, Boeing Vertol Company, IOM 8-7451-5-112, November 19, 1971.

4. Jacobs, R., Freeman, R., VERTOL'S 1969 PRD 49-1 TEST RESULTS, Boeing Vertol Company, IOM 8-7482-1-370, March 26, 1970.

5. Spitko, R. J., REINFORCED COMPOSITE MATERIALS ALLOWABLE DOCUMENT, Boeing Vertol Company, Report SRR 7, Revision Vol. IIC, December 22, 1972.

6. HRH-10 NYLON FIBER/PHENOLIC RESIN HONEYCOMB, Hexcel Aerospace, Data Sheet, DS 4000, March 1, 1971.

7. MODERATE TEMPERATURE CURING STRUCTURAL ADHESIVE SYSTEM, Boeing Vertol Company, Boeing Material Specification BMS 5-51C, Revised 5-1-69.

8. VERTOL PROCESS SPECIFICATION, Boeing Vertol Company, Process Specification D8-0224.

9. STRUCTURAL SANDWICH COMPOSITES, Department of Defense, MIL-HDBK-23A, December 30, 1968.

10. MILITARY STANDARDIZATION HANDBOOK, METALLIC MATERIALS AND ELEMENTS FOR AEROSPACE VEHICLE STRUCTURES, VOLUME I, Department of Defense, MIL-HDBK-5A, September 1, 1971.

11. PLASTICS FOR AEROSPACE VEHICLES, PART 1, REINFORCED PLASTICS, Department of Defense, MIL-HDBK-17A, January 1971.

12. Robinson, John, PRELIMINARY DESIGN OF ARBITRARY SECTION SEMI-MONOCOQUE STRUCTURES, Boeing Vertol Company, Program S-25, October 10, 1963.

13. STRESS MANUAL D6-22695, COMMERCIAL AIRPLANE GROUP, The Boeing Company, January 1972.

14. STRUCTURAL DESIGN GUIDE FOR ADVANCED COMPOSITE APPLICATIONS, VOLUME II, ANALYTICAL METHODS, SECOND EDITION, Advanced Composites Division, Air Force Materials Laboratory, Air Force Systems Command, Wright-Patterson Air Force Base, Ohio, January 1971.

APPENDIX

MATH MODEL LOGIC AND INPUT VALUES

The math model logic flows, codes for variables, and values used are given herein.

```
**OPERATING COSTS PER YEAR
  FOR BASE CONFIGURATION
  COSBMM*FMA*12.*(YPL-1.)/YPL*QOB
  FOR ALTERNATIVE CONFIGURATIONS THE FOLLOWING ARE
  ADDED
  NO. OF DIRECT PERSONNEL = HDS = NCO*RCO+NCE*RCE+RMP
  FMA = (YP*FMP+YW*FMW)/YPL
  CREW PAY = NCO*RCO*COPCO+NCE*RCE*COPCE
  CREW TRAINING = NCO*RCO*CTCO*RTO+NCE*RCE*CTCE*RTE
  MAINT PAY = RMP*COPM
  MAINT TRAINING = RMP*CTM*RTE
  NO. OF SUPPORT PERSONNEL = HDSS = HDS*RISP
  SUPPORT PAY = HDSS*(RISO*COPSO+(1.-RISO)*COPSE)
  SUPPORT TRAINING = HDSS*(RISO*RTO*CTSO+(1.-RISO)*
  RTE*CTSE)
  MEDICAL & ARMY WIDE = (HDS+HDSS)*CAW
  P.O.L. COST = (1.2+CF*FC)*(FMP*YP+FMW*YW)*12./YPL
  SPARES CONSUMPTION = ((COSAFM+COSBMM)*FMA*12.+
  (COSEFM*FMA*12.)+COSVFM+COSRFM)*(YPL-1.)/YPL*
  (QO-QOB)

**TOTAL OPERATING COSTS ARE THE SUM OF ABOVE TIMES
  OPERATIONAL YEARS PER AIRCRAFT

**LIFE-CYCLE COST EFFECTIVENESS IS THE SUM OF ABOVE
  NONRECURRING, INITIAL INVESTMENT AND TOTAL OPERATING
  COSTS

**DISCOUNTING
  NONRECURRING COSTS ARE SPREAD EQUALLY OVER THE FIRST
  FOUR YEARS
  INITIAL INVESTMENT COSTS ARE SPREAD EQUALLY OVER THE FIFTH
  THROUGH NINTH YEARS
  OPERATING COSTS ARE SPREAD EQUALLY OVER TEN YEAR PERIODS
  STARTING WITH THE YEAR THE INITIAL INVESTMENT WAS MADE
  TOTAL COST FOR EACH YEAR IS DISCOUNTED AT THE AVERAGE OF THE
  DISCOUNTING FACTORS FOR YEAR START AND YEAR END

**DISCOUNTED LIFE-CYCLE COST EFFECTIVENESS VALUE IS THE
  SUM OF THE ANNUAL DISCOUNTED COSTS FOR THE FULL PROGRAM
  LIFE

**THE CONCEPT HAVING THE LOWEST DISCOUNTED LIFE-CYCLE COST
  RANKS HIGHEST
```

```
**OPERATIONAL FACTORS
  YP=YPL-YW
  WE=WS+WB+WY
  EU=WG-WE-WL-WM
  QO-QP/(1.+RMF+AP*FMP*12.*YP+(AWO+AWH)*FMW*12.*YW)
  QM-QO*RMF
  QA=QP-QO-QM
  AVAILABILITY = 1 - DOWNTIME / TOTAL TIME
  AV=((1.-((MP+MCAP+MCBP)*FMP/RPH+ETP*FMP)/730.)*YP+
  (1.-((MP+MCAW+MCBW)*FMW/RPH+ETW*FMW)/730.)*YW)/YPL
  FOR BASE CONFIGURATION
  QPS=QP
  QOB=QO
  QMB=QM
  AVB=AV
  ULB=EU

  FOR ALTERNATIVE CONFIGURATIONS
  RMFA=(QMB+(QOB*AVB/AV-QOB))/QOB
  QO=QOB*ULB/EU
  QM=QO*RMFA
  QA=QO*(AP*FMP*12.*YP+(AWO+AWH)*FMW*12.*YW)
  QP=QO+QM+QA

**NONRECURRING COSTS
  (CNEB+CNTB+CNPB+CNFB+CNAF)*(1.+CNMF)

**INITIAL INVESTMENT COSTS
  FOR BASE CONFIGURATION
  CIFB*QPS+CISBF*CIFB*QOB+CIGFB*CIFB*QOB
  FOR ALTERNATIVE CONFIGURATIONS THE FOLLOWING ARE
  ADDED TO EVALUATE THE EFFECT OF THE COMPONENT ON
  THE AIRCRAFT SYSTEM
  (CIFA+CIFB+CIFE+CIFV+CIFR)*(QP-QPS)
  (CISAF*CIFA+CISBF*CIFB+CISEF*CIFE+CISVF*CIFV+CISRF
  *CIFR)*(QO-QOB)
  (NCO*RCO*CTCO+NCE*RCE*CTCE+RMP*CTM)*(QO-QOB)
  (FSF*CF*FC*FMA*12.)*(QO-QOB)
  (CIGF*(CIFA+CIFB+CIFE+CIFV+CIFR))*(QO-QOB)
  (CINF*(NCO*RCO+NCE*RCE+RMP)*(QO-QOB)
```

MATH MODEL INPUT DATA

LOC	CODE	ITEM	PROD QTY	BV CON-CEPT	VALUE	UNITS	SOURCE*
10	CNEB	Nonrecurring engineering design cost for component		1 2 3	157892 248913 208867	$	Boeing
11	CNTB	Nonrecurring tooling cost for component		1 2 3	544251 896040 859892	$	Boeing
12	CNPB	Nonrecurring prototype cost for component		1 2 3	360108 532685 538443	$	Boeing
13	CNFB	Nonrecurring fatigue test article cost for component		1 2 3	95947 139559 140797	$	Boeing
14	CNAB	Nonrecurring static test article cost for component		1 2 3	95947 139559 140797	$	Boeing
15	CIGFB	Investment GSE cost factor for component	1000	1 2 3	.04932 .03559 .03478	-	Boeing
			500	1 2 3	.08791 .06217 .06088		

LOC	CODE	ITEM	PROD QTY	BV CON-CEPT	VALUE	UNITS	SOURCE*
16	CIFB	Investment flyaway cost for component	1000	1	22901	$	Boeing
				2	31739		
				3	32480		
			500	1	25701		
				2	36344		
				3	37109		
17	COSBMM	Component maintenance material cost per flight hour	1000	1	5.14	$/FH	Boeing
				2	5.20		
				3	5.21		
			500	1	5.17		
				2	5.26		
				3	5.27		
18	WB	Weight of component		1	145	Lb	Boeing
				2	154		
				3	170		
19	WTMCBP	Maintenance man-hours per flight hour for component - peacetime			.05769	MH/FH	Boeing
20	WTMCBW	Maintenance man-hours per flight hour for component - wartime			.05769	MH/FH	Boeing
21	ETP	Elapsed time/flight hour for component inactive maintenance - peace			.23077	HR/FH	Boeing
22	ETW	Elapsed time/flight hour for component inactive maintenance - war			.23077	HR/FH	Boeing

LOC	CODE	ITEM	PROD QTY	BV CON-CEPT	VALUE	UNITS	SOURCE*
23	AWH	Attrition rate per flight hour due to hostile action for aircraft system		1 2 3	.0000116 .0000115 .0000109	-	Boeing
24	C	Total life-cycle cost, not discounted				$	Program
25	CN	Total component nonrecurring cost, not discounted				$	Program
26	CI	Total investment cost for component and effect on system				$	Program
27	CO	Total life cycle O&M cost for component and effect on system				$	Program
28	EU	Useful load				Lb	Program
29	EA	Availability				Percent	Program
30	ETR	Hostile attrition rate				-	Program
31	CNMF	Nonrecurring systems management factor			.08	-	Boeing
32	CIFA	Investment flyaway cost of airframe less component	1000 500		446000 541000	$	PLACE
33	CIFE	Investment flyaway cost of engine			85000	$	Lycoming

LOC	CODE	ITEM	PROD QTY	BV CON-CEPT	VALUE	UNITS	SOURCE*
34	CIFV	Investment flyaway cost of avionics			20000	$	101-20, Boeing
35	CIFR	Investment flyaway cost of armament			80000	$	101-20, Boeing
36	CISAF	Initial spares factor for airframe less component (% flyaway)			.37	-	Boeing
37	CISCF	Initial spares factor for component (% flyaway)	1000	1	.0265415	-	Boeing
				2	.0235017		
				3	.0233221		
			500	1	.0253522		
				2	.0225037		
				3	.0223619		
38	CISEF	Initial spares factor for engine (% flyaway)			.27	-	Boeing
39	CISVF	Initial spares factor for avionics (% flyaway)			.27	-	Boeing
40	CISRF	Initial spares factor for armament (% flyaway)			.05	-	Boeing
41	CIGF	Aircraft related ground support equipment factor (% flyaway)			.10	-	Boeing
42	CINF	Non-aircraft supplies factor (cost per man)			6000	$	Boeing
43	COSAFM	Airframe consumed spares cost per flight hour			106	$/FH	101-20

LOC	CODE	ITEM	PROD QTY	BV CON-CEPT	VALUE	UNITS	SOURCE*
44	COSEFM	Engine consumed spares cost per flight hour			0	$/FH	Boeing
45	COSVFM	Avionics consumed spares cost per aircraft per year			2361	$/YR	101-20
46	COSRFM	Armament consumed spares cost per aircraft per year			34028	$/YR	101-20
47	COPCD	Officer crew pay and allowances per year			14000	$/YR	Planning Boeing
48	COPCE	Enlisted crew pay and allowances per year			8100	$/YR	Planning Boeing
49	COPM	Maintenance man pay and allowances per year			6400	$/YR	Planning Boeing
50	COPSO	Support officer pay and allowances per year			12000	$/YR	Planning Boeing
51	COPSE	Support enlisted pay and allowances per year			6400	$/YR	Planning Boeing
52	CTCO	Officer crew training cost per man			34658	$	Planning
53	CTCE	Enlisted crew training cost per man			3854	$	Planning
54	CTM	Maintenance man training cost per man			2582	$	Planning

LOC	CODE	ITEM	PROD QTY	BV CON-CEPT	VALUE	UNITS	SOURCE*
55	CTSO	Support officer training cost per man			6992	$	Planning
56	CTSE	Support enlisted training cost per man			3398	$	Planning
57	CAW	Medical and Army wide cost per man per year			2961	$/Yr	Planning
58	CF	Cost of fuel			.104	$/Gal	101-20
59	WG	Gross weight			9500	Lb	Bell
60	WS	Weight of structure, excluding component			962.8	Lb	Bell
61	WY	Weight of all systems			4409.1	Lb	Bell
62	WL	Fixed useful load			458.2	Lb	Bell
63	WM	Mission equipment weight			245.9	Lb	Bell
64	QT	Quantity of prototype aircraft			5	-	Army
65	QP	Basic quantity of production aircraft	1000 500		1000 500	-	Army
66	FMP	Flight hours per month - peace			40	FH/Mo	Army
67	FMW	Flight hours per month - war			100	FH/Mo	Army
68	YPL	Operational years per aircraft			10	Yr	Army

LOC	CODE	ITEM	PROD QTY	BV CON-CEPT	VALUE	UNITS	SOURCE*
69	YW	Years of war during operational life			3	Yr	Army
70	RMF	Basic maintenance float ratio to operational quantity			.1	-	Boeing
71	NCO	Crew officers per aircraft			2	-	TOE
72	NCE	Crew chiefs per aircraft			1	-	TOE
73	WTMP	Preventive maintenance man-hours per flight hour			0	MH/FH	Boeing
74	WTMCAP	Corrective maintenance man-hours per flight hour for aircraft less component - peace			6.67	MH/FH	101-20, Boeing
75	WTMCAW	Corrective maintenance man-hours per flight hour for aircraft less component - war			6.67	MH/FH	101-20, Boeing
76	RCO	Officer crew manning ratio			1.2	-	Boeing
77	RCE	Enlisted crew manning ratio			1.0	-	Boeing
78	RMP	TOE, DS, GS, Depot maintenance men per aircraft - peace			14.93	Men/ A/C	101-20, Boeing
79	RMW	TOE, DS, GS, Depot maintenance men per aircraft - war			14.93	Men/ A/C	101-20, Boeing
80	RMIOF	Maintenance operational factor			1	-	Boeing

LOC	CODE	ITEM	PROD QTY	BV CON-CEPT	VALUE	UNITS	SOURCE*
81	RISP	Support personnel ratio to direct - peace			2.2	-	AVSCOM
82	RISW	Support personnel ratio to direct - war			2.2	-	AVSCOM
83	RISO	Support officer ratio to total support personnel			.112	-	AVSCOM
84	RPH	Maintenance personnel in Org/DS per aircraft for airframe and engine			2.84	Men/ A/C	TOE
85	RTO	Officer turnover ratio % per year			.15	-	AVSCOM
86	RTE	Enlisted turnover ratio % per year			.27	-	AVSCOM
87	FSF	Initial fuel stock factor % of first year			.25	-	Boeing
88	FC	Fuel consumption rate gal per flight hour			97	Gal/Hr	101-20
89	AP	Operational attrition rate per flight hour - peace			.0000717	-	Report 1

LOC	CODE	ITEM	PROD QTY	BV CON-CEPT	VALUE	UNITS	SOURCE*
90	AWO	Operational attrition rate per flight hour - war			.0000717	-	Report 1
91	DISRA	Discount rate			.1	-	37-13
92	RADS	Start year for nonrecurring expenditures			1	-	Boeing
93	RADE	End year for nonrecurring expenditures			4	-	Boeing
94	VESS	Start year for recurring investment			5	-	Boeing
95	VESE	End year for recurring investment			9	-	Boeing

*SOURCES

Army	-	USAAMRDL
Boeing	-	Values are estimated by the appropriate functional group or groups in the Boeing Vertol organization
PLACE	-	Boeing Vertol Parametric Life-Cycle Army Cost Estimator
101-20	-	FM 101-20-1, Field Manual, United States Army Aviation Planning Manual
570-2	-	AR 570-2 Headquarters, Dept. of the Army, Manpower and Equipment Control, Organization and Equipment Authorization Tables - Personnel
37-13	-	AR 37-13 Headquarters, Dept. of the Army, Financial Administration, Economic Analysis of Proposed Army Investments
Planning	-	Dept. of the Army, Army Force Planning Cost Handbook
AVSCOM	-	Headquarters, U.S. Army Aviation Systems Command Letter AMSAV-EET dated 3 Nov. 1972, CH-47A and B Modernization Program
TOE	-	TOE 17-111H, Attack Helicopter Company
Report 1	-	Boeing Report D210-10267-1 to U.S. Naval Air Development Center, Helicopter Escape and Personnel Survival Accident Data Study, Contract No. N62269-70-C-0094
Bell	-	Bell Helicopter Co. Report No. 209-099-143 dated 14 Jan. 1968, Actual Weight and Balance Report, Detail Type, for the Last FY '66 Model AH-1G Helicopter, S/N 66-15357